Development of new immunoassay platforms for rapid serological diagnosis of Lyme borreliosis

Dissertation

zur

Erlangung des Doktorgrades

der Naturwissenschaften

(Dr. rer. nat.)

dem

Fachbereich Pharmazie der

Philipps-Universität Marburg

vorgelegt von

M.Sc. Mohammed Abdelsalam Abdelkader Alasel

aus Ägypten

Marburg/Lahn 2016

Erstgutachter: Prof. Dr. Michael Keusgen

Zweitgutachter: Prof. Dr. Udo Bakowsky

Eingereicht am_____

Tag der mündlichen Prüfung am_____

Hochschulkennziffer: 1180

Table of Contents

Acknowledgment

List of abbreviation

3-DPESB	3-dimensional porous solid surface sinter bodies
ABICAP	Antibody Binding Immune Column for Analytical Purpose
AFM	atomic force microscopy
APTES	(3-aminopropyl)triethoxysilane
ASTM	American Society for Testing and Materials
AuNPs	gold nanoparticles
BSA	bovine serum albumin
BSK	Barboure-Stoennere-Kelly
CBC	casein buffer concentrate
CDC	US Centers for Disease Control and Prevention
Con A	concanavalin A
CSF	cerebrospinal fluid
DNA	deoxyribonucleic acid
DSC	N,N´-disuccinimidyl carbonate
EDC	N- (3-dimethylaminopropyl)-N`-ethylcarbodiimide hydrochloride
ELISA	enzyme-linked immunosorbent assay
EM	erythema migrans
FDA	US Food and Drug Administration
FTIR	Fourier transform infrared spectroscopy
g	gram(s)
h	hour(s)
HRP	horseradish peroxidase enzyme
IgG	immunoglobulin G
IgM	immunoglobulin M
L	liter(s)
min	minute(s)
mM	millimol L^{-1}
mL	milliliter(s)
NHS	N-hydroxysuccinimide
OspC	outer surface proteins C

PBS	phosphate buffered saline
PCR	polymerase chain reaction
POC	point of care
QCM	quartz crystal microbalance
RIA	radioimmunoassay
SEM	scanning electron microscopy
SPR	surface plasmon resonance
TMB	3,3',5,5'-tetramethylbenzidine
UV	ultra violet

1. Introduction

Bioanalysis, a fundamental research area of analytical chemistry, concerns the identification and quantification of molecules in biological systems. One of its major interests is human health, which focuses on detection of biomolecules that exist, for example, as a result of a certain infectious disease. Antibodies, for instance, can be detected in body fluid, indicating the presence of an infection. The early detection of such biomolecules would allow an early treatment of the disease successfully via antibiotic; and this would assist further in prohibiting the transition of the infectious disease as well as would reduce the risk of more advanced sever health problems. Therefore, a simple, rapid, and sensitive test is needed to detect and quantify the infecting agent. Besides the test should be cost effective and easy to interpret.

Ligand-binding immunoassay is the most commonly used analytical procedure to detect antibodies in body fluids. This is due to its high sensitivity, besides its high specificity.

In the presented thesis, a *Borrelia* infection (one of the most common infectious diseases in North America and Europe) was taken as a model to develop novel ligand-binding immunoassay platforms for rapid point of care testing.

1.1 Immunoassays

Immunoassay is a widely used laboratory and on-site test; it enables a high specific and sensitive detection of analytes, ranging from small molecules (1) to intact cells (2). The main concept of the assay performance is based on a high specific interaction between antibody, the key component, and antigen. The antigen or the antibody is used to recognize the immune agent (analyte); following, detection of the produced antibody-antigen complex (immune complex) can be easily conducted. In effect, detection of the infectious disease is accomplished (Figure 1).
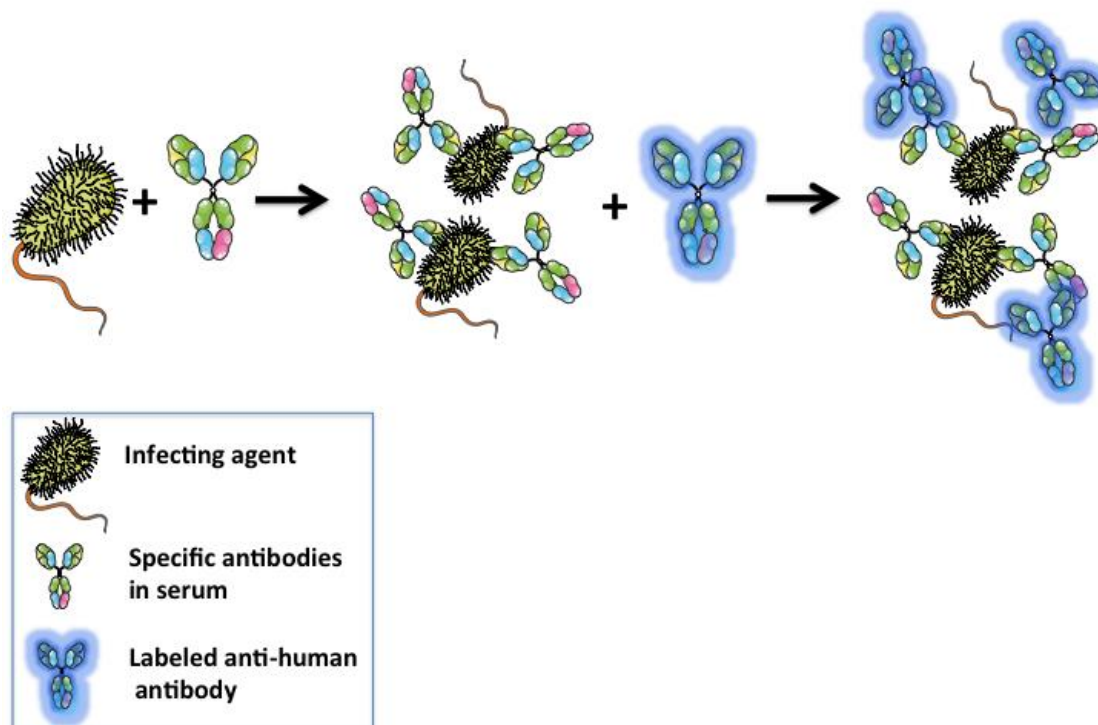
Figure 1 *A scheme illustrates the employment of immunoassays in detection of infectious diseases. Antibodies are used to recognize the antigen (infecting agent) in sample. A label can then be added to monitor the interaction.*

Since the first immunoassay that was developed by Yalow and Berson for insulin determination in 1960 (3), this type of antigen-antibody interaction dependent techniques have been developed and found their applications in diverse areas; it has been applied in determination of chemical molecules, biomolecules and even whole cells. For example, determination of toxins (4), cancer biomarkers (5), environmental contaminants (6), whole cells (7), proteins concentration, as well as determination of small molecules in clinical samples, such as body fluids, could be applicable. Yalow and Berson developed a highly sensitive assay based on a radioisotope labeled antigen or antibody in a competitive analysis way, radioimmunoassay technique (RIA).

RIA was extensively used subsequently in diverse areas of biomedical and clinical diagnosis such as measurement of pepsinogen in porcine blood samples (8), and determination of vasopressin in plasma (9). Yet, RIA possesses some drawbacks that limited the further use of such approach. Namely, the special and long arrangement for requisition and handling of the radioactive materials, the short living nature of the radioisotope label, which causes

subsequently shortening the shelf-life of the labeled antibody or antigen, the hazard health the radioisotopes constitutes, and the waste disposal problems. Besides, RIA is not adequate for the direct determination of samples, since the decrease in detected signal could be arisen by other factors rather than a specific antibody-antigen interaction (10).

As alternative, immunoassays have been evolved to using enzymes for detection instead of radioisotopes. Enzymes have the ability to undergo chemical reactions, providing a sensitive and a clear detection. A single copy of an enzyme can generate many product molecules, which in turn would decrease the detection limit of the measurements by amplifying the signal. An enzyme that is coupled to either the antigen or the antibody reacts with a substrate producing a physically or chemically detectable product, mostly a colored precipitate. The colored products can then be easily measured using a spectrophotometer. Electrochemical detection could be also employed to detect the enzyme reaction (detection of electrons movement between an electrode and a substrate is mainly possible after an enzymatic reaction) (11).

The quantitative measurements of immunoglobulin G (IgG) antibodies in rabbit serum using alkaline phosphatase enzyme (12) and the quantitative determination of human chorionic gonadotropin in urine using horseradish peroxidase enzyme (HRP) (13) are considered the pioneer studies in using enzymes for detection in immunoassays.

HRP has become the most common used enzyme in immunoassays since then; the reason is due to that, HRP has the ability to oxidize numerous of chromogenic substrates, e.g. 3,3',5,5'-tetramethylbenzidine (TMB), 3,3',4,4'-biphenyltetramine, and 2,2'-azino-bis(3-ethylbenzothiazoline-6-sulphonic acid) (ABTS). These chromogenic substrates convert in turn into colored products, which can be easily monitored, in the presence of an oxidizing agent such as hydrogen peroxide (14). TMB substrate can be oxidized by HRP to form a cation radical intermediate, which in turn could be combined to form a charge-transfer complex. The complex can be seen easily at acidic pH as a blue precipitate; besides it can be measured at 650 nm (14). The cation intermediate can also further oxidized to form a yellow colored diimine derivative that can be measured at 450 nm (Figure 2).
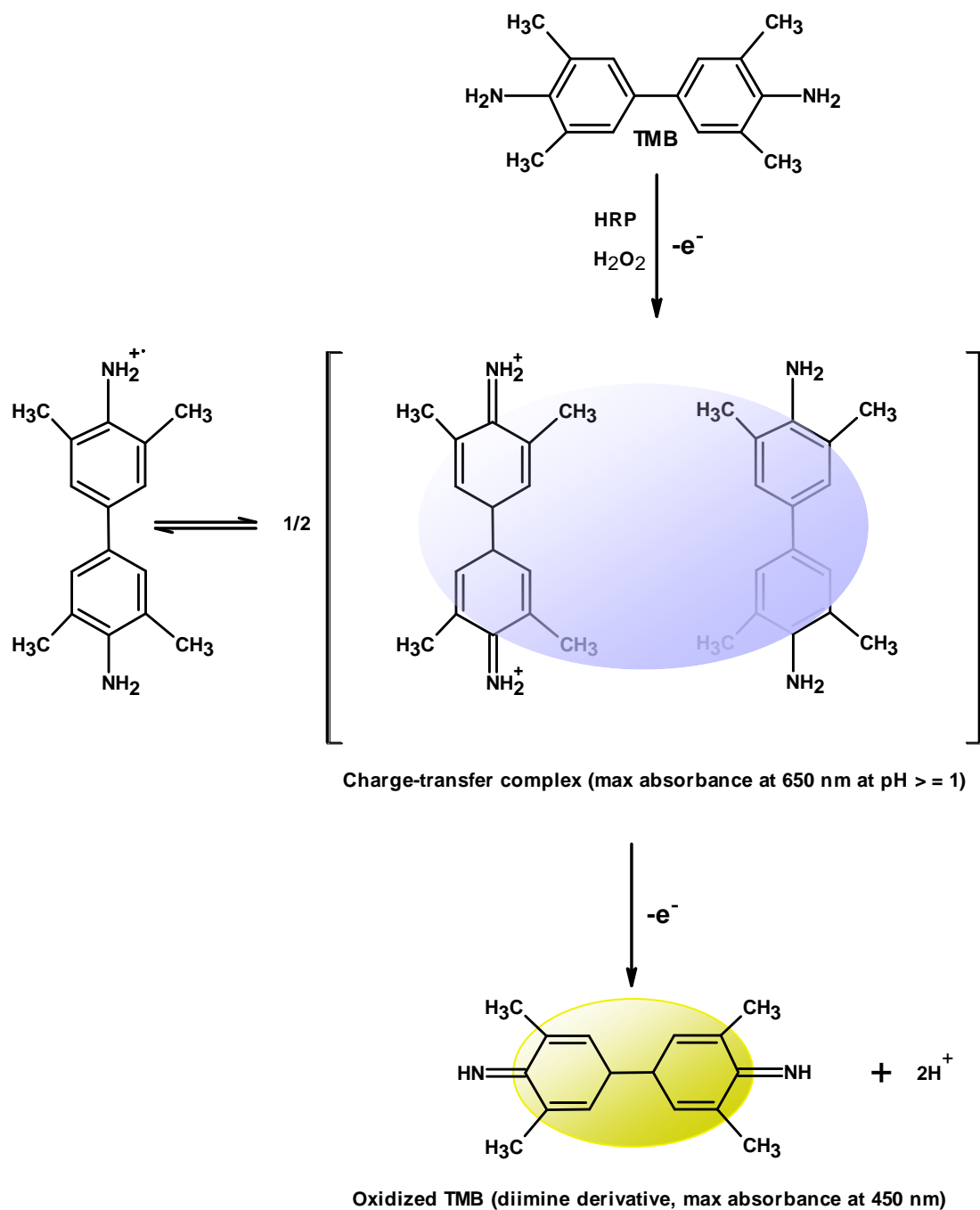
Figure 2 *Oxidation of TMB using HRP enzyme in presence of oxidizing agent (H_2O_2). Oxidation reaction results in a charge-transfer complex, which can be seen at acidic pH as a blue precipitate. The maximum absorbance of the blue precipitate can be measured at 650 nm. Further oxidation of TMB would result in a yellow diimine derivative that has maximum absorbance at 450 nm.*

Although enzymes enhanced the signal and decreased the limit of detection, other studies have been conducted to increase the immunoassay sensitivity even more.

Woodhead reported more sensitive test in 1985. The test is based on using chemiluminescence, a label capable of emitting light after a chemical reaction (15). Woodhead developed an immunoassay based on using acridinium ester as labels; it has the advantage of producing light under mild conditions with no requirements for a catalyst. The reaction takes place under aqueous conditions at basic pH in presence of hydrogen peroxide. As a result an excited product is formed, which emits light after it relaxes to its ground state (Figure 3). The photons can be emitted as a result of relaxation of an exited product to its ground state after an exoergic reaction; the intensity of the emitted light is related to the concentration of the tested sample.

Figure 3 *Mechanism of chemiluminescence reaction of acridinium ester. An excited product is formed in presence of oxidizing agent, which emits light after it relaxes to its ground state.*

Furthermore, diverse labels have been reported for immune complex detection; all have a main concern of enhancing the assay sensitivity. For example, nanoparticles, dyes, and fluorogenic reporters have been used as labels for detection.

For many years, immunoassays have been performed on a fixed platform, like microtiter plate, where the protein probe is fixed on a solid support. However, the assay possesses the disadvantage of that large volume of the sample is needed. Alternatively, microfluidics technique was evolved; a technique that manipulate and process the sample in very small amounts (10^{-9} – 10^{-18} L); the sample in a fluid moves freely in channels with diameter of ten to hundreds micrometers (16). Microfluidic immunoassays have a distinct characteristic of the diversity of designs and fabrications, which enable the analysis of different biomolecules. In addition, this type of microfluidic system characterized by the short analysis time and the low cost because of the low volume of reagents. As a disadvantage, the sensitivity is not enough in many applications. Nevertheless, many strategies based on microfluidic technique have been developed to amplify the test signal (17). More about design and fabrication of microfluidic techniques and its application can be found in this review (18).

Another platform was also employed in immunoassay, which bring the chromatographic technique and immune chemical reaction together, is immunochromatographic assay. It is simple, cheap and suitable for on-site detection (19). Considering the need to obtain a simple, cheap and sensitive test, many other platforms have been also developed. For example, flow cytometric immunoassays (20), electrochemical immunoassays (21) and nanoparticle-based immunoassays (22).

1.2 Classification of immunoassays

As mentioned above, antigen or antibody in immunoassay is used to catch the immune agent (analyte) from the sample. Based on whether the bound analyte and unbound analyte are separated by a washing step or not, immunoassays can be classified into homogeneous or heterogeneous (23). Heterogeneous immunoassay is considered when the antigen or the antibody is immobilized on a solid surface; then loading of the other immune agent containing solution comes afterwards. An immune complex produced as a result, which can be detected using a labeled protein. The unbound proteins should be washed away before the detection step. The signal produced by the labeled protein is related in this case to the bound immune agent (24). Considering the detection of antibodies in sample, immunoassay is homogeneous when the antigen, the target antibody, and a well-controlled concentration of the labeled antigen are mixed in one solution. The antigen competes with the labeled antigen to antibody binding sites. A signal is generated due to a change in marker's activity when

coupled. Unlike the heterogeneous, there is no separation of unbound antigen or labeled antigen to get accurate signal (25). Figure 4 shows the difference between a homogeneous and a heterogeneous immunoassay.
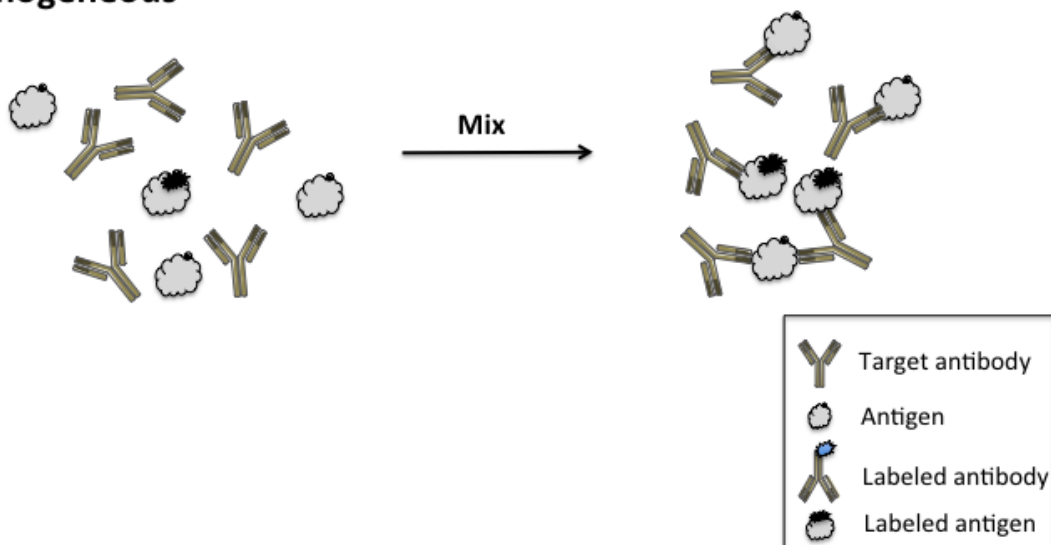
Figure 4 *An illustration of the difference between heterogeneous and homogeneous immunoassays. In contrast to homogeneous assay, a washing step is needed in the heterogeneous assay in order to separate the bound and unbound analyte.*

Immunoassay can be designed in either competitive or noncompetitive manner. In competitive immunoassays an immobilized antibody has a limited binding sites; an antigen and a labeled antigen competes to those limited sites. The antigen can displace the labeled antigen on the antibody sites, as a result the higher the antigen concentration in the sample is, the lower the labeled antigen bind to the antibody and the lower the detected signal is (26). The unbound antigen and unbound labeled antigen can be easily washed, and bound labeled antigen concentration can be then detected. Competitive immunoassay is mostly used in determination of small molecules such as drugs.

In noncompetitive immunoassays, either antibody or antigen with high quantity is immobilized on a solid surface. Following, analyte is applied to the surface, and finally a secondary labeled antibody is loaded, which can be easily monitored (27). One common platform of noncompetitive immunoassays is sandwich enzyme-linked immunosorbent assay (ELISA), in which, a primary antibody is immobilized and a labeled antibody can bind to an antigen, which is previously bound to the primary antibody; in sandwich ELISA the antigen should have two epitopes. Schematic representations of competitive and noncompetitive immunoassays are shown in Figures 5 and 6.
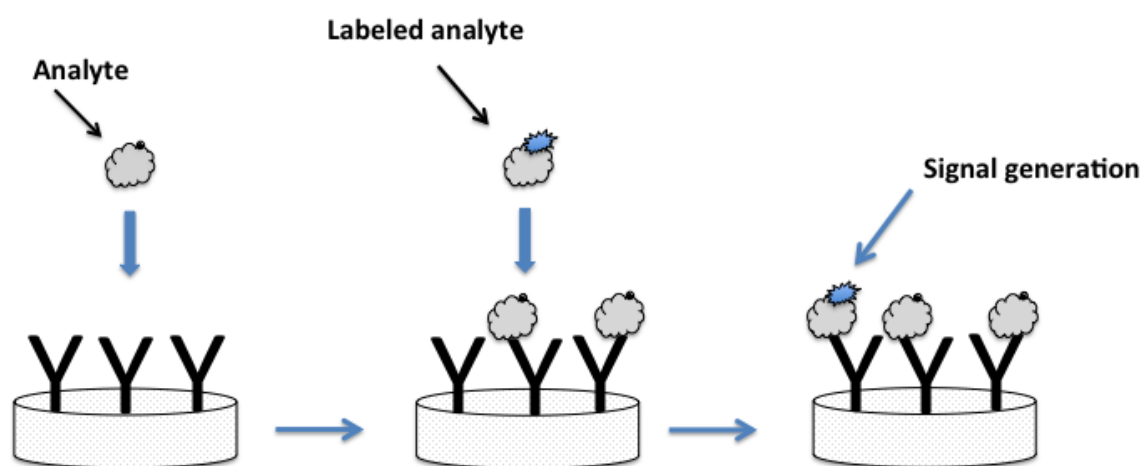
Figure 5 *Schematic representation of a competitive immunoassay; analyte is applied first followed by a labeled analyte. Higher concentrations of analyte would result in lower concentrations of bound labeled analyte and lower detected signal.*
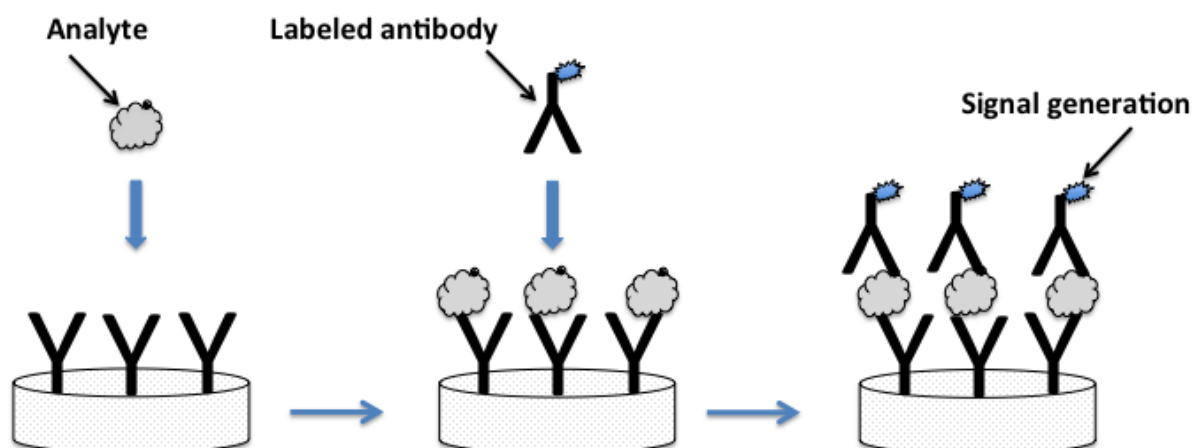
Figure 6 *Schematic representation of a non-competitive immunoassay; a secondary labeled antibody is added to detect the interaction. The target antigen binds to the immobilized antibody as well as binds to the labeled antibody. Higher detected signal indicates of high analyte concentration.*

1.3   Antibody

Antibodies are the key components of an immunoassay; a biomolecule, which has the ability to bind foreign harmful antigens (such as bacteria, fungi, viruses, parasites and chemicals) in human body through a specific recognition sites in their structures. The binding results in forming an immune complex (28), which can then be removed from circulation through phagocytosis by macrophages. Lymphocytes are white blood cells able to secret antibodies after their stimulation; this takes place through one type of its cells known as plasma cells (29). Lymphocytes are considered the major cells involved in the immune system because they determine the structure specificity of antibody.

An antibody or an immunoglubin is a glycoprotein composed of 4 polypeptide chains that can be visualized as a Y shape. Each polypeptide chain has an amino terminal group and a carboxyl terminal group. Two polypeptides are long (440 amino acids approximately), identical and called heavy (H) chains with a molecular mass of 50-75 KDa. The other two are shorter (220 amino acids approximately), identical and called light (L) chains with a molecular mass of about 25 KDa (30). Moreover, each polypeptide chain consists of a constant region (C) and a variable region (V).

Light chains can be divided into one variable (V_L) and one constant (C_L) domain, while the heavy chains can be divided into one variable (V_H) and three or four constant domains. Starting from the amino end to the carboxyl end of polypeptide, constant chains can be named C_{H1}, C_{H2}, C_{H3}, and C_{H4}. The variable regions of both heavy and light chains are homologous and similar in length; in the same manner the constant region of light chain is homologous and similar in length to the constant regions of the heavy chain (31).

Heavy chains are linked to each other and to the light chains by disulphide bridges, in addition to some non-covalent forces such as electrostatic, hydrogen bonding and Van der Waals forces. A flexible domain can be found in antibody, which enables the arms of the Y shape to be flexible and able to move based on the antigen's position. This domain sequence, known as hinge region, can be found between the constant regions of the heavy chains C_{H1} and C_{H2}.

Variable domains contain small number of amino acids that are able to identify antigens and interact specifically to them. Variable domains differ from antibody to another, giving the antibody its unique interacting behavior. As a result antibodies function in different types of immune responses, opposing different types of antigens.

On the other hand, the constant regions do not differ from antibody to another. Nevertheless, antibody directed to a certain antigen can be divided into 5 different classes or isotopes, IgG, IgM, IgA, IgE and IgD, based on a difference in the amino acid sequence of the constant regions of the heavy chains (effector site), which known as γ, μ, α, ξ and δ respectively. This difference enables the antibody to function in different stages of the disease (32). Figure 7 shows a typical structure of immunoglobulin (antibody) protein.
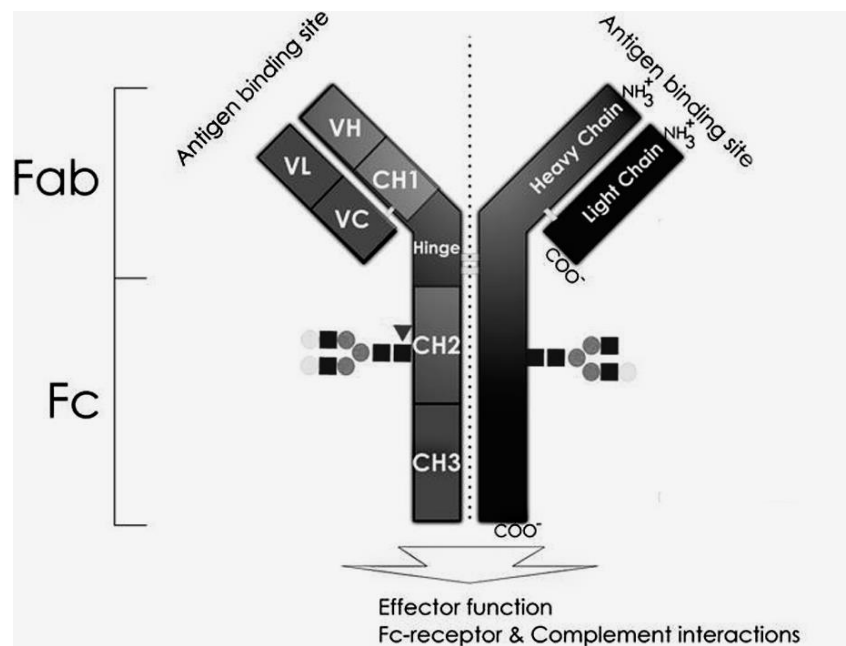
Figure 7 *Schematic structure of an IgG molecule. An IgG consists of two heavy and two light chains that contain several domains: the variable domains variable light (VL) and variable heavy (VH) that form the antigen-binding site and the constant domains CL (constant light) and CH1–3 (constant heavy) building the framework. The IgG can be furthermore divided into the Fab (fragment antigen binding) and Fc (fragment crystallizable), which induce the effector functions. Modified from Higel et al. (33)*

1.4 Antibody-antigen interaction

Antibodies are produced when the **B** lymphoid cells are stimulated by antigen; they are capable of detecting and binding a specific conformational region on the antigen (epitope or antigenic determinant). The antibody detects the epitope through some amino acid residues, mostly aromatic (tyrosine, tryptophan, and phenylalanine). The residues are contained in six loops of the amino-terminal region of the antibody (complementarity determining regions) (34). Three of these loops are from the light chain and three are from the heavy chain (the tip of the Y shaped antibody structure) (Figure 7). This high specific interaction brings the value of the antibody up in experimental biology, biomedical research, diagnostics and therapy.

When antibody and antigen are in a precise alignment to each other, the interaction of both proteins takes place and forms the immune complex.

The interaction takes place only when the concentrations of antibodies and antigens are sufficiently high to ensure the formation of immune complex, more than 50 % of antibody and antigen should be bound. The immune complex is mainly stable because of noncovalent forces; namely, hydrogen bonding, ionic (coulombic) interaction, hydrophobic interaction, Van der Waals forces, and steric repulsion forces. These forces are extremely sensitive to the distance between the interacting groups; each of these forces is not strong by itself but when they combined, a very tight interaction takes shape (35). Nevertheless the immune complex can be detached by applying a high salt concentration, detergent, or non-physiological pH.

A visible effect such as a precipitation reaction, an agglutination reaction, or a flocculation reaction can be observed as a result of the antibody-antigen interaction (Figure 8) (36). Agglutination of *Leptospira* spp. in the microscopic agglutination test (37) and precipitation of *Aspergillus* spp. antigen and serum antibody in an agar gel
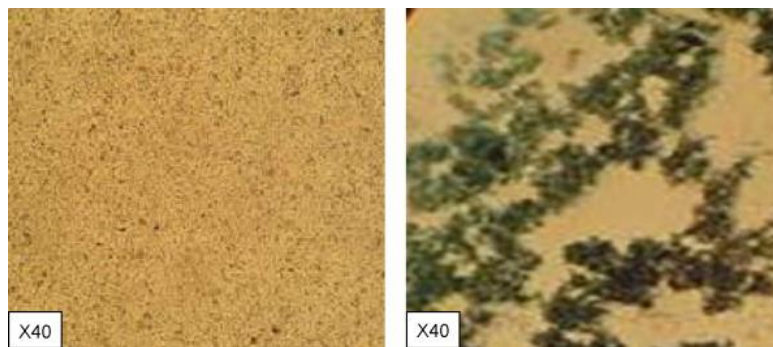
Figure 8 *Latex agglutination test; visible agglutination reaction (right) can be detected after formation of antibody-antigen complex and negative control (left) that lacks antibody-antigen complex formation.*

diffusion test (38) are two examples of visible reactions caused after an antibody-antigen interaction.

Most of immune complexes are not visible; detection of such complexes is significant in vitro analysis, thus many techniques have been developed to detect this kind of interaction. The immune complex can be detected using a colorimetric reaction (39), or an electrochemical reaction (40). Detection can be also performed in a label-free environment; for example, quartz crystal microbalance (QCM) device, and plasmon resonance (SPR) device enable the detection in real time in label free environment. (41)

Most commonly used techniques, however, are the labeled-based immunoassays, which monitor the interaction after applying a label that produce observable signal (42).

1.5 Lyme borreliosis

Lyme borreliosis is one of the most common infectious diseases in North America and Europe; it is transmitted to human by specific *Ixodes* spp. ticks. The transmission takes place during the tick feeding through injection of the tick saliva. 36 hours, as feeding period is usually needed for infection (43).

In 1982, Burgdorfer and colleagues successfully isolated and detected spirochete bacterial species from adult *Ixodes dammini*. The bacteria showed a specific binding to immunoglobulins of patients, who were convalescing from Lyme disease. The bacteria were found in the *Ixodes* midgut, which were collected in an endemic Lyme disease (Shelter Island, New York). The bacteria were named later as *Borrelia burgdorferi* and considered the cause of the Lyme borreliosis (44).

Total of 12 species belong to the genus *Borrelia burgdorferi*; at least five genospecies are pathogenic in human. *Borrelia afzelii* and *Borrelia garinii* are the main cause of the disease in Europe; *Borrelia burgdorferi sensu stricto* is a main cause of Lyme borreliosis in North America. In addition to *Borrelia spielmanii, and Borrelia bavariensis* (45).

Borrelia burgdorferi is phylum spirochetes bacteria with, helically shaped thin long cells, outer cell membrane, and flagella (46) The outer cell membrane surrounds the protoplasmic cylinder, the inner cell membrane and the peptidoglycan (47). The flagella are located in the space between the outer cell and the protoplasmic cylinder parallel to the long axis of the organism with average diameter of 18 nm. The flagella give the *Borrelia* its motility even in viscous medium (48). Structure and morphology of *Borrelia* burgdorferi can be seen in Figure 9.
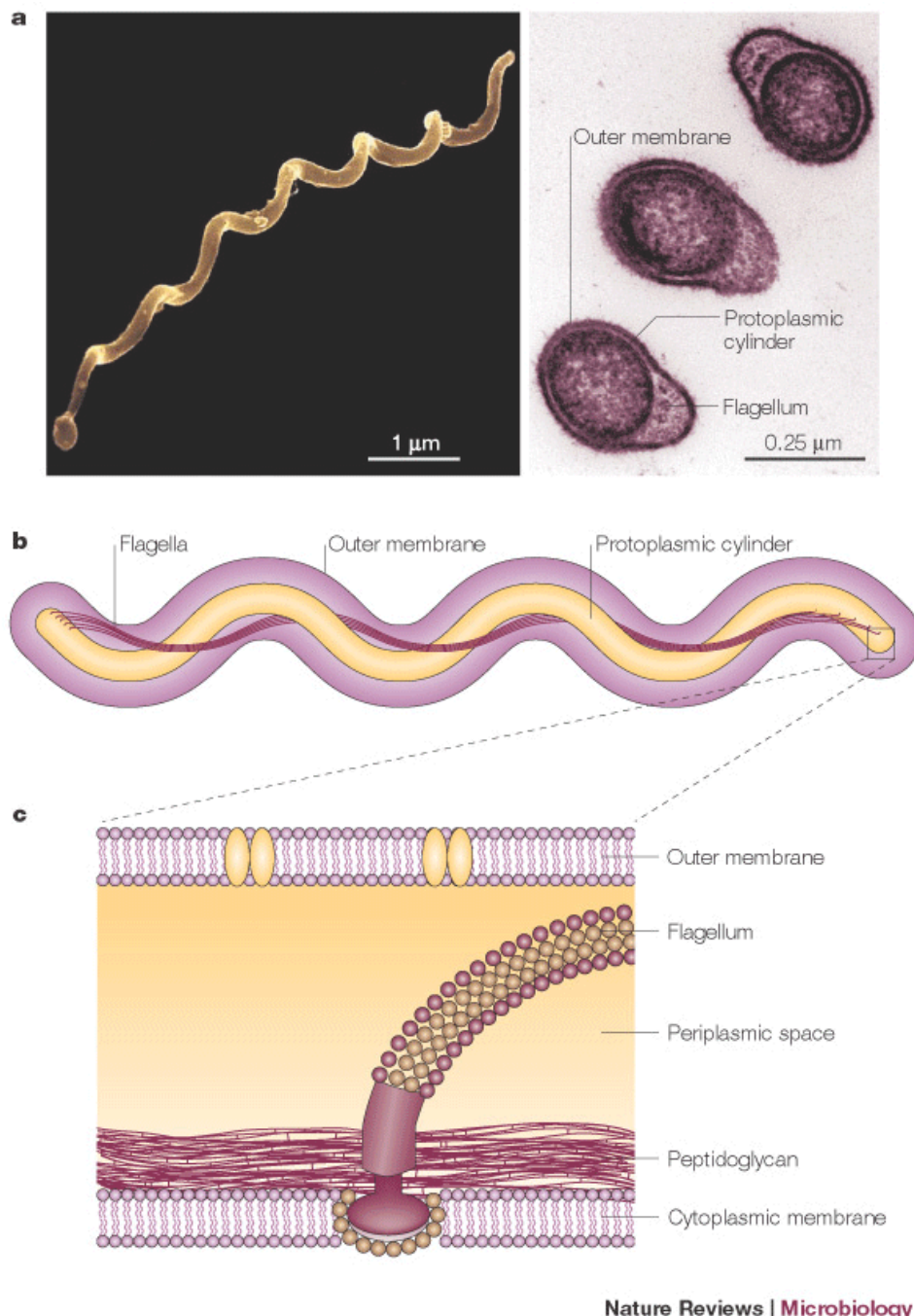
Figure 9 *Structure and morphology of Borrelia burgdorferi.* **a** *Scanning (left) and transmission (right) electron micrographs of Borrelia burgdorferi. The helical shape of Borrelia (visible in the scanning electron micrograph) is imparted by the periplasmic flagella, which can be seen in the cross-sectional view of the spirochaete in the transmission electron micrograph.* **b** | *Diagram of the spirochaete. Flagellar insertion points are located near the termini of the spirochaete. Bundles of flagella wind around the flexible, rod-shaped protoplasmic cylinder of Borrelia and overlap in the middle. The outer membrane constrains*

*the flagellar bundles within the periplasm. **c** | Detailed diagram of flagella. Each flagellum is inserted into the cytoplasmic membrane and extends through the cell wall into the periplasm. Flagella are multi-component, complex structures. Spirochaetal motility results from coordinated rotation of the flagella. Source: figures and caption was adapted from he burgeoning molecular genetics of the Lyme disease spirochaete (46).*

The life cycle of *Borrelia burgdorferi* can be concluded in four steps*: i) Borrelia occurs first in the tick vectors, ii) Borrelia is transmitted to the host, iii) Borrelia occurs in the hosts, and iv) it is transmitted to the tick* (Figure 10). More details can be found in this review (49).
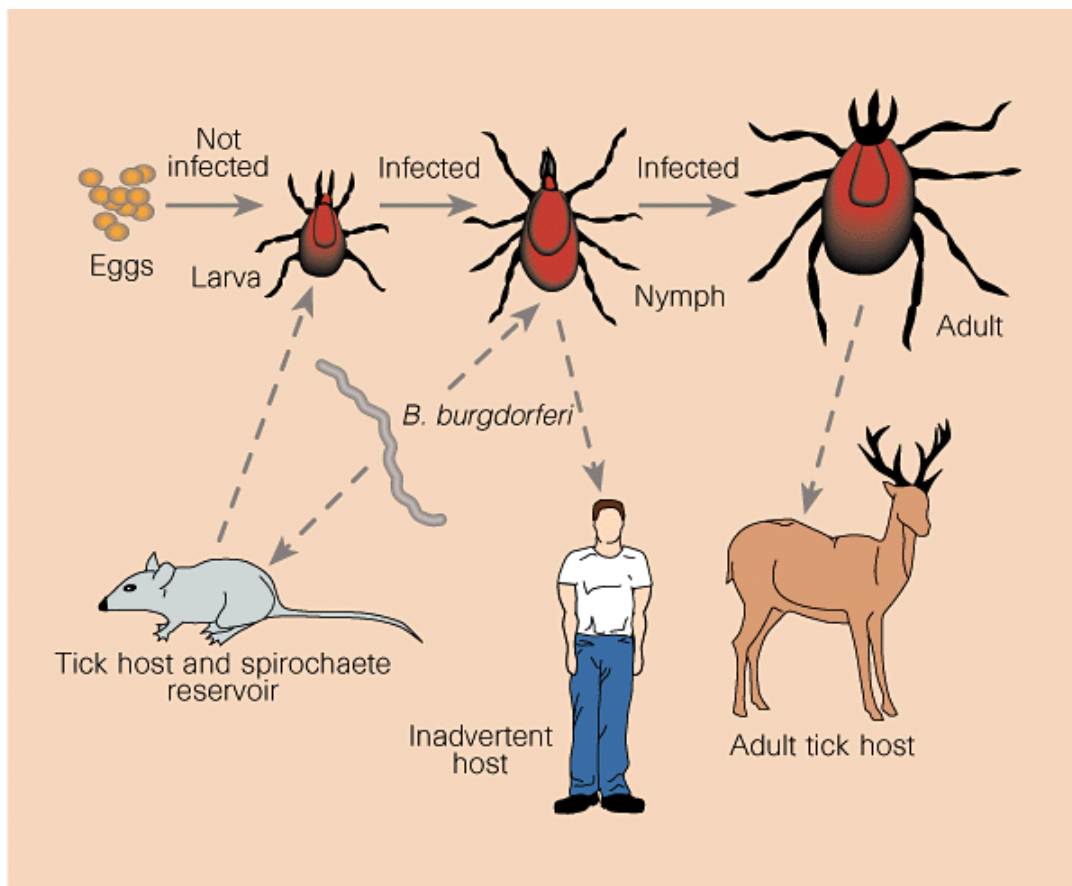
Figure 10 *Life cycle of Ixodes tick vectors of Borrelia burgdorferi. Small rodents, such as mice, are reservoirs for B. burgdorferi. The tick becomes infected from feeding on a mouse and remains infected as it changes to nymph and then adult. The spirochaetes are transmitted by infected nymphs to other mice and to humans, which are inadvertent hosts. Deer are important hosts for adult ticks, but are not effective reservoirs for B. burgdorferi (50).*

Three clinical stages could appear and may overlap at the patient of Lyme borreliosis (48): i) erythema migrans (EM), a rash increase centrifugally, appears after days to few weeks of the tick bite (51), ii) spreading of *Borrelia* into bloodstream causing clinical signs of the early dissemination; many organs may be affected at this stage including nervous system, the joints, and the heart; this stage appears after few weeks to months from infection (52), and iii) if Lyme borreliosis is not treated, the third stage that appears as chronic organ involvement occurs, persistent joint inflammation and joint swelling. In addition, direct involvement of the eye could take place at this stage (53). Additionally, other pathognomonic symptoms could express the presence of *Borrelia* infection; namely, lymphadenosis cutis benigna, meningopolyneuritis Bannwarth, and acrodermatitis chronica atrophicans. In this case a test for Lyme borreliosis detection is recommended.

1.5.1   Laboratory diagnosis of Lyme borreliosis

Laboratory diagnosis is necessary when the patient shows the typical borreliosis symptom, EM with fever following a tick bite in an endemic Lyme disease area. The diagnosis is commonly based on the direct or the indirect detection of the infecting agent; *Borrelia* detection can be performed employing four different techniques: i) the direct detection of intact *Borrelia* spirochetes using microscope based observation (54) ii) cultivating of *Borrelia* followed by microscopic detection of spirochetes (55), iii) detection of *Borrelia* specific deoxyribonucleic acid (DNA) sequence using the polymerase chain reaction (PCR) (56), and iv) the indirect detection based on measurement of *Borrelia* specific IgG or immunoglobulin M (IgM) antibodies using serological immunoassays (57). In case of Lyme borreliosis suspicion, direct microscopic detection of the spirochete *Borrelia* in clinical samples comes as a first approach; however this method is limited in laboratory diagnosis because of the limited sensitivity arose from the sparseness of organisms in clinical samples, in addition to the subjective interpretation of the microscopy results.

Alternative approach could be employed for detection is the cultivation of the causative agent followed by the microscopic monitoring of the spirochetes; a typical *Borrelia* culture is Barboure-Stoennere-Kelly (BSK) (58), a liquid medium of CMRL-1066 with bovine serum albumin fraction V, rabbit serum and N-acetylglucosamine supported with other ingredient; the cultivation takes place at 30° to 34°C for up to 12 weeks.

The presence of *Borrelia* spirochetes is then detected in culture supernatant by dark-field microscopy or by fluorescence microscopy after a staining step. Culture is a time-intensive process; patient should wait up to 12 weeks before being declared positive or negative. Other limitations should be considered in such a method; for example, culturing of samples other than skin and blood is limited due to the scarcity of organisms, the difficulty in culturing some organisms, the slow growth of other organisms and the dangerous to culture other organisms.

The small number of *Borrelia* in clinical specimen can be overcome through detection of the amplified *Borrelia* DNA in early Lyme disease in skin, cerebrospinal fluid (CSF), and synovial fluid samples using the PCR; as disadvantages, diagnosis of blood and CSF samples using PCR has shown to be uncertain for laboratory use because of the low sensitivity the test showed in this special case (usually, PCR is very sensitive). Also PCR does not differ between dead and live organisms, as well as accidental contamination with target DNA could take place in laboratory; that would lead to false positive results even after clinical treatment (59). Due to their high specificity, the three techniques are still in use. Nevertheless developing an alternative has been one main concern in clinical diagnosis; that comes on the basis of the shortcomings those conventional methods posses.

As mentioned above ligand binding assays (serological diagnosis) as an indirect detection method mainly comes in laboratory as a confirmatory test due to the high specificity and high sensitivity, as well as short time of the test. Hence, most of developed methods can been seen based on serological diagnosis.

1.5.2   Serological diagnosis of borreliosis

When a clinical diagnosis suspects a Lyme borreliosis from the symptoms, serological diagnosis comes as a confirmatory test. The test aims mainly to detect the immune response to the *Borrelia burgdorferi* antigens, particularly IgG and IgM. Serological diagnosis has been considered the only test, which has been approved by the US Food and Drug Administration (FDA) for borreliosis diagnosis.

After the vector bite, the body takes 2 to 6 weeks to produce antibodies against antigens; obtaining positive result using serological diagnosis at this stage is infrequent (less than 50 %).

This limited sensitivity in early infection can be neglected since the infection is confirmed by the clinically diagnosis after recognition of the presence of EM. After 2-6 weeks, serological diagnosis is mainly positive with one tier test; however it might yield false positive results that caused by other spirochete infections. Therefore two-tiered serological testing (60) was recommended by US Centers for Disease Control and Prevention (CDC) and European guidelines (61). Two-tiered testing starts with a sensitive enzyme immunoassay that detects IgG or IgM, followed by immunoblotting of the positive or intermediate samples acquired from the first test. The enzyme immunoassay should be at least a second-generation test, i.e. a recombinant antigen that show low cross reactivity to other non-pathogenic bacteria should be used. The two-tiered testing is recommended also in particular when the patients are not presenting with EM or the infection took place in area where Lyme borreliosis is not an endemic disease. An alternative to the two-tiered testing, a specific and accurate one-tier testing could be acquired when a highly specific recombinant antigen or synthetic peptide would be utilized. The used antigen should cover the wide antigenic variety of several relevant *Borrelia* subspecies; simultaneously, it should avoid the cross reaction with the other non-pathogenic *Borrelia* strains and other cross-reactive agents. In addition, the antigen should have a measurable immune response from the infected host in all phases of infection and should distinguish between fresh, past or healed infection. In the presented work recombinant antigens have been used to develop a specific one-tiered testing, which can be used as an alternative for the time consuming two-tiered testing.

1.6   Antigens immobilization and carriers

One main step when developing a new immunoassay is to immobilize antigen on the support or carrier surface through a gentle and straightforward coupling procedure. Developed immobilization methods have aimed at preserve the structure and function of the biomolecules under reaction conditions; also the method should enable a high storage stability of the antigen. Immobilization techniques can be generally classified into physical, covalent, entrapment, crosslinking, and affinity immobilization (62).

Physical and ionic adsorption of proteins is one approach, which utilizes some weak binding forces, e.g. hydrogen bonds, Van der Waals forces, multiple salt linkages, hydrophobic and electrostatic interactions. The non-specifically adsorbed proteins can be removed by washing afterwards.

Introduction

This method is considered easy and fast, however, the adsorbed proteins could be detached due to a change in pH, temperature or ionic strength, affecting the performance of the assay (63). Entrapment of proteins in matrices is another approach that has been also developed for protein immobilization. It considers the caging of the proteins within a matrix such as gels, polymers, pastes, or inks via covalent or non-covalent bonds. The biomolecules and the matrix are well mixed and applied simply on the carrier surface. We can find also the crosslinking technique, where the proteins are to be attached to the carrier via bi or multifunctional reagents, e.g. glutaraldehyde, bis(diazo)benzidine, tannic acid, or dimethyl adipimidate (64).The most used immobilization technique depends mainly on covalent bonding. The bond is created through the reaction of reactive groups at the protein surface, such as the N-terminus lysine amino groups, hydroxyl, sulfhydryl, or phenolic functional groups with corresponding functional groups at the surface of the solid support, carrier (65).

In the present work, two platforms were served as carriers, 3-dimensional polyethylene sinter bodies and gold nanoparticles (AuNPs). Polyethylene evolved into a very good candidate as a carrier in biotechnology applications, including biosensors and bioassays. This arises as a result of its low cost, low energy requirements for processing and its high chemical stability. Besides, polyethylene posses a highly optical transparency to the detection wavelength in light intensity measurement based devices. Polyethylene can be produced by the polymerization of ethene; the polymer surface is naturally inert and highly hydrophobic (66). Physical and chemical properties of polyethylene, however, could be controlled during production process. This would provide variety of characteristics for the polymer, which can be employed in various applications. Numerous techniques were developed to manipulate the polyethylene with the desired characteristics during synthesis; for example living or controlled alkene polymerization (67), implementation of chain transfer reactions and controlled copolymerization of alkene with functional monomer (68).

Yet, activation and surface modification of the polyethylene low surface energy should be performed, boosting the polyethylene adhesion, biocompatibility and hydrophilic properties without any effect on its bulk properties. Consequently, a proper surface for biomolecules immobilization is provided. Introducing functional groups on the surface of the cheap commodity polyethylene has been studied using several techniques. Namely, inducing copper (II) ion adsorptivity on polyethylene surface via γ-ray irradiation(69), generating peroxides on the surface via ozonation (70), introducing bioactive compounds via ultraviolet light (UV) light (71) and oxidation of polyethylene surface using wet chemistry(72).

Introduction

Surface modification based on polymerization of monomeric blocs has been also successfully carried out via plasma (73), γ-ray irradiation (74) and UV irradiation.

Photografting of monomers, mostly polar, using UV light is one of the most convenient methods to activate chemical bonds and to introduce functional groups on the polyethylene surface. The versatility application of the process is a consequence of the low cost and the easy in controlling the grafting process with high density of monomer molecules on the surface; this yield on a high and long-term chemical stability of the grafted layer. Likewise, UV radiation has a neglected effect on the bulk properties of the polymer and the substrate. UV light in its full range of wavelength is generally used to achieve the grafting process; nevertheless, it was elucidated that below 300 nm the UV light enhance the initiation of graft polymerization (75).

Photografting can be carried out either in one-step or two-step process. In one-step process, the polymer is dipped in a solution that contains both the monomer and the photoinitiator, and then it is exposed to the UV radiation, initiating the grafting process (76). While in the two-step process, a solution of photoinitiator is added to the polymer and irradiated; following, a second step takes place; a solution of the monomer is introduced to the polymer, which in turn will be grafted on the polymer surface during irradiation (77). Although the overall result of the two processes is similar. The one step process is favorable in industrial perspective due to the short time and the easy of performing, while the two-step process is preferred in scientific research since the grafting process including the density of grafting layer can be controlled.

The photografting process starts with absorbing the UV light by the photoinitiator; the excitation of molecules to a short-lived singlet state takes place and then relaxes to more stable triplet state (intersystem crossing) forming bi-radicals; then the bi-radicals abstracts hydrogen from the polymer surface leaving the polymer as a macro-radical. The monomer could be, eventually, abstracted by the polymer surface forming a new layer of the polymerized monomer. In two-step photografting process the photoinitiator first reacts with the surface of the polymer surface through radical reaction then it is replaced by the monomer afterwards in the second step. A schematic illustration of one-step grafting process can be seen in Figure 11.

Initiation step
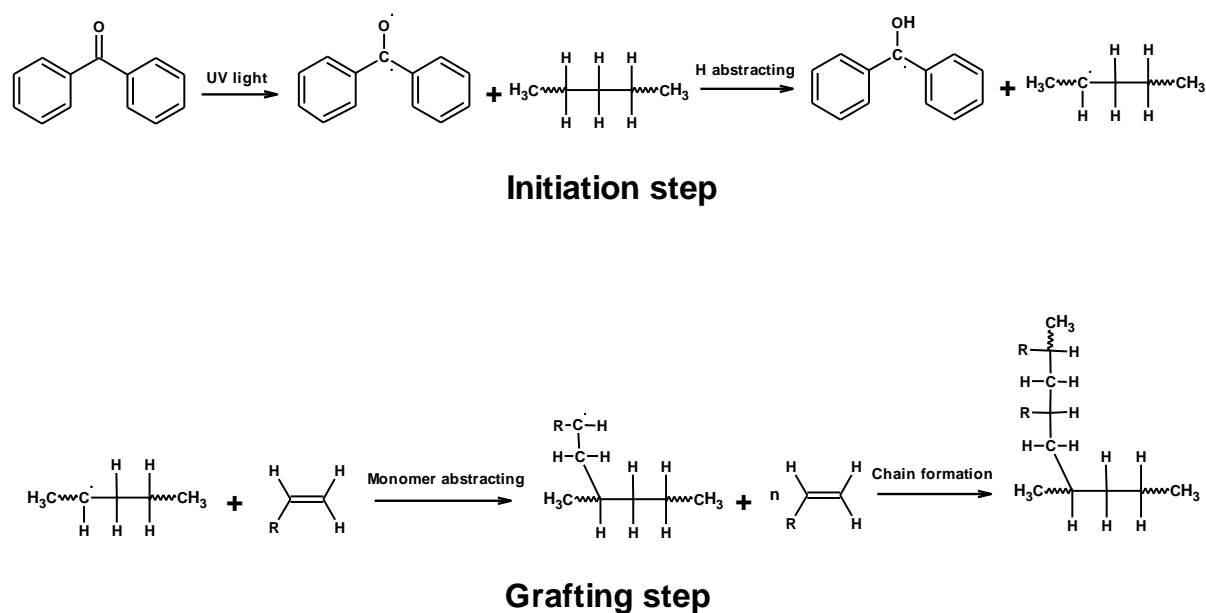
Grafting step

Figure 11 *Schematic illustration of one-step UV photografting process. Benzophenone act as photoinitiator; it absorbs UV light, turning into radical. The radical abstracts hydrogen atom from the polymer surface, exposing active carbon. The active carbon can abstract the monomer subsequently, forming a layer of polymerized monomer.*

AuNPs as a second platform served as proteins carrier, assisting in developing a new rapid serological test. According to the American Society for Testing and Materials (ASTM), terminology for nanotechnology ASTM international 2006, nanoparticles can be defined as any particles that are synthesized under controlled size and shape with average length of 1 to 100 nm in two or three dimensions. Nanoparticles possess some unique chemical, optical and electrical properties when compared to its relative bulk materials. Among them is the high surface-to-volume ratio, which permits the functionalization of nanoparticles with biological active components, such as peptides, proteins and DNA. This phenomenon facilitates nanoparticles to be utilized in development of many biological applications, such as drug delivery (78), imaging (79), development of biosensing applications (80), and improving the chromatographic separation of protein (81). Nanoparticles based on noble metal such as gold possess a unique property that distinguishes themselves from other nanoparticles, semiconductor quantum dots, magnetic nanoparticles and polymeric nanoparticles. AuNPs is characterized by its SPR; a phenomenon takes place at the nano-scale level of gold particles.

Conduction electrons are triggered to collectively oscillate with a resonant frequency when certain wavelengths of electromagnetic radiation interact with its surface (Figure 12). This phenomenon is responsible for the strong absorption and scattering of visible light that incident to the nanoparticles, giving the nanoparticles its intense color (82). The change in size and shape of nanoparticles resulted in change in the SPR; this explains the ability of AuNPs to possess a diversity of light scattering
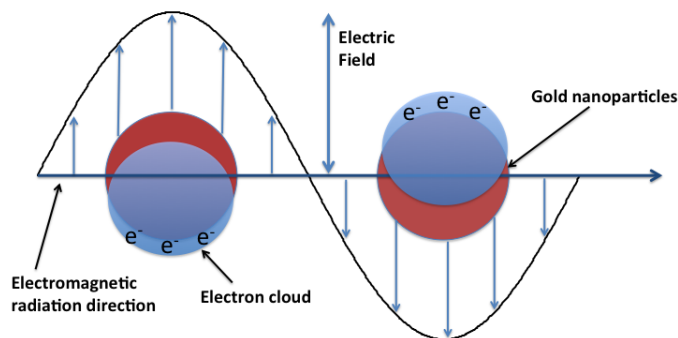
Figure 12 *Schematic illustration of AuNPs surface plasmon resonance. Collective oscillation of conduction electrons takes place after interaction with the light radiation, resulting in extinction of light (absorption and scattering).*

and absorbance. As a consequence color of gold nanoparticles can be diverse from red to blue. Distance between gold nanoparticles in suspension showed to have a very crucial impact on AuNPs color. Decreasing this distance cause a change in SPR, which appear as a shift in maximum absorbance of nanoparticles to higher wavelengths. This phenomenon enabled AuNPs to be serving as intense label in immunoassay, biochemical sensors, and surface-enhanced spectroscopies. This type of colorimetric biosensing methods caught the attention because they are simple and promising for point-of-care testing. Mirkin and coworkers developed the first established assay based on aggregation of AuNPs for DNA detection in 1996 (83). This phenomenon has been exploited since then in different applications; namely, detection of thiocyanate (84), detection of cancer cells (85), and detection of heavy metals (86).

When nanoparticles based on noble metal (such as gold) being synthesized, a reducing agent and a capping agent are necessary to complete the synthesis process; the reducing agent reduce the metal ions to form the inorganic core of the particles while the capping agent is responsible for stabilizing the core from aggregation through electrostatic repulsion between nanoparticles. Many approaches have been developed for AuNPs synthesis in order to improve their stability, biocompatibility, and aqueous dispersion. AuNPs can be synthesized in different shapes and sizes with diameter ranging from 3 to 200 nm. The most widely used method based on the reduction of gold hydrochlorate solution by citrate ions; a method

developed by Turkevich in 1951 (87) and latter optimized by Frens in 1972 (88). In this method citrate acts as both a reducing agent and capping agent. The method allows synthesis of spherical AuNPs in aqueous solution in the range from 10 to 25 nm smaller particles are hard to obtain and bigger particles were clumped. However, other established approaches showed the potential to obtain bigger sizes of AuNPs using Turkevich method with some modifications.

Brust and Schiffrin (89) reported another widely used method in 1994 that have the advantage of synthesizing small AuNPs in organic solution with 1- 3 nm. The method based on using two-phase (water-toluene) reduction of gold hydrochlorate by sodium borohydride in the presence of an alkanethiol; this results in the direct synthesis of surface-functionalized AuNPs.

Many other methods have been developed to improve the synthesis of AuNPs including, using plant extracts to reduce gold salt and colloidal gold fabrication in what so called 'green synthesis' (90), using chemical radiation such as UV and Y-ray for reduction of gold ions in presence of surfactants (91), and reduction of gold salt in presence of polymers which acts as a surface coating for the AuNPs that can improve the long-term stability, enhancing hydrophobicity, and improving biocompatibility (92).

Compatible AuNPs surface should be obtained for bio-conjugation purposes. Using Turkevich method, synthesized AuNPs possess a high affinity to be modified with biomolecules; this comes as a result of the negative charge on the surface (which assumed is arising from adsorbed $[AuCl_2]^-$ ions) (93). Also, the biomolecules can be easily attached via hydrophobic interaction or via linkers. The attachment can be conducted based on self-assembling of bi-functional ligand via electronic attraction of positively charged sites on biomolecules and negatively charged AuNPs, adsorption through the hydrophobic sites on protein binding to the metal surface, or covalent binding of gold to a chemical group (dative bonding); the latter ensures the constant binding of protein to the nanoparticle surface and ensures the avoidance of possible denaturing of protein. This straightforward functionalization of AuNPs supports AuNPs to be used in broad applications; for example, in diagnostics as labels, in microscopy as probes, in biosensors as a platform, and in drug delivery as carrier. A widely used method for AuNPs functionalization is to fabricate AuNPs with monolayer-protected clusters (MPCs) during synthesis; alkanethiolate (C_3-C_{24}) is used for AuNPs functionalization using Schriffin method (94); subsequently, ligand exchange techniques can be used to transfer the AuNPs from organic to aqueous solution; this

techniques based on exchange the alkanethilate MPCs with water-thiol-acid molecules. Finally, the attachment of the biomolecules could be easily acquired (95).

In general, the minimum amount of biomolecule needed to prevent AuNPs aggregation is added plus 10-20 % excess for the functionalization process. In addition, a blocking agent, such as polyethylene glycol, bovine serum albumin, and solution of dried milk, is added to completely coat the remaining free sites on the gold surface; this helps in reduce the nonspecific interactions during assay performance as well as assist in stabilizing AuNPs colloid.

2   Aims and objectives

In laboratory diagnosis, detection of anti-*Borrelia* antibodies in sera sample mainly comes as a confirmation test for Lyme borreliosis diagnosis. This is as mentioned due to the high specificity and high sensitivity of the test as well as its short time. Many assays have been developed for serological diagnosis of borreliosis.

Three major techniques were used for the detection: i) immunofluorescent antibody staining (IFA) (96), ii) enzyme-linked immunosorbent assays (ELISA) (97) and iii) western immunoblot tests (98). However, most of these assays are time-consuming and some are labor-intensive; also ELISA utilizing whole *Borrlia burgdorferi* as the antigen structure yields some false-positive reactions. Thomas B. Ledue developed a fully automated random-access analyzer, which employs two-step chemiluminescence immunoassay technology for Lyme borreliosis diagnosis (99). The system is promising, sensitive, selective, and can be used as alternative to conventional immunoassays based on using enzyme for detection. Yet, the test could not be considered for point of care testing, where some significant factors should be respected such as well-trained personnel able to perform the test and interpret the results (100).

Therefore, the aim of this work was to develop new immunoassay platforms for rapid and sensitive serological diagnosis of borreliosis. Main goal of the work was to develop a point of care test; in addition, the platforms should be transferred to further immunoassays.

The work aimed also to test two antigens, a recombinant VlsE antigen and the 26-mer peptide from the VlsE antigen sixth invariable, C6, region, in the proposed platforms. Both antigens induce a strong antibody response that can be detected from early to late phase during the disease in humans infected with *Borrelia burgdorferi* or with European genospecies including *Borrelia afzelli* and *Borrelia garlnii.* Simultaneous they showed low cross-reaction with other non-pathogenic *Borrelia* strains.

The objective of the present work was to employ two novel platforms, i) 3-dimensional porous polyethylene sinter bodies (3-DPESB) and ii) two-antigen modified gold nanoparticles, in a simple and rapid immunoassay for the detection of antibodies directed to infectious diseases.

Based on the desired objectives, the study included:

1- Utilizing ABICAP^{TM} technology along with a small 3-DPESB (2×2.5 mm) to develop a point of care test.

2- Surface activation of the 3-DPESB for antigens immobilization.

3- The intention to combine the high specificity of a recombinant fusion protein and a modified 3-DPESB to conduct a rapid and easy serological test. The work aimed to modify the 3-DPESB with a polysaccharides mannan, which allows fixation of genetically designed fusion protein, C6 region of VlsE, fused with Concanavalin A, by self-organization. Therefore, choosing of a convenient technique to immobilize mannan on the surface was of a main interested in the work. Final step was to investigate the proposed platform in the detection of anti-*Borrelia* antibodies in human sera samples; detection should be conducted colorimetrically in an ELISA-like manner using HRP labeled secondary antibody.

4- The direct immobilization of VlsE antigen on the 3-DPESB. Hydrophobic and covalent immobilization techniques were proposed to achieve the fixation of antigen on the surface, which would be used further in testing human sera samples in an ELISA-like manner. Moreover, we aimed to examine different labels, HRP labeled antibody, AuNPs modified with protein A, as well as Sudan IV nanoparticles modified with HRP enzyme, to improve the sensitivity of the platform.

5- Investigating the potential to use two-antigen modified gold nanoparticle to obtain a rapid one-step serologic test. Work aimed to synthesize different sizes of spherical AuNPs followed by its functionalization with two antigens, Protein A and VlsE *Borrelia* antigen. Finally, verifying the feasibility of modified AuNPs in detection of antibodies in human sera samples should be performed.

3 Experimental:

3.1 Chemicals:

If not otherwise mentioned, chemicals were obtained from Fluka, Sigma-Aldrich or Merck, Germany, in analytical quality. Benzophenone and 4-dimethylaminopyridine were obtained from Merck-Schuchardt, Germany. N,N´-disuccinimidyl carbonate $\geq$ 95% (NMR), sodium acetate anhydrous, anti-human IgG (γ-chain specific)-biotin antibody, mannan from *Saccharomyces cerevisiae* and (3-aminopropyl) triethoxysilane 99%, 11-mercaptoundecanoic acid 95%, nitric acid 65%, and N- (3-dimethylaminopropyl)-N`-ethylcarbodiimide hydrochloride (EDC) were from Sigma-Aldrich, Steinheim, Germany. Allyl alcohol 99.5% (GC), ethanolamine 99%, and manganese chloride tetrahydrate 99 % were from Fluka, Germany. Acetone 99.5%, hydrochloric acid S.G. 1.16 (32%), and methanol were from scientific, UK. Ethanol, di-potassium hydrogen phosphate, sodium dihydrogen phosphate, sodium carbonate, N-hydroxysuccinimide (NHS),   sodium dihydrogen phosphate dihydrate, di-sodium hydrogen phosphate dihydrate, and sodium hydrogen carbonate were from Merck, Darmstadt, Germany. Sodium chloride 99.8%, boric acid 99.8%, 4-(2-hydroxyethyl)-1-piperazineethanesulfonic acid (HEPES), PUFFERAN® $\geq$ 99.5%, magnesium chloride 98.5% water free, calcium chloride 94%, Coomassie -solution Roti1-Quant, 5 x concentrate, and acetic acid glacial 100%, bovine serum albumin (BSA), albumin fraction V, biotin free $\geq$ 98% for molecular biology were from Carl Roth, Karlsruhe, Germany. Sodium hydroxide 99% was from Grüssing, Filsum, Germany.

Anti-human IgG-HRP and 3,3',5,5'-tetramethylbenzidine (TMB/substrate solution) were from Seramun Diagnostica, Heidesee, Germany. ABICAP^{TM} column, ABICAP^{TM} sinter bodies, size of 2×2.5 mm and pores 100 μm wide, were from Senova Gesellschaft für Biowissenschaft und Technik mbH, Germany.

Blocking solution based on chemically modified and fragmented highly purified casein was purchased from Candor, Wangen, Germany. 5.5% casein buffer concentrate (CBC) and conjugate buffer [antibody/antigen (poly HRP) conjugate stabilizer (AA1)) were from Stereospecific Detection Technologies, Baesweiler, Germany.

Nanoparticles based on bovine serum albumin (BSA) and Sudan IV, which are conjugated with streptavidin and horseradish peroxidase (HRP), particle size: 541 nm, was supplied by research center of medical technology and biotechnology (fzmb), Bad Langensalza, Germany.

Experimental

Gold (III) chloride hydrate 99.999% trace metals basis, trisodium citrate dehydrate, and silver enhance kit (silver enhancer solution A and solution B) were from Sigma-Aldrich, Schnelldorf, Germany. Servapor dialysis tubing, MWCO 12000 – 14000, diameter 21 mm and pore diameter 25 Å was from SERVA electrophoresis GmbH, Heidelberg, Germany.

3.2   Buffers and solutions

- Carbonate-bicarbonate buffer (CBB) pH 9.6

    160 ml 100 mM sodium carbonate (Na_2CO_3) (MW 105.99 g/mol)

    +   340 ml 100 mM sodium hydrogen carbonate ($NaHCO_3$) (MW 84.01 g/mol)

- Phosphate buffered saline (PBS) pH 7.4

    10.4 mM di–potassium hydrogen phosphate (K_2HPO_4) (MW 174.18 g/mol)

    1.8 mM sodium di-hydrogen phosphate monohydrate ($Na_2HPO_4.H_2O$) (MW 137.99 g/mol)

    150 mM sodium chloride (NaCl) (MW 58.44 g/mol)

    pH adjusted with HCl or NaOH

- Acetate buffer pH 4.8

    200 ml 100 mM acetic acid (CH_3COOH) (MW 60.05 g/mol)

    +   300 ml 100 mM sodium acetate (CH_3COONa) (MW 82.03 g/mol)

- Borate buffer pH 7.4

    100 mM boric acid (H_3BO_3) (MW 61.83 g/mol)

    200 mM sodium hydroxide (NaOH) (MW 39.997)

    pH adjusted by adding NaOH to boric acid solution

- Borate buffer pH 9

    10 mM boric acid (H_3BO_3) (MW 61.83 g/mol)

    200 mM sodium hydroxide (NaOH) (MW 39.997)

    pH adjusted by adding NaOH to boric acid solution

- HEPES buffer pH 7.4

    10 mM 4-(2-hydroxyethyl)-1-piperazineethanesulfonic acid (MW 238.31 g/mol)

    1 mM calcium chloride ($CaCl_2$) (MW 110.99 g/mol)

    1 mM manganese chloride tetrahydrate ($Cl_2Mn.4H_2O$) (MW 197.91 g/mol)

    1 mM magnesium chloride ($MgCl_2$) (MW 95.22 g/mol)

    pH adjusted by NaOH or HCl

- MES buffer pH 5.5

    100 mM 2-(N-morpholino)ethanesulfonic acid ($C_6H_{13}NO_4S.H_2O$) (MW 213.25 g/mol)

    pH adjusted with NaOH

- Phosphate buffer pH 7.4

    50 mM sodium dihydrogen phosphate dihydrate (NaH_2PO_4)$\cdot 2H_2O$ (MW 156.007 g/mol)

    50 mM di-sodium hydrogen phosphate dihydrate (Na_2HPO_4)$\cdot 2H_2O$ (MW 177.98 g/mol)

    pH adjusted with mixing two stock solutions

- Washing solution: 10 mM PBS pH 7.4 + 0.1% BSA + 0.05% tween20

- Antibody dissolving solution: CBC buffer diluted 4 times with PBS buffer.

- Coomassie –solution diluted 5 times with water

- Blocking solution (1): PBS pH 7.4 + 0.2% BSA

- Blocking solution (2): chemically modified and fragmented highly purified casein

- Drying buffer: PBS pH 7.4 + 1% BSA + 5% sucrose

- Discoloration solution: 181 mL water + 19 mL glacial acetic acid + 50 mL methanol

3.3 Antigens

VlsE *Borrelia* antigen was supplied by Seramun Diagnostica, Heidesee, Germany. Full-length 56 kDa VlsE *Borrelia* recombinant antigen was supplied in PBS (0.15 M NaCl), pH 7.2 - 7.4, *Borrelia afzelii*. Protein was expressed in *E.coli* with Glutathione-S-Transferase and purified with affinity chromatographic techniques. Purity is > 90% as detected by SDS-PAGE.

Concanavalin A-C6 fusion protein was produced in our group. Following is a brief description of its production: the genes of Concanavalin A and C6 (VlsE epitope of *Borrelia*) were fused together into the expression vector pET15b according to the procedure described in previously published article (101). *E. coli* BL21 DE3 cells were transformed with the genetic material and protein expression was performed under 37° C for 4 h after IPTG induction at an optical density of 0,6 at 600 nm. The cells were harvested and the fusion protein was derived from the cells via inclusion body purification. After purification, the inclusion bodies were dissolved in a buffer containing 6 M guanidiniumhydrochloride, 500 mM sodiumchloride, 10% (v/v) glycerol in 50 mM PBS buffer at pH 7.5. The protein solution was stored at -20 °C till further use.

Protein A-soluble extracellular from *Staphylococcus aureus* capable of binding to the Fc portion of immunoglobulins was from Sigma-Aldrich, Schnelldorf, Germany.

Experimental

3.4   Sera samples

Sera samples were provided by Seramun Diagnostica, Heidesee, Germany. Samples were tested by Seramun Luminescence immunoassay LIA-006 for IgG, positive human-sera anti-VlsE (IgG), derived from patients with assumed Lyme borreliosis, negative human-sera are from normal blood donors. Positive and negative samples are listed in Table 1.

Positive sera samples	Negative sera samples
CL-007	CL-457
CL-029	CL-360
CL-040	CL-421
CL-068	CL-550
CL-144	CL-551
CL-146	SB-2207
CL-149	SB-2013
CL-154	SB-2019
CL-156	SB-2022
CL-235	SB-2039
CL-264	SB-2028
CL-268	SB-2030
CL-271	SB-2023
CL-272	SB-2040
CL-274	SB-2035
CL-053	SB-1974
Hd3	SB-1976
	SB-1982
	SB-1983

Table 1 *List of positive and negative sera samples used in assays development.*

3.5 Instruments

Instruments that have been used in the work are listed in Table 2.

Instrument	Manufacturer
Bruker ALPHA FTIR spectrometer with ATR-measuring unit	Bruker, Germany
JEOL JSM-7500F field emission scanning electron microscope	JEOL Ltd. Tokyo, Japan
Atomic force microscopy JPK Nano Wizard	JPK Instruments, Berlin, Germany
Atomic force microscopy cantilevers (NSC16/ Si_3N_4/AlBS)	Micromasch, Estonia
ABICAP^{TM}-photometer with read out at 650 nm and 520 nm	Senova Gesellschaft für Biowissenschaft und Technik mbH, Germany
pH meter Lab 850	Schott instruments, Germany
Heraeus Pico 17 centrifuge	Thermo Scientific, Thermo Elektro LED GmbH, Osterode, Germany
Heraeus UV lamp	Original Hanau, Hanau, Germany
Diaphragm vacuum pump	Vacuubrand, Wetheim, Germany
Shimadzu UV-2401 spectrometer	Shimadzu Suzhou Instruments, Suzhou, Jiangsu, China
Jenway Genova plus life science spectrophotometer fitted with micro-cuvette holder	Bibby Scientific, UK
Vortex Yellow Line TTS2	IKA, Wilmington, USA
Plasmonic SPR device	Plasmonic Biosensor AG, Wallenfels, Germany

Table 2 *List of used instruments in the presented work.*

4   Methods

4.1   UV irradiation of 3-dimensional polyethylene sinter bodies (3-DPESB)

Polyethylene sinter bodies have been activated using UV irradiation. The activated sinter bodies could be further used for covalent immobilization of biomolecules. Activation was established based on photografting of 2-propenol; 2-propenol in turn would form polyalcohol groups on the surface, exposing active hydroxyl groups. 3-dimensional polyethylene sinter bodies (3-DPESB) with dimensions of 2×2.5 mm were used in all steps. The presented method was used for the functionalization of 13 sinter bodies jointly as follow: firstly, the 3-DPESB were washed with 96% ethanol for 10 min under reduced pressure to remove any impurities. Then, 3-DPESB were incubated in a reaction mixture of 2 ml methanol containing 3% (w/v) of benzophenone and 0.5 ml of 2-propenol. The solution was placed with stirring for 6 h in front of a 400 Watt UV lamp that emits UV light at 254 nm. Irradiation of the samples was carried out at room temperature. After UV irradiation, the 3-DPESB were washed 3 times with methanol followed by washing 3 times with double distilled water each for 5 min under reduced pressure while stirring. Finally the sinter bodies were dried at 40° C for 2 h. During UV irradiation, partially evaporation of methanol was observed, which was compensated by addition of 0.5 mL methanol after 3 h.

4.2   Characterization of the UV treated 3-DPESB

Surface characterization of the UV treated 3-DPESB was performed using Fourier transform infrared spectroscopy (FTIR), scanning electron microscopy (SEM) and atomic force microscopy (AFM). FTIR spectra (Bruker ALPHA FTIR spectrometer with ATR-measuring unit) were collected in the $375 - 4000$ cm^{-1} region with a resolution of 4 cm^{-1}. Typically 24 scans were collected to obtain sufficient signal to noise ratio. Microscopic visualization of the surface was carried out using a JEOL JSM-7500F field emission scanning electron microscope (SEM) at an accelerating voltage of 5 kV. AFM measurement of the polyethylene surface was performed using the JPK Nano Wizard. AFM cantilevers (NSC16/ Si$_3$N$_4$/AlBS) with ultra-sharp tips and a length of about 230 mm were used. The resonance frequency was 170 kHz and the nominal force constant was 45 N/m. The measurements were done in intermittent contact mode under dry conditions.
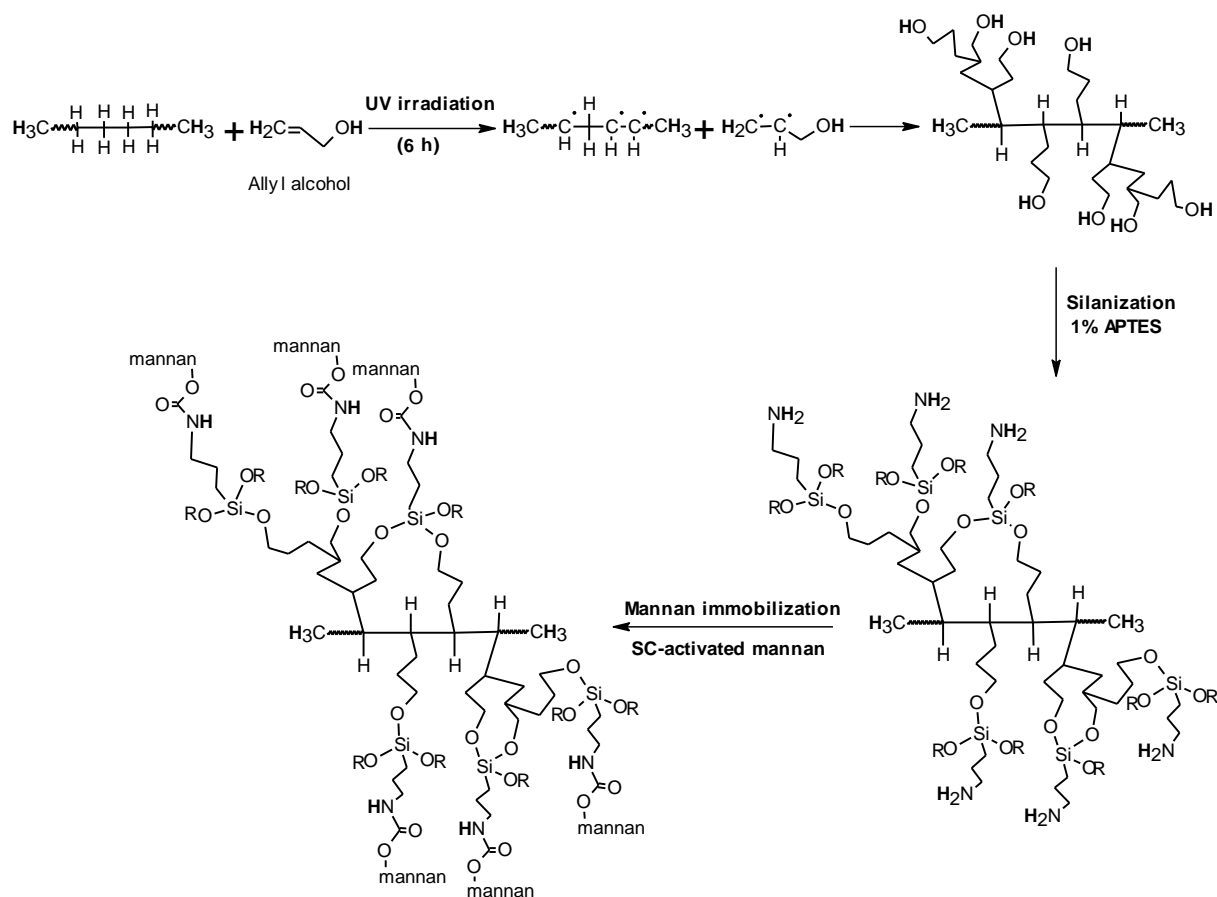
4.3 Covalent immobilization of mannan on the UV treated 3-DPESB

Firstly, the formed polyalcohol-layer was stabilized by a silane layer. 3-DPESB were incubated in 1% (v/v) APTES in 2 mL dry acetone for 10 min under reduced pressure while stirring. The 3-DPESB were then dried at 40° C for 2 h and stored in a desiccator before further use.

To allow a smooth immobilization of the mannan, mannan hydroxyl groups were activated firstly following a slightly modified protocol from Miron and Wilchek, which was deduced from the Zalipsky method (102). In brief, 30 mg of mannan was dissolved in 3.5 mL of dry dioxane. The solution was carefully heated in a water bath until complete dissolution of the mannan. Then, 6 mM of DSC solved in 1 mL dry acetone was added to the mannan solution and finally 6 mM of 4-dimethylaminopyridine in 1 mL of dry acetone was added in aliquots during 1 h. The solution was stirred for 6 h at room temperature. Precipitate of succinimidyl carbonate (SC)-mannan was obtained by addition of 2 volumes of diethyl ether and the precipitate was re-dissolved in dry acetone.

This step was repeated two times more (last step without dissolution in acetone). The resulting solid product was dried under reduced pressure and stored in the refrigerator until used. The 3-DPESB with the freshly prepared silane layer were incubated with the SC-mannan in 0.1 M MES buffer pH 5.5 while stirring overnight at 4° C; this results in covalent binding of mannan to the surface (Scheme 1). For each 3-DPESB, 0.75 mg mannan was used for immobilization. Afterwards, the 3-DPESB were incubated for 1 h with 80 mM ethanolamine in 2 mL MES buffer to passivate all active ester groups followed by blocking further unspecific binding sites using 2 mL of the casein based blocking solution 2 for 2 h. Finally, the 3-DPESB were dried under reduced pressure for 2 h and stored in a desiccator before further use.

Scheme 1 *Surface functionalization of polyethylene using UV light followed by APTES coating and mannan immobilization.*

4.4   Covalent immobilization of VlsE antigen on the UV treated 3-DPESB

For covalent immobilization of VlsE antigen on UV treated 3-DPESB, primary activation of hydroxyl groups on 3-DPESB surface was carried out following Miron and Wilchek's protocol (102). Activation was accomplished after incubating the 3-DPESB in a solution of 1.5 mL of dry dioxane, 0.5 ml 6 mM of N, N´-disuccinimidyl carbonate solved in dry acetone and 0.5 ml 6 mM of 4-(dimethylamino) pyridine in dry acetone; the latter was added in aliquots during 1 h. The solution was gently stirred for 6 h at room temperature. The 3-DPESB were then dried under reduced pressure. 3-DPESB were finally incubated overnight at 4 °C with VlsE antigen (0.5 µg for each sinter body) in MES buffer pH 5.5 (Scheme 2).

Methods

Active carbamate groups were passivated using ethanolamine. 3-DPESB were incubated with 40 mM ethanolamine in 2 mL MES buffer pH 5.5 for 35 minutes. Next, 3-DPESB were washed two times 5 minutes each with MES buffer, and finally, the free unspecific binding sites were blocked after 75 min incubation in 2 ml PBS buffer pH 7.4 containing 0.5% BSA and 5% sucrose. The functionalized 3-DPESB were dried under reduced pressure and stored at 4 °C until used for further experiments.
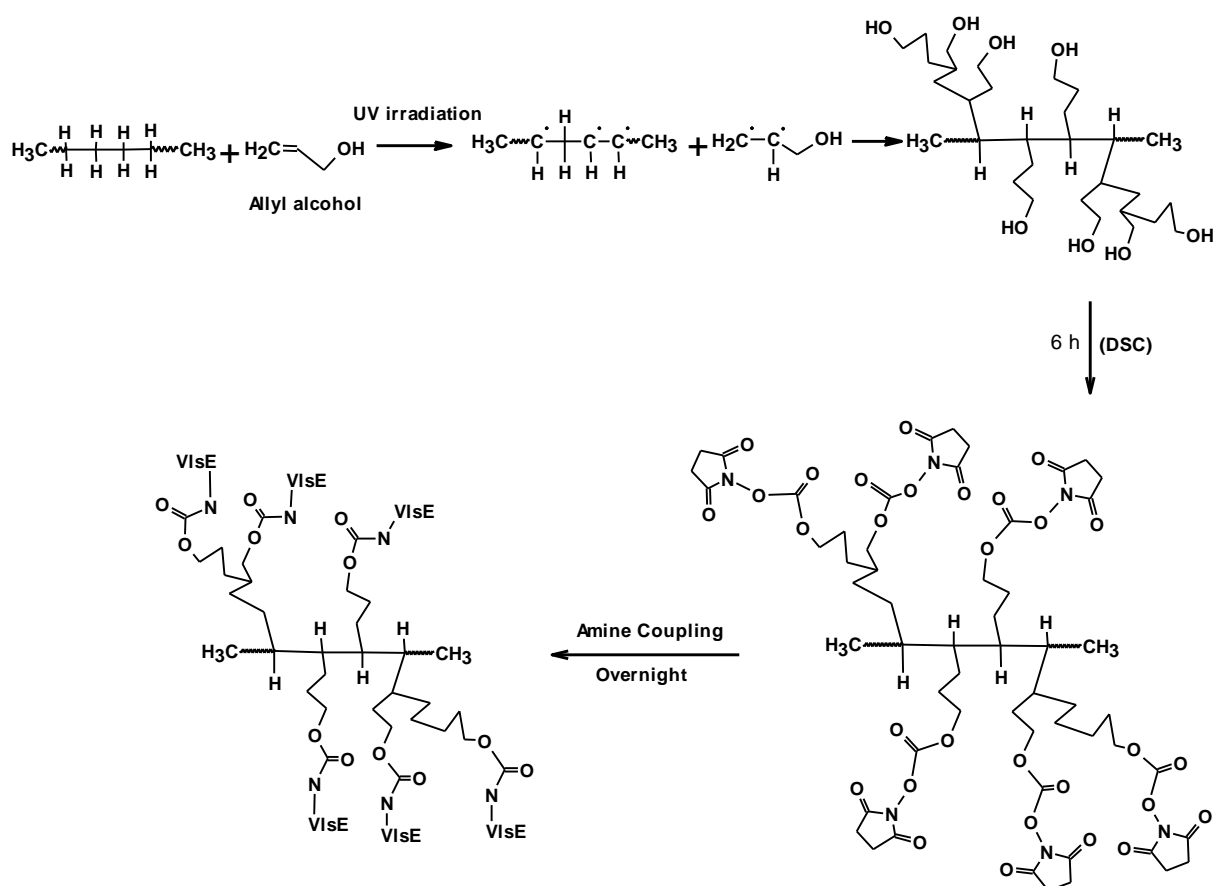
Scheme 2 *Surface functionalization of polyethylene using UV light followed by antigen coating using amine-coupling procedure.*

4.5 Hydrophobic immobilization of VlsE antigen on the surface of 3-DPESB

Hydrophobic immobilization of VlsE antigen on the surface of the 3-DPESB was performed based on a previously published procedure with some modifications (103). In a brief, the sinter bodies were washed with 96% ethanol for 10 minutes followed by 10 minutes washing

with 50% ethanol in water. 3-DPESB were washed 3 times 10 minutes each with 0.1 M carbonate-bicarbonate buffer pH 9.6. Next, 3-DPESB were incubated with the VlsE antigen in the carbonate bicarbonate buffer over night; 0.3 µg of antigen for each sinter body was used. The 3-DPESB were incubated for 1 h in the blocking solution 1 to block the free unspecific sites followed by two hours incubation in the drying buffer. Finally, 3-DPESB were dried under reduced pressure and stored at 4° C until used for the assay. All immobilization steps were carried out under reduced pressure with stirring at room temperature.

4.6 Gold nanoparticles synthesis

AuNPs was synthesized after the reduction of gold hydrochlorate solution using Turkevich's method (87). Briefly, glassware was firstly carefully cleaned using hydrochloric acid and nitric acid in a volume ratio 3:1, respectively. Then, the glassware was rinsed with deionized water and finally dried in an oven at 100 °C for one hour before use. Using a reflux process in order to prevent evaporation during the synthesis, a solution of 0.612 mM sodium citrate (50 ml of double distilled water) in three-necked round-bottomed flask was heated with vigorous stirring until boiling. 1 ml of gold (III) chloride hydrate solution was added afterwards; 19 mM, 20.5 mM and 23 mM were used to synthesize 20, 30, and 40 nm particles, respectively. The solution was kept boiling for 10 min. The heating system was switched off and the solution was kept stirring for 30 min. The cold solution was stored at 4 °C until further use.

4.7 Hydrophobic functionalization of gold nanoparticles with protein A

30 nm AuNPs was functionalized with protein A in order to serve as a label in integration with the polyethylene sinter bodies' platform. Adsorption of protein A was carried out following a procedure developed by Thobhani (104). Firstly, the colloidal gold solution was dialyzed for 24 hours in distilled water. The pH of 2 mL dialyzed gold solution was adjusted between 7 and 7.5 using about 1 µL 0.2 M NaOH and later centrifuged for 30 min at 3500 rpm. The supernatant was discarded and the gold pellets were re-suspended in 2 mL 100 mM borate buffer pH 7.4 containing 20 µg mL^{-1} protein A. The resulting suspension was gently stirred for 30 min in dark at room temperature; following, 200 µL 10% BSA in borate buffer

pH 7.4 was added and stirred further for 15 min. The suspension was centrifuged two times for 30 min at 3500 rpm. The supernatant was discarded and the gold pellets were re-suspended in borate buffer pH 7.4. After second centrifugation, gold pellets were re-suspended in storage buffer (0.5 mL 100 mM borate buffer pH 7.4 containing 0.1% BSA).

4.8 Evaluating the feasibility of AuNPs modification with protein A using SPR device

Plasmonic SPR device was used to evaluate the feasibility of the AuNPs modification with protein A. The working principle of the used plasmonic instrument (Wallenfels, Germany) is based on the SPR technique (Figure 13). An optical method in which the refractive index of a very thin layer of gold (50 μm) adsorbed on a metal sensor surface is measured. As the analyte binds to the ligand immobilized on the surface, the mass increases; as a
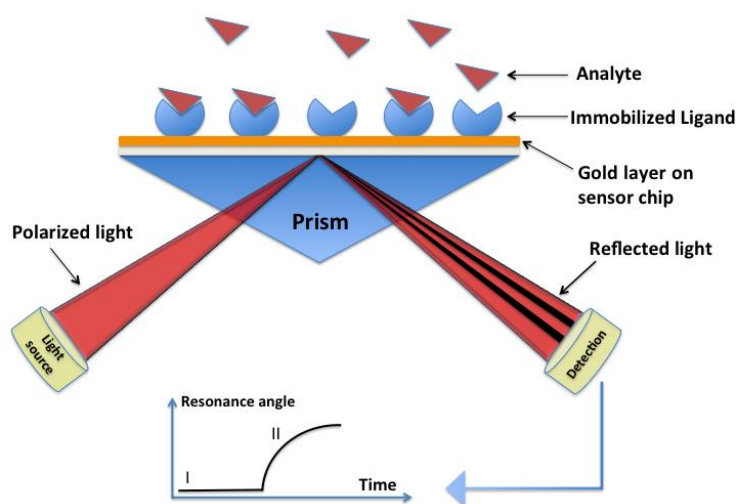
Figure 13 *Surface plasmon resonance principle and a typical sensogram of resonance signal change with time. Refractive index of gold layer changes, as the analyte binds to the ligand. The change can be measured as resonance units.*

result the refractive index increases (105). The change in the refractive index causes a change in resonance angle in turn, which can be measured in real time. The result can be plotted as a response or resonance units versus time. In our experiments AuNPs modified with protein A was added after antibody-antigen interaction. The interaction of AuNPs to antibodies could be monitored, confirming the feasibility of the nanoparticles for further experiments.

OspC *Borrelia* antigen was first immobilized by hydrophobic adsorption on highly hydrophobic SPR prism coated with octadecyltrimethoxysilane (C18 chip). C18 can be immobilized following a protocol published by Höbel et al. (106). Briefly, SPR gold prism was cleaned in acetone for 10 min followed by a rinsing step in Millipore water. The gold surface was incubated afterwards in a mixture of 0.1 M KOH and 30% H_2O_2 (1:1, v/v) for 20

min at 60 °C. The surface was rinsed with water and then dried under vacuum. The gold surface was incubated in octadecyltrimethoxysilane (1% w/w in toluene) for 6 h at room temperature on a shaker (250 rpm). The prism was then rinsed in toluene, methanol, and water respectively. Finally, the prism was dried under reduced pressure until used.

Using the C18 chip, an immunoassay has been conducted as follow: 10 µL 500 µg mL^{-1} OspC antigen in PBS buffer (0.15 M, pH 7.4) was injected to the SPR chip and incubated for 15 min. Surface was washed with PBS to remove any unbound antigens. Following, 10 µL 200 µg mL^{-1} BSA was added to block the free unspecific binding sites on the chip surface. 10 µL positive human serum, 100- fold dilution, was added subsequently, and finally, 10 µL of the AuNPs suspension modified with protein A was added (Figure 14). As a control, 10 µL AuNPs modified (blocked) with BSA was added after serum sample.
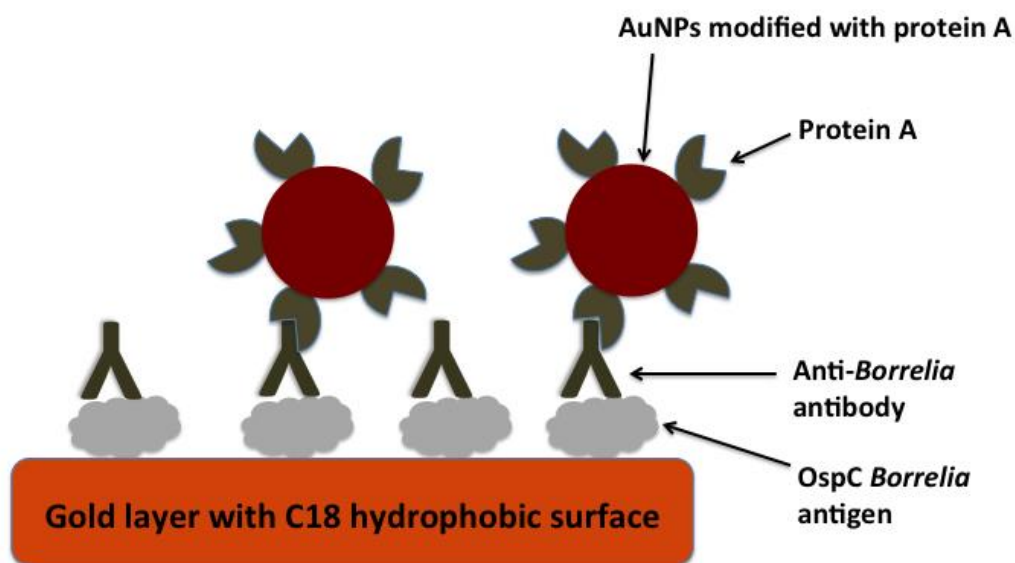
Figure 14 *A schematic representation of SPR immunoassay used to evaluate the feasibility of AuNPs modification with protein A. AuNPs attached to the surface due to a specific interaction between protein A and antibody. AuNPs blocked with BSA result in no binding response.*

4.9 Two-protein modified gold nanoparticles preparation

To accomplish the second platform, AuNPs (20, 30, and 40 nm) were covalently modified with two antigens, protein A and *Borrelia* VlsE. Prior to antigen immobilization, AuNPs was capped with 11-mercaptoundecanoic acid as follow: NaOH 0.2 M was used to adjust the pH of 2 mL gold between 7 and 7.5; the solution was centrifuged for 40 min at 4000 rpm. The supernatant was discarded and the pellets were re-suspended in 2 mL double distilled water. To the 2 mL suspension, 4 µL of 0.2 M NaOH was added; following, 5 µL of 1mg mL^{-1} 11-mercaptoundecanoic acid (dissolved in ethanol) was slowly added while stirring. The solution was gently stirred for two hours at room temperature followed by stirring 24 h at 4 °C. Gold suspension was finally cleaned after two times centrifugation for 40 min at 4000 rpm and the pellets were re-suspended in 10 mM borate buffer pH 9.

Immobilization of the two antigens was achieved using EDC/NHS coupling procedure. 10 µL 1 mg mL^{-1} VlsE and 12 µL 1 mg mL^{-1} protein A were added to a 2 mL carboxylated nanoparticles. A freshly prepared mixture of 10 µL 0.2 mM NHS and 5 µL 0.25 mM EDC, which have been dissolved in 10 mM borate buffer pH 9, was directly added afterwards. The solution was gently stirred over night at room temperature. Next, the suspension was centrifuged two times at 4000 rpm for 40 min and the pellets were re-suspended in 10 mM borate buffer pH 9. Finally the gold pellets were re-suspended in storing buffer, 0.5 mL 50 mM phosphate buffer pH 7.4 containing 1.5 mg bovine serum albumin. Figure 15 illustrates a schematic representation of AuNPs surface modification, followed by antigens immobilization.
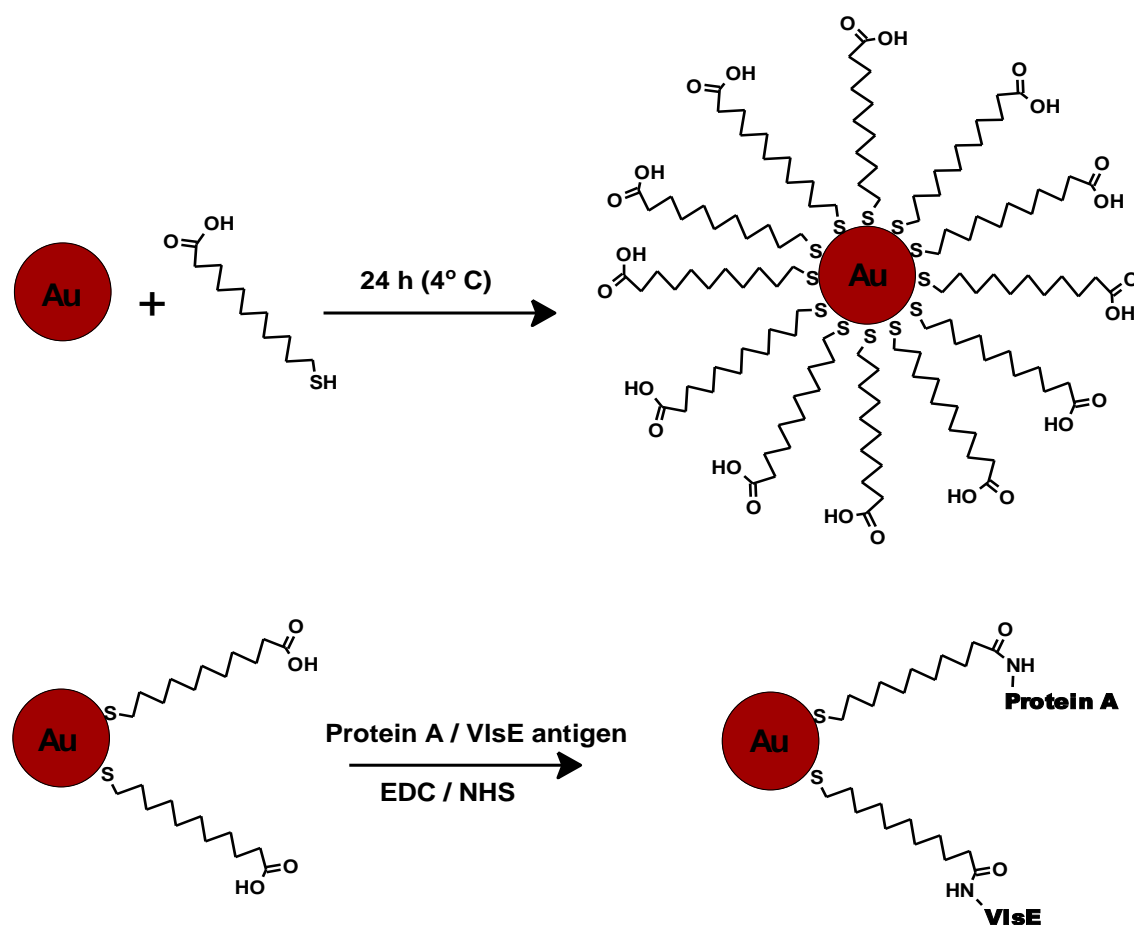
Figure 15 *Schematic representation illustrates the modification of AuNPs with VlsE Borrlia antigen and protein A. AuNPs capped first with MUA; following, antigens were immobilized using EDC/NHS coupling procedure.*

4.10 Assay workflow using VlsE-modified 3-DPESB (detection by HRP labeled secondary antibody and Sudan IV-streptavidin-HRP-nanoparticles).

After modifying the 3-DPESB with VlsE antigen, borreliosis positive and negative human sera were applied to evaluate the performance of the platform. Firstly, the functionalized 3-DPESB was placed inside a polycarbonate cartridge on top of an unmodified 3-DPESB, which has been passivated with 1% BSA solution (ABICAP^{TM}, Figure 16). Alternatively a pipette tip of a volume of 1 mL can be used in order to perform the entire assay in this tip. The sera were either diluted 1000-fold (5.5% CBC buffer) when VIsE antigen hydrophobically immobilized or 500-fold when VIsE antigen covalently immobilized.

200 µL of the diluted serum sample was always loaded to the ABICAP™ column. The colorimetric detection of immune interaction was sequentially performed using ABICAP™ photometer. The assay workflow was conducted using HRP labeled antibody and nanoparticles based on Sudan IV for detection.
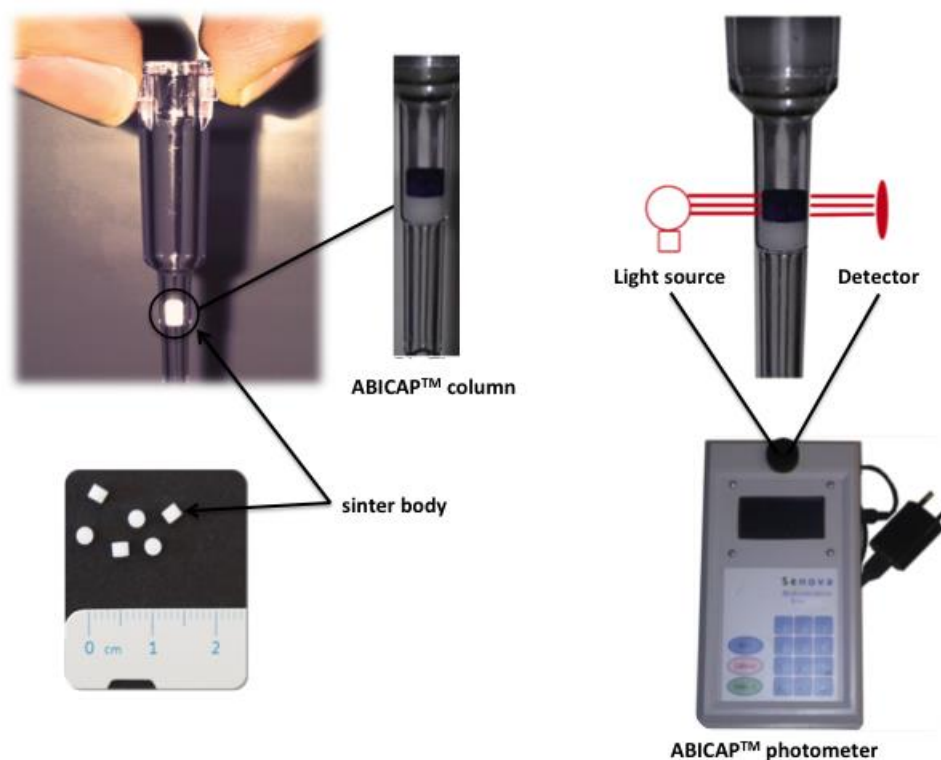
Figure 16 *Assay set up. 2 × 2.5 mm 3-DPESB were placed inside a small column or a pipette tip. Optical density after HRP enzymatic reaction can be measured at 650 nm using ABICAP™ photometer. HRP secondary antibody or Sudan IV nanoparticles modified with HRP were used for detection.*

Firstly, detection using HRP labeled antibody was performed in integration with both 3-DPESB modified with hydrophobic adsorption and 3-DPESB modified with covalent bonding; the detection was pursued after serum loading as follow: applying 250 µL of HRP labeled antibody (1 µg mL^{-1}) in (AA1) buffer, equilibration of the 3-DPESB using 250 µL acetate buffer pH 4.8, and then loading of TMB substrate; finally, 250 µL acetate buffer pH 4.8 was loaded (Figure 17). Detection using Sudan IV nanoparticles modified with HRP was only used with the covalently modified 3-DPESB; detection was pursued after serum loading as follow: 250 µL 1000-fold dilution of biotinylated primary antibody (0.6 mg mL^{-1} protein

content), loading of 250 µL of nanoparticles diluted in PBS buffer pH 7.4 with the desired dilution (100 – 133-fold). Equilibration of 3-DPESB with 250 µL acetate buffer pH 4.8 followed by loading the TMB substrate was then conducted; Finally 250 µL acetate buffer pH 4.8 was added (Figure 18). The incubation times for the serum, labeled secondary antibody or nanoparticles, and the substrate TMB were 3 min each. Washing steps using washing buffer were performed after each step. The optical density was quantified using the ABICAP[TM] photometer at 650 nm in triplicate. Raw data were processed by ORIGIN[TM] software package.
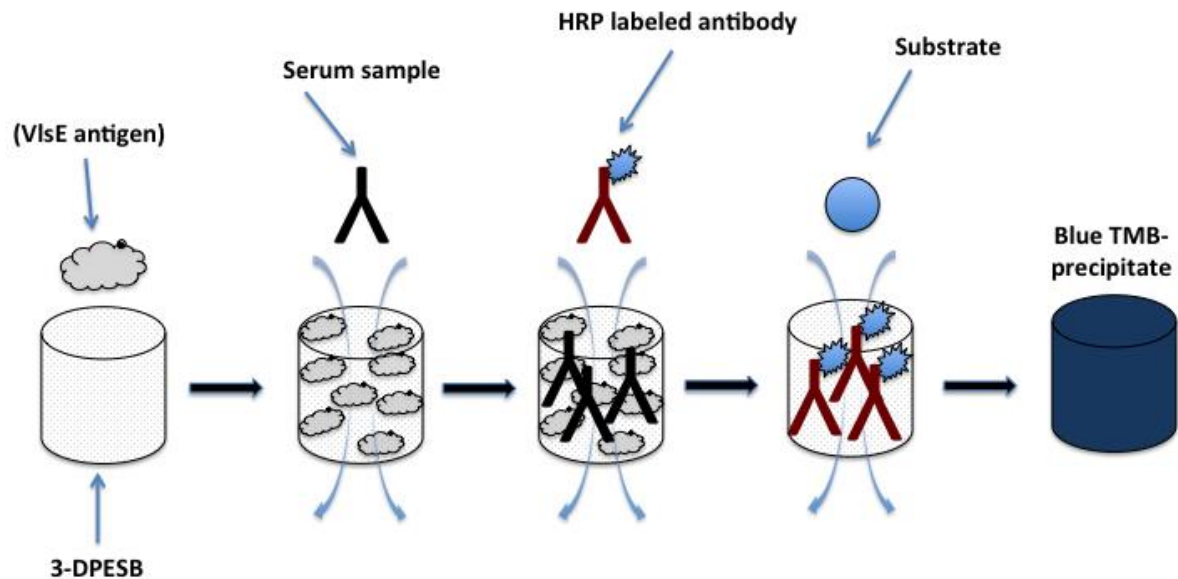
Figure 17 *Borreliosis assay on antigen coated 3-DPESB. HRP labeled antibodies was used for detection. The optical density of the resulting blue TMB-precipitate can be measured at 650 nm.*
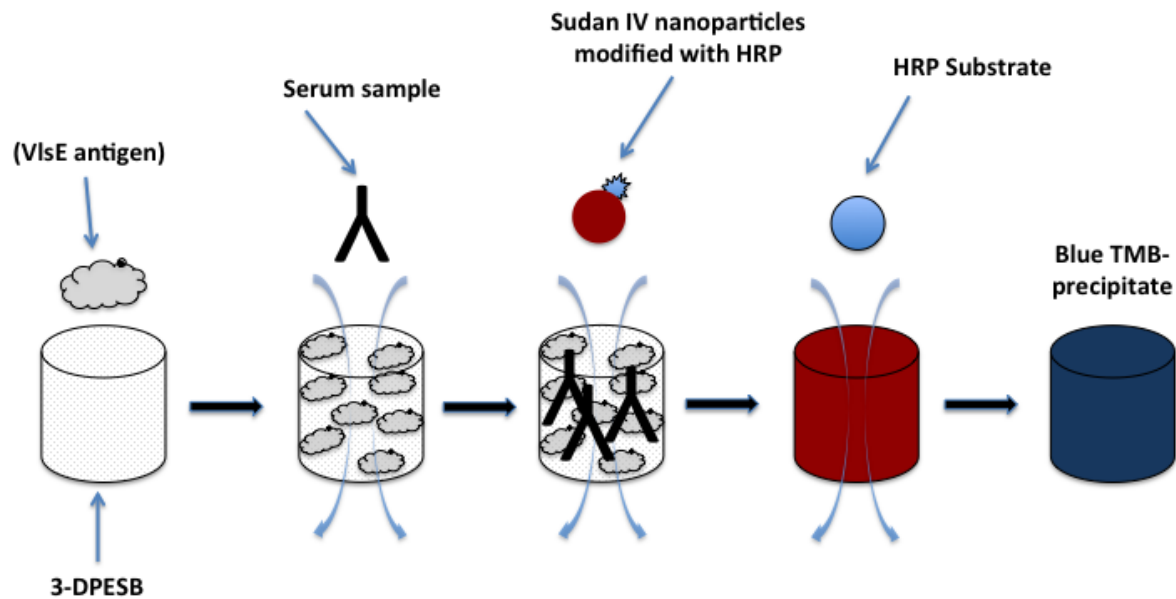
Figure 18 *Borreliosis assay workflow on antigen coated 3-DPESB. Sudan IV-HRP nanoparticles was used for detection. Red nanoparticles can be measured at 520 nm; differently, the blue TMB-precipitate can be measured at 650 nm.*

4.11 Assay workflow using VlsE-modified 3-DPESB (detection by gold nanoparticles).

Gold nanoparticles was used for detection in integration only with 3-DPESB that have been modified using hydrophobic adsorption. In the here case, 200 μL 250-fold dilution of serum sample was applied, instead, to the ABICAP^{TM} column enclosing the 3-DPESB followed by a washing step with 250 μL washing buffer; 200 μL protein A-colloidal gold solution (5-fold dilutions in PBS buffer) was loaded subsequently. Finally, the optical density was measured at 650 nm.

Silver enhancer solution was used to enhance the signal as follow: 150 μL of silver enhancer solution (silver enhancer solution A and silver enhancer solution B, 1:1) was loaded after protein A-colloidal gold (Figure 19). Following, a washing step with double distilled water was needed. The incubation times for the serum and AuNPs were 3 min each.

Washing step using washing buffer was performed after serum loading. Finally measurement of the optical density was conducted at 650 nm in triplicate. Raw data were processed by ORIGIN^{TM} software package.
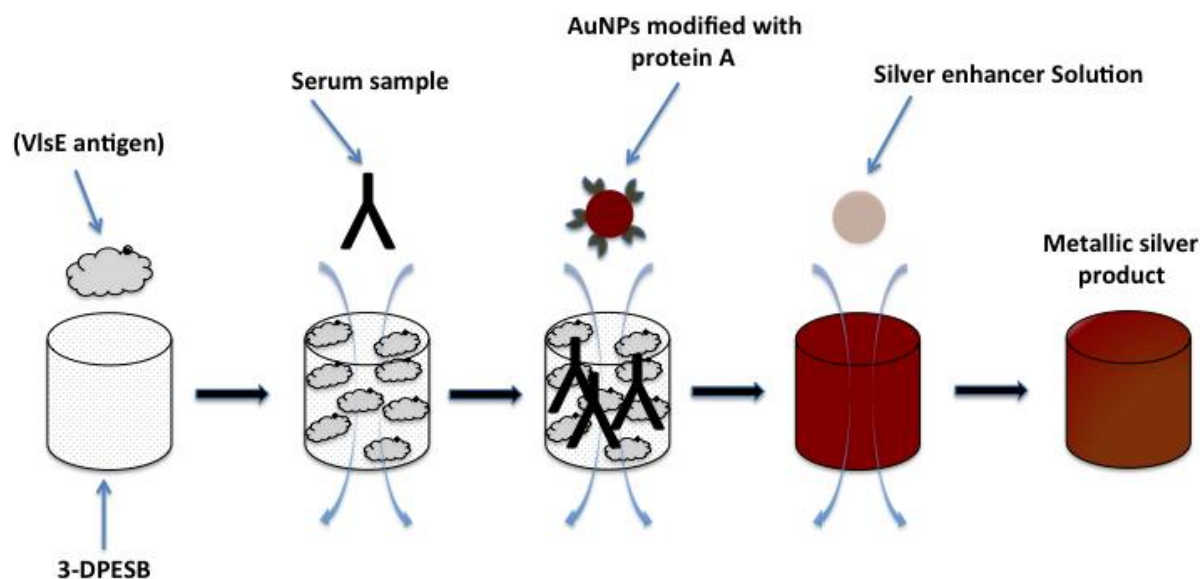
Figure 19 *Borreliosis assay workflow on antigen coated 3-DPESB. AuNPs modified with protein A was used for detection. AuNPs or metallic silver absorbance can be measured at 650 nm.*

4.12 Assay workflow using mannan-modified 3-DPESB (detection by HRP labeled secondary antibody)

Firstly, the mannan-modified 3-DPESB was fixed inside an ABICAP^{TM} cartridge above an unmodified sinter body as spacer, which has been previously washed with casein based blocking solution 2. The spacer adjusts the position of the 3-DPESB during the optical density measurements. 250 μL of the fusion protein solution (3 μg mL^{-1}, consisting of the lectin binding domain ConA and the *Borrelia* surface antigen C6) in 10 mM HEPES buffer pH 7.4 was loaded to the cartridge; the ConA part interacts specifically with the immobilized mannan, while the antigen part is free for serum diagnosis. For analysis, 250 μL of 1000-fold diluted human serum in 5.5 % CBC was loaded to the cartridge (107). The detection was performed as follow: applying 250 μL of HRP labeled antibody (1 μg mL^{-1}) in (AA1) buffer, equilibration of the 3-DPESB using 250 μL acetate buffer pH 4.8, and then loading of TMB substrate; finally, 250 μL acetate buffer pH 4.8 was loaded (Figure 20). The incubation times for the fusion protein, serum, labeled secondary antibody and the substrate TMB were 3 min

each. Washing steps using washing buffer were performed after each step. Optical density was measured at 650 nm in triplicate. Raw data were processed by ORIGIN^{TM} software package.
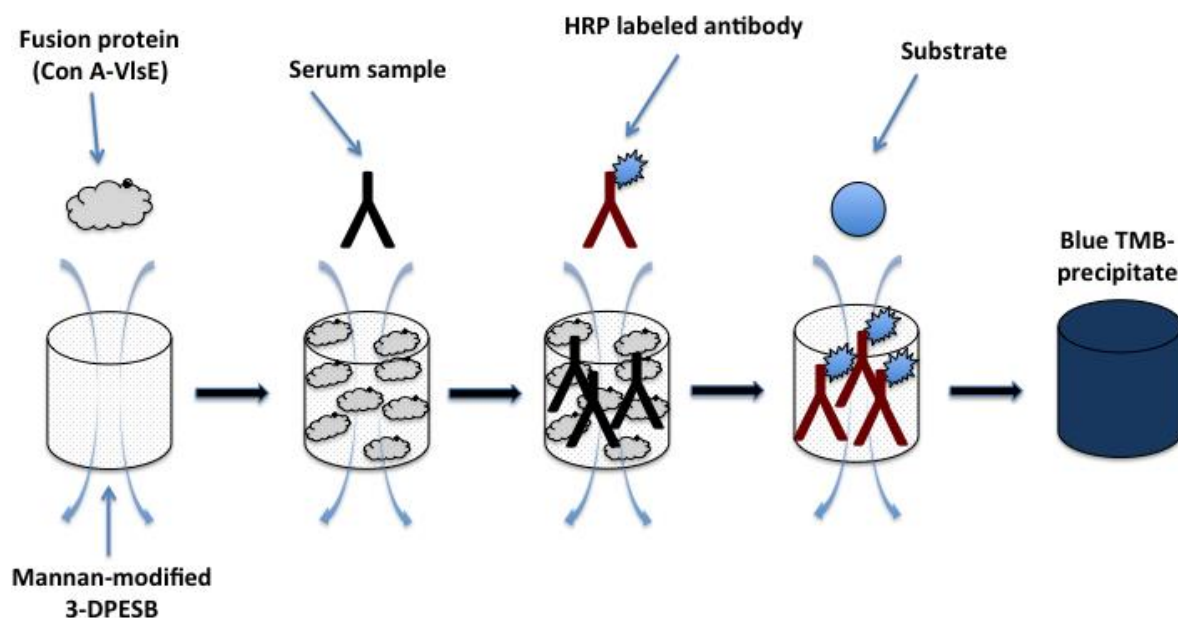
Figure 20 *Borreliosis assay workflow on mannan-coated 3-DPESB. The fusion protein is caught by the mannan, exposing the antigen part for antibodies detection. HRP labeled antibody was used for detection. Blue TMB-precipitate can be measured at 650 nm.*

4.13 Assay setup using the two-antigen modified gold nanoparticles

100 μL phosphate buffer pH 7.4 containing the serum sample with the desired dilution was loaded in a micro-cuvette; 20 μL of modified AuNPs was then added to the solution. The solution was incubated at room temperature until measurements (Figure 21). UV–vis spectra were collected on a Shimadzu UV-2401 spectrometer for the qualitative analysis. Absorbance intensities of AuNPs were measured at 590 nm for quantitative analysis using Genova plus life science spectrophotometer fitted with micro-cuvette holder. Experiments were performed in triplicate. Raw data were processed by ORIGIN^{TM} software package.
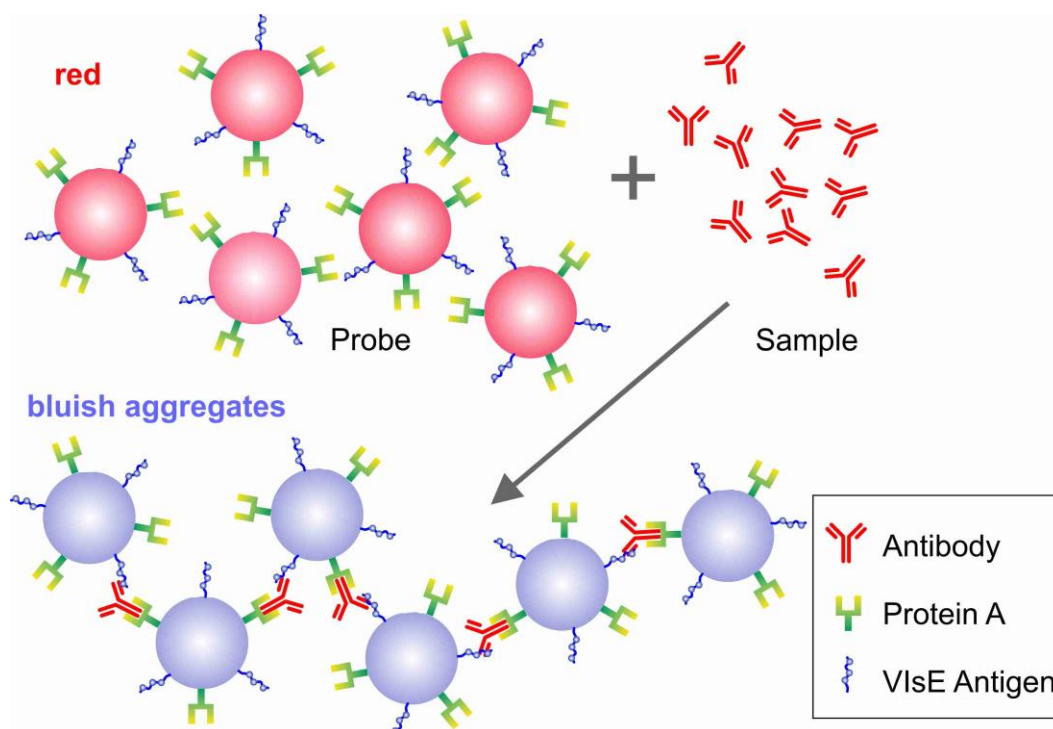
Figure 21 *Aggregation of gold nanoparticles as a consequence of antibodies interaction with the immobilized antigens. As a result coupling of the SPR of the adjacent particles takes place and aggregation appears as a change in color from red to blue.*

5 Results

5.1 Activation of 3-DPESB using UV photografting

Firstly, different amounts of 2-propenol were tested in order to select a convenient concentration, which results in monomer's grafting. Best results were found, if 2-propenol makes up to 25% volume of the reaction mixture, while volume ratios like 1:1 and strongly diluted solutions like 5% of 2-propenol did not give any advantage in the obtained FTIR spectra. It is assumed that the ratio between the used benzophenone and the 2-propenol is of importance. In summary, it turned out that 25 % of 2-propenol is sufficient for the following derivatization steps. Different irradiation times were tested additionally for photografting of 2-propenol in order to find the optimal loading with OH-groups. 3-DPESB were treated for 1h, 3h and 6h followed by FTIR analysis (Figure 22).
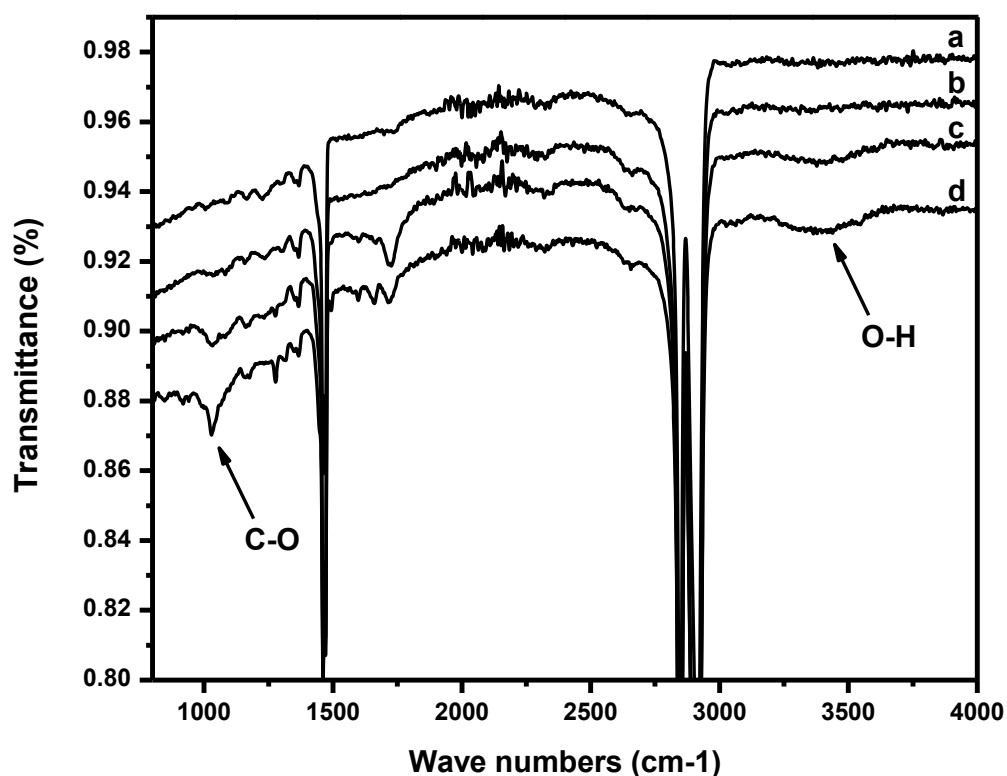
Figure 22 FTIR spectra after 2-propenol photografting on 3-DPESB as a function of time. Unmodified 3-DPESB (a), 1h UV-irradiation (b), 3h UV-irradiation (c), and 6h UV-irradiation (d).

It is clearly visible that after 3h and 6h of irradiation OH-related absorption bands appeared. One broad band is located between 3720 and 3200 cm^{-1}, centered at about 3450 cm^{-1}, which could be attributed to O–H stretching of alcohols and another band located between 1135 and 1000 cm^{-1} could be assigned to C–O stretching of alcohols.

The scanning electron microscopy images of the unmodified 3-DPESB and the UV treated 3-DPESB with 2000-fold magnification (scanned area 10 μm x 10 μm) can be shown in Figure 23.
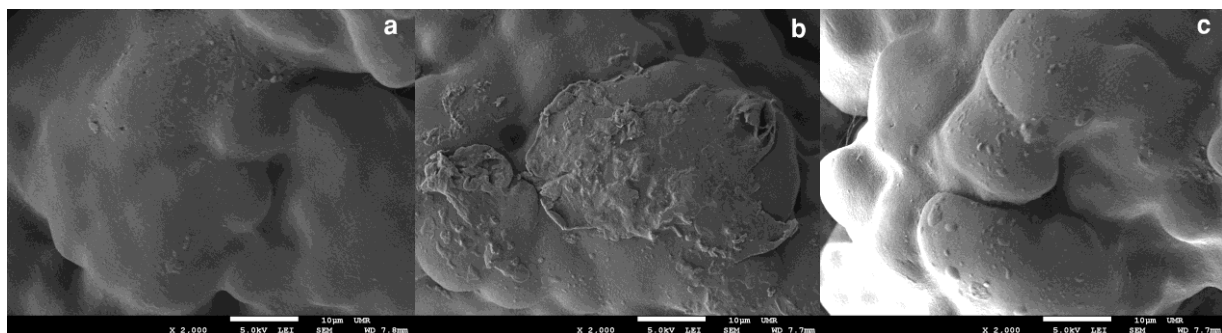
Figure 23 *Scanning electron microscopy (SEM) images of unmodified 3-DPESB (a), UV modified 3-DPESB and one place with a multilayer (b) and UV modified 3-DPESB with uniform coating (c); scanned area (10 × 10 μm).*

Atomic force microscopy measurements (scanned area 10 μm x 10 μm, resolution was 512 x 512 pixels) that confirm the SEM results are given in Figure 24.
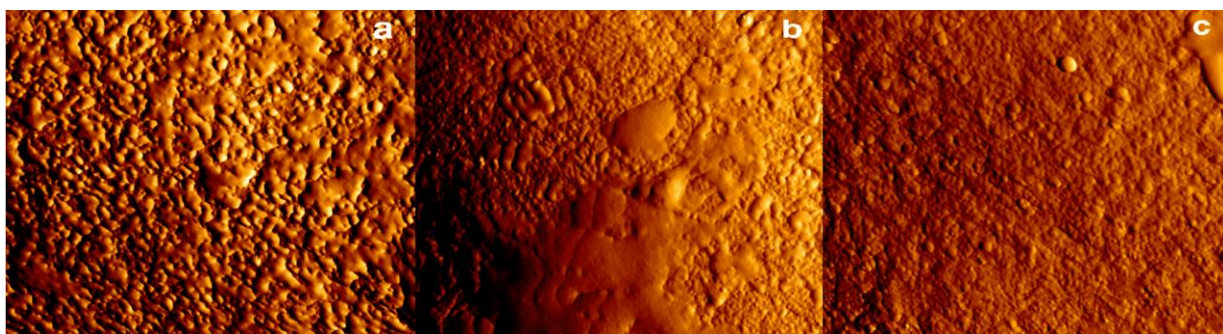
Figure 24 *Atomic force microscopy (AFM) images of unmodified 3-DPESB (a), UV-modified 3-DPESB and one place with a multilayer (b) and UV-modified 3-DPESB with uniform coating (c); measured area (5 × 5 μm).*

By both techniques, the surface of the unmodified 3-DPESB (23a, 24a) has been significantly modified after UV irradiation and photografting (23b, c; 24b, c). The so modified 3-DPESB were covered with some kind of cross-linked structure, which can be explained by polymerization of 2-propenol. However, polymerization is not even over the entire surface. At some places, coating seems to be more or less regular (Figures 23c and 24c). At other places, a rather thick multilayer has been formed, which might be physically instable (Figures 23b and 24b). The reason for punctual multilayer formation could not been found but might be supported by longer exposure times.

5.2 Silanization of UV treated 3-DPESB by APTES for mannan immobilization

In the next step, the UV treated 3-DPESB surface was grafted with APTES for mannan immobilization (Scheme 1). By this procedure, amino groups for further immobilization steps were introduced. Detection of amino groups and its distribution on the surface was carried out utilizing Coomassie Brilliant Blue Dye-G250 absorption at 520 nm in a so called 'protein quantitation assay' according to Bradford following a protocol published by Kehrel et al. (108). The silanized 3-DPESB were placed right above a spacer sinter body inside a cartridge (compare Figure 16), sinter bodies were wetted by 250 µL 50% aqueous ethanol solution followed by incubation with 250 µL Coomassie–solution for 5 min. After washing, optical density at 520 nm was determined (Figure 25). The photometer was adjusted with one blank 3-DPESB wetted with 50% ethanol. Unmodified (without photografting) 3-DPESB but treated with APTES as well as unmodified 3-DPESB without any treatment were used both as a control. In the presence of amino groups, a deep blue color occurs (Figure 25-c). The color distribution seems to be rather homogenous indicating the presence of amino groups over the entire surface. Additionally, 3-DPESB were dissected to control color development inside the sinter bodies; the color distribution was found to be rather regular. The two controls (Figure 25a and 25b) exhibited a much weaker coloration, which can be explained by unspecific binding of the dye (Figure 25a) or a partial APTES coating even without any hydroxyl groups at the 3-DPESB's surface (Figure 25b).
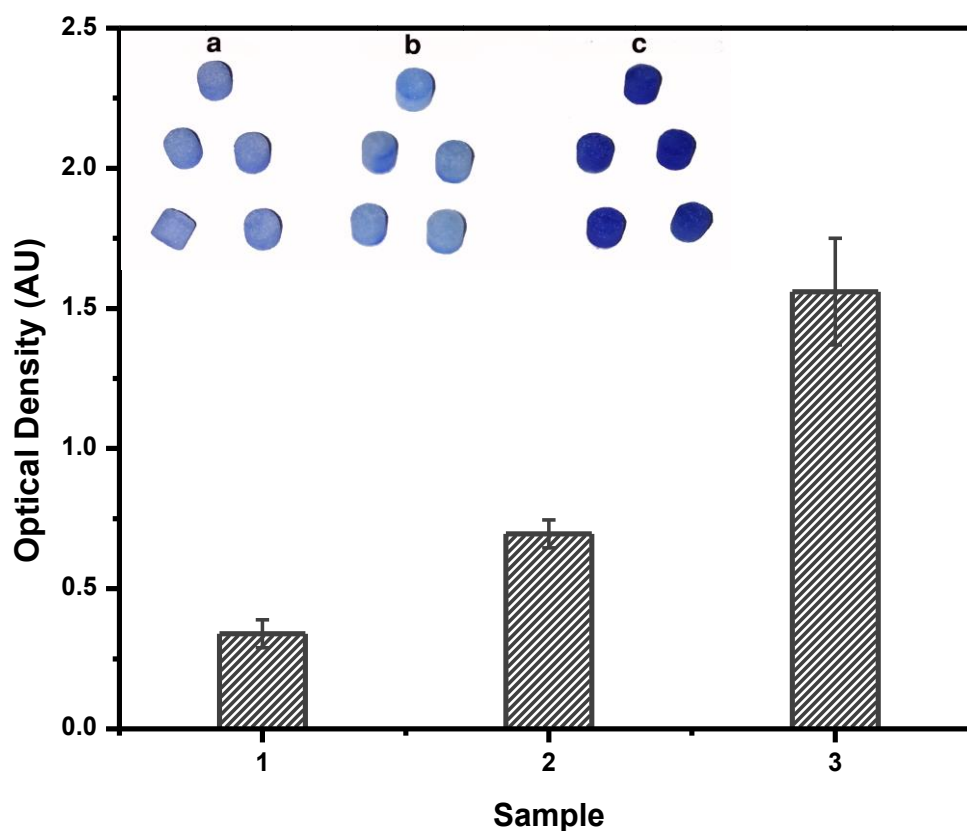
Figure 25 *Optical densities of 3-DPESB after staining of the APTES-layer by Coomassie Brilliant Blue Dye-G250. Unmodified 3-DPESB (1 and a), unmodified 3-DPESB treated with APTES, but without photografting step (2 and b) and UV- modified 3-DPESB with APTES (3 and c).*

The functionalized 3-DPESB showed an optical density of about 1.56 with standard deviation of ±0.20, the unmodified 3-DPESB treated with APTES showed a signal at about 0.70 with standard deviation of ±0.05 and the unmodified 3-DPESB with no treatment gave an optical density of 0.34 and standard deviation of ±0.05. These differences between these three measurements are significant, indicating a successful coating with APTES for the 2-propenol modified surface. However, APTES can be also grafted to unmodified 3-DPESB to a certain extend. But the latter experiment as depicted in Figure 25b gave a much lower loading with amino groups as it could be obtained after photografting (Figure 25c).

5.3 Mannan coating

To get the 3-DPESB ready for the assay as depicted in Figure 20, a mannan coating is necessary. Mannan can be covalently immobilized by acid amide binding. Therefore, SC-mannan seems to be suitable (Scheme 1). This activation prior to immobilization is necessary to allow a smooth immobilization of the carbohydrate. Mannan has been chosen because it is chemically stable, shows low unspecific binding and allows attachment of lectins by self-organization. After mannan immobilization, free amino groups were blocked by ethanolamine and unspecific binding sites were passivated by a blocking solution. The so prepared mannan-coated 3-DPESB should be stored over several months and can be loaded by the fusion protein shortly before usage.

5.4 Serological diagnosis using mannan modified 3-DPESB

The workflow of the assay is depicted in Figure 20. Firstly, the ConA-C6 fusion protein has been applied shortly before the assay was performed. This protein displays a lectin-binding site on one end allowing immobilization on the mannan surface by self-organization and a specific antigen structure at the other end facilitating anti-*Borrelia*-IgG-detection. In the final detection step, anti-IgG-antibodies coupled to HRP were applied and TMB was used as color reagent.

Results are shown in Figure 26. A blue TMB-precipitate was produced when Borreliosis-positive sera were applied (Figure 26a) while only little coloration was visible when negative sera (Figure 26b) were added. Also the two negative controls were more or less colorless (Figure 26c, d).
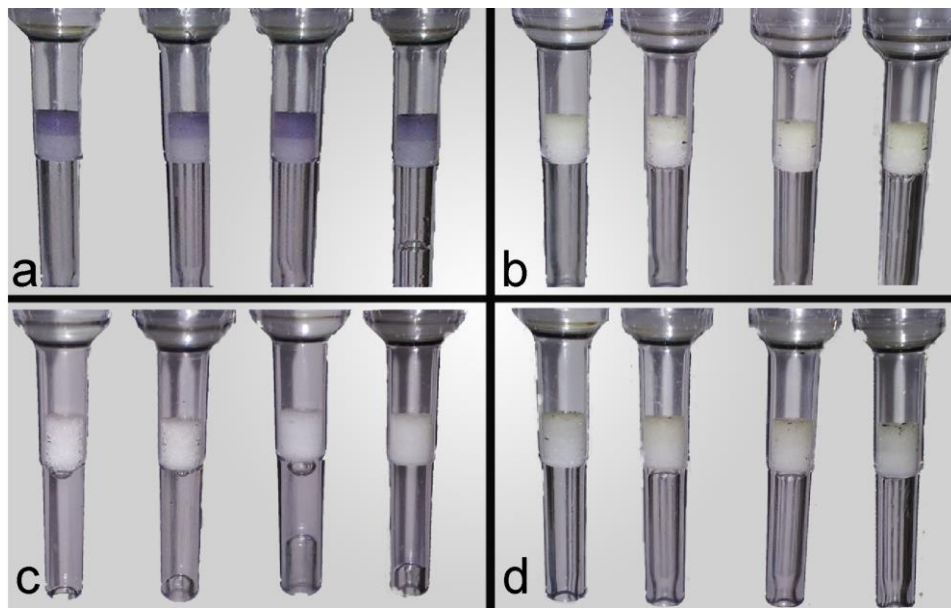
Figure 26 *Color development obtained after HRP detection. Cartridges are filled with an unmodified spacer followed by the probe. Two positive sera (a), two negative sera (b), two positive sera with control 1, 3-DPESB without photografting and silanization (c), and two positive sera with control 2, 3-DPESB without fusion protein (d).*

Quantitative analysis of a larger variety of real serum samples is displayed in Figure 27. As indicated by the horizontal cut-of-line, a differentiation between positive and negative sera, which is important for borreliosis therapy, can be clearly deduced from obtained data. Again, two controls were introduced leaving out an immobilization step or the fusion protein. Differences between positive and negative sera were significant, meaning that it is unlikely that a false-positive or false-negative result occurs.
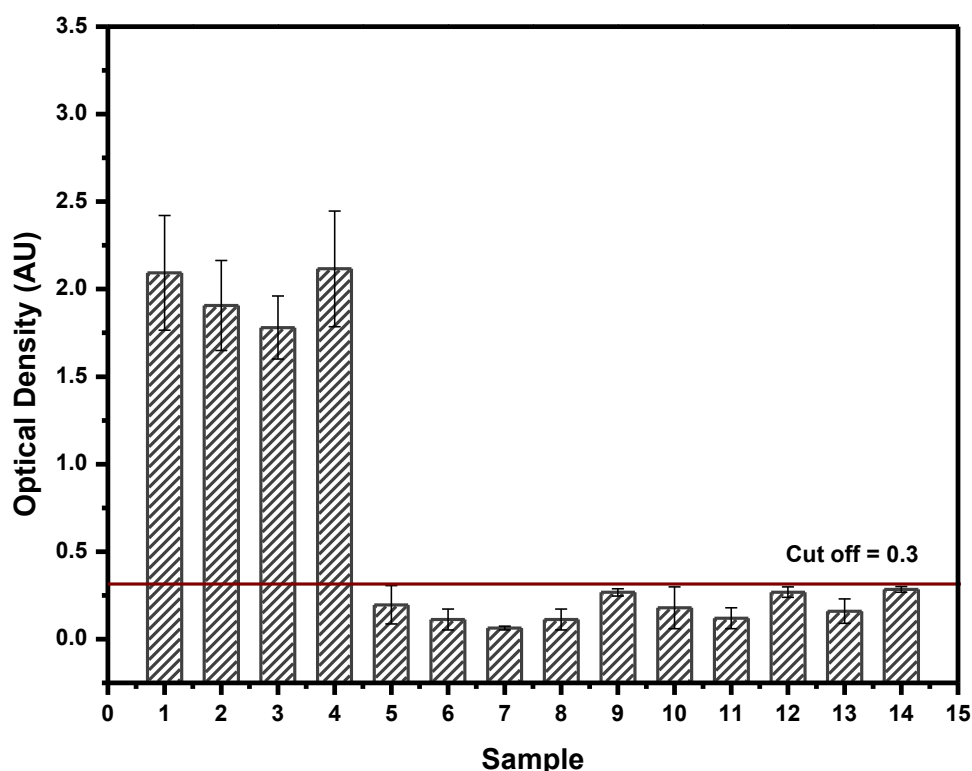
Figure 27 *Results of the borreliosis assay with real human sera. Positive sera (1,2,3,4), negative sera (5,6,7,8), control 1 (9,10,11,12; 3-DPESB without photografting and silanization) and control 2 (13,14; 3-DPESB without fusion protein).*

5.5 Serological diagnosis using hydrophobically modified 3-DPESB

The used polyethylene has a rather high affinity to proteins; this in turn allows a rather easy hydrophobic immobilization of VlsE antigen on the 3-DPESB. With a special washing routine, VIsE could be adsorbed to the 3-DPESB surface in sufficient amounts; that contributes consecutively in enhancing the assay sensitivity. After loading sera samples, two labels were used for detection: i) HRP labeled secondary antibody and ii) gold nanoparticles modified with protein A. Based on the used label, assay optimal conditions have been changed; this includes the concentration of immobilized antigen as well as the dilution of serum sample. Firstly, the optimum amount of VlsE antigen needed for immobilization was investigated. Using the adsorption immobilization procedure mentioned in section 4.5, concentrations of 1, 0.5 and 0.3 µg per sinter body were tested.

5.5.1 Detection using HRP secondary labeled antibody

Using an ELISA like assay, 500-fold dilution of sera samples were analyzed first using the prepared 3-DPESB to select the optimum amount of the immobilized VlsE. When 1 or 0.5 µg of VlsE antigen was immobilized using the hydrophobic adsorption technique, some positive samples resulted in optical densities higher than the detection range of the ABICAP^{TM} photometer (2.5 AU). While immobilization of 0.3 µg of VlsE antigen could regulate the optical densities of the positive serum samples in the detection range. As a next step, approximate anticipation of the optimum serum dilution was tested using 0.3 µg VlsE modified 3-DPESB. Different dilutions of two positive samples were tested; obtained signals can be seen in Figure 28.
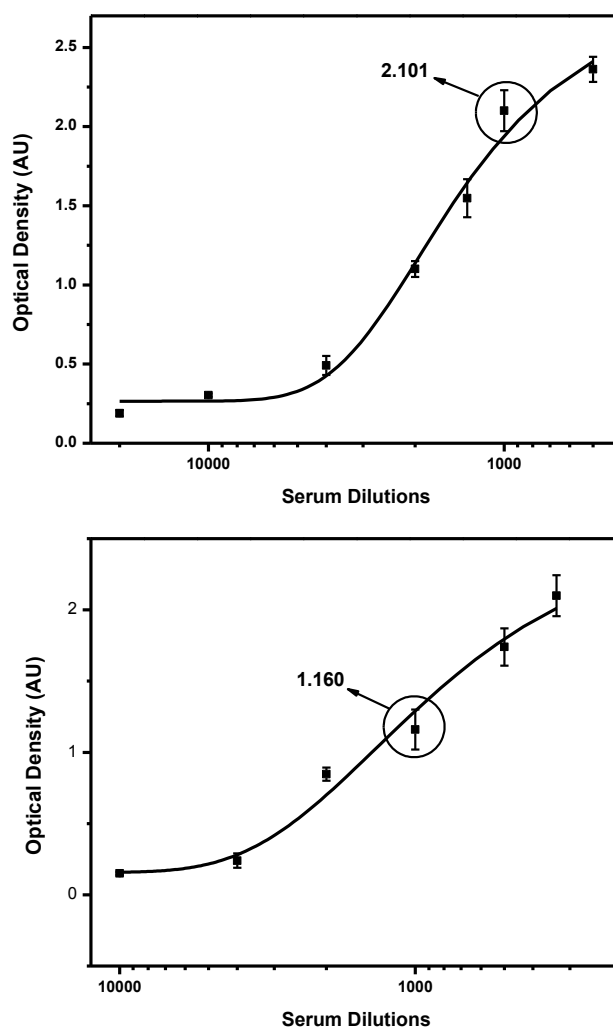
Figure 28 *Calibration curves of two positive sera. Different dilutions of sera were tested with 0.3 µg VlsE modified 3-DPESB. Highlighted spots are related to 1000-fold dilution (n=3).*

Results showed that between 500-fold and 2000-fold dilution, the detection signals were obtained between 2.3 and 0.84. Serum dilutions above 2000- fold resulted in low signals, which might not yield convenient signal when other positive samples are being tested. Dilutions below 500- fold resulted in signals out of the detection range. Consequently, 1000-fold dilution as an optimum was chosen for further experiments. It must be pointed out that the absolute amount of antibodies in the sera, which is directed against VIsE cannot be determined. In these cases, the dilution factor of the sample is a value for sensitivity.

Using the optimized conditions, 17 positive and 20 negative real human sera were tested. Results were summarized with some examples of the obtained 3-DPESB after TMB color reaction in Figure 29. One control was introduced leaving out the immobilization step. The controls as well as the negative sera were display with more or less colorless. In contrast to the positive samples, which appear with dark blue color, indicating the presence of the infection.

As indicated also here by the horizontal cut-of-line, a differentiation between positive and negative sera can be clearly deduced from obtained data. For 16 of the 17 positive sera there is a clear differentiation from the negative sera. There is only a problem with sample 11, which is false negative.
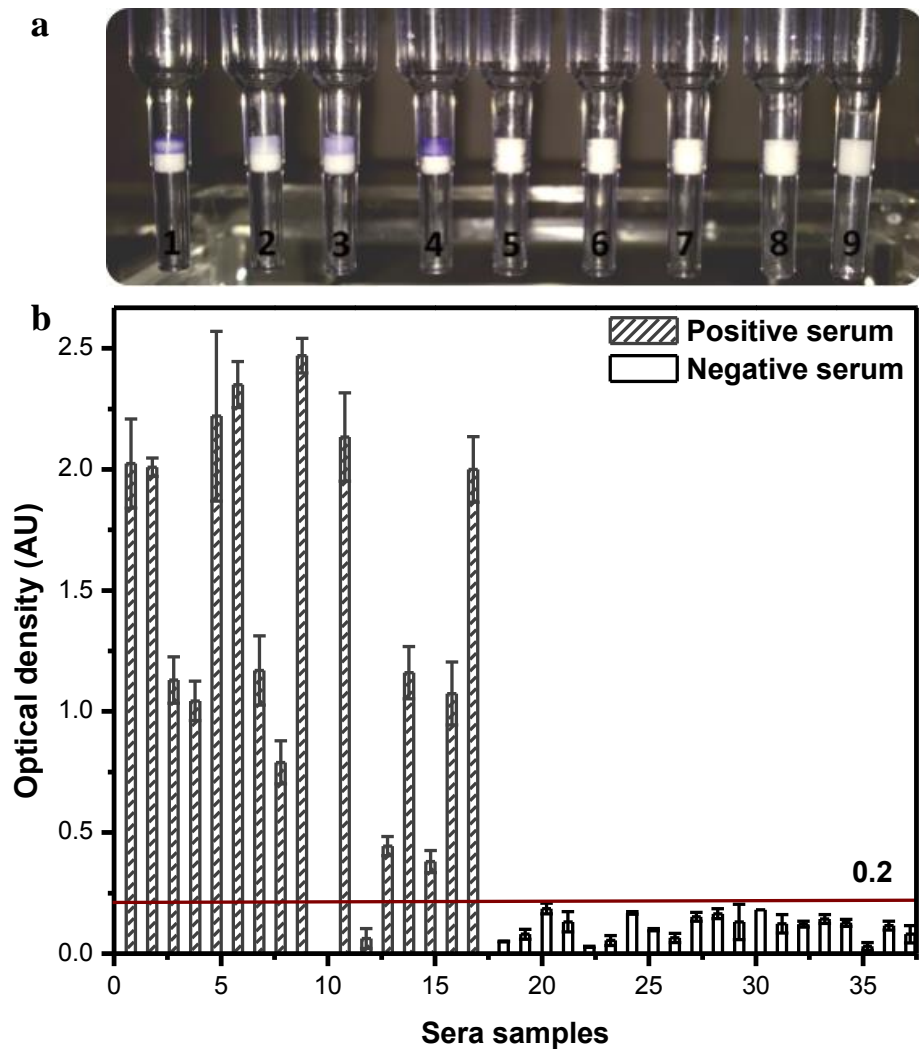
Figure 29 *(a) Color development of 4 positive sera (1-4) and 4 negative sera (5-8) and one control (9) after performing the assay on 3-DPESB that have been modified using hydrophobic adsorption and (b) optical densities of 17 positive and 20 negative sera samples tested on 3-DPESB modified with VlsE antigen using hydrophobic adsorption. Detection was conducted using HRP secondary labeled antibody; cutoff was found at 0.2 (n=3).*

5.5.2 Evaluating the feasibility of AuNPs modification with protein A for detection

Protein A, which binds to the Fc part of antibodies, was immobilized on gold nanoparticles. Interaction of protein A on AuNPs surface with anti-*Borrelia* antibodies could be monitored using SPR device, confirming the feasibility of the nanoparticles as a label for ABICAP^{TM} system. At first, SPR chip has been modified with OspC *Borrelia* antigen, which capture the anti-*Borrelia* antibodies. Successful adsorption of the OspC antigen on the surface could be seen as 23 AU increase in the signal. After a washing step using PBS buffer, blocking of the surface was conducted using BSA; no detected signal was obtained; this indicates to the absence of free binding sites on the surface. The immobilized amount of antigen was sufficient to cover the surface. Therewith, the OspC antigen could capture the antibodies from the serum, which appear as increasing in the signal with 10 AU after serum loading. Finally, interaction of protein A with the antibodies could be observed; 15 AU as a signal indicates the capture of nanoparticles on the surface (Figure 30). The binding is caused by a specific interaction of antibodies with protein A; this can be confirmed when nanoparticles, which has been totally blocked with BSA, was injected as a control after the positive serum. Using the same setup, only 2 AU as increased signal could be obtained (Figure 31). In conclusion, functionalization of AuNPs with protein A was successful, producing an applicable label for the ABICAP^{TM} system.
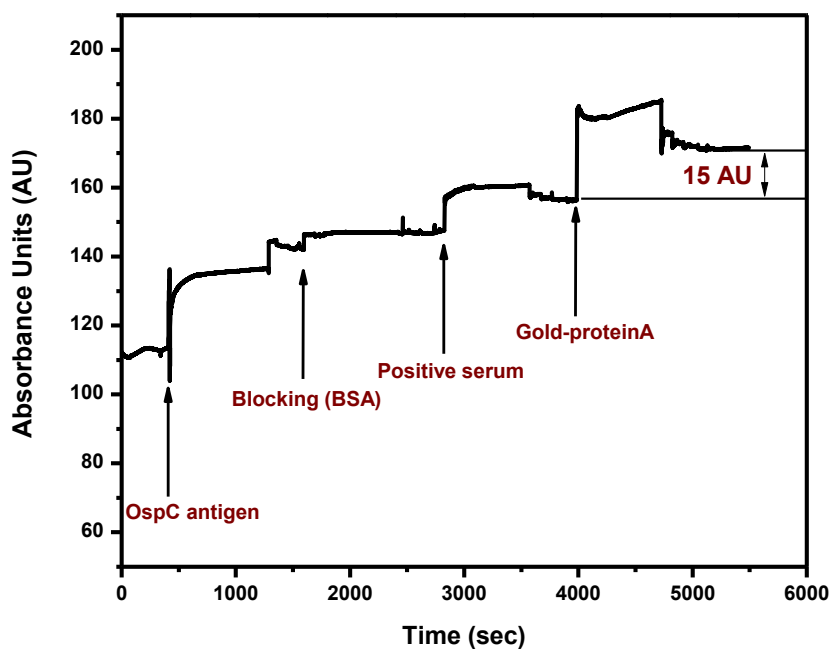
Figure 30 *High affinity response of AuNPs modified with protein A to antibodies on SPR chip. Antibodies in human serum sample were attached to the surface due to a specific interaction with OspC Borrelia antigen. Antigen has been hydrophobically adsorbed to SPR chip.*
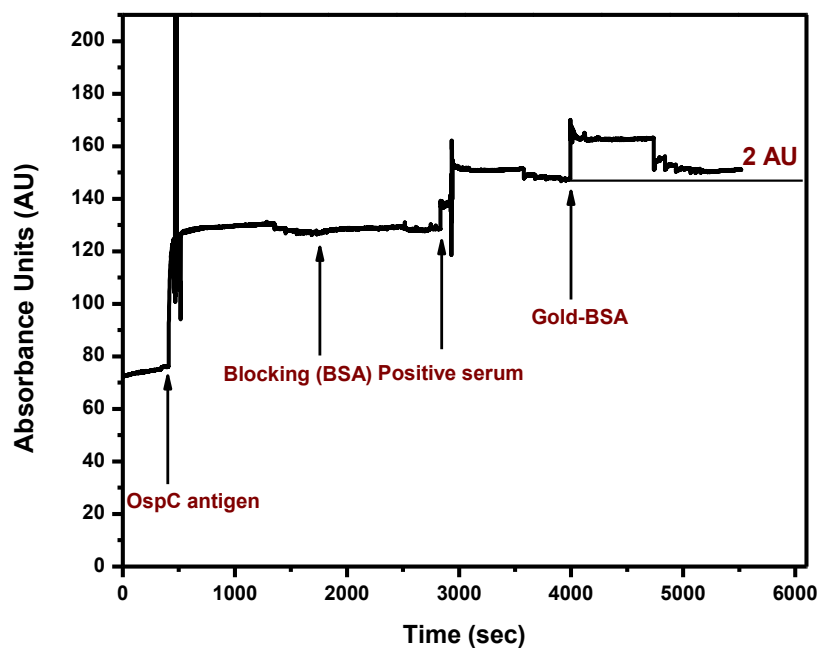
Figure 31 *Weak affinity of AuNPs blocked with BSA to antibodies on SPR chip. Antibodies in human serum sample were attached on the surface due to a specific interaction with OspC Borrelia antigen. Antigen has been hydrophobically adsorbed to SPR chip.*

Results

5.5.3 Detection using AuNPs modified with protein A

A second approach based on AuNPs integrated with the hydrophobically modified 3-DPESB was developed. The addition of the AuNPs modified with protein A after serum application allowed direct and convenient differentiation between positive and negative sera. In addition, loading silver enhancer solution after AuNPs could enhance the signal two times. AuNPs are able to reduce the silver ions on its surface to elementary silver, giving a strong absorption of visible light that in turn would improve the assay sensitivity.

Firstly, assay conditions were optimized using silver enhancer solution; one positive and one negative sera sample were used and results are summarized in Table 3.

AuNPs Dilution	Serum sample	Antigen (VlsE)	Optical density	Standard deviation
5 fold	Positive	3 µg / sinter body	0.436	0.004
5 fold	Negative	3 µg / sinter body	0.163	0.076
5 fold	Positive	5 µg / sinter body	0.577	0.069
5 fold	Negative	5 µg / sinter body	0.288	0.049
10 fold	Positive	3 µg / sinter body	0.21	0.021
10 fold	Negative	3 µg / sinter body	-0.018	0.019
10 fold	Positive	5 µg / sinter body	0.47	0.089
10 fold	Negative	5 µg / sinter body	0.041	0.012

Table 3 *Optical densities obtained after testing different dilutions of colloidal gold suspension and different concentrations of the immobilized VlsE antigen (3 and 5 µg / sinter body). One positive and one negative sera sample were used. Experiments 7 and 8 gave best results, 10-fold dilution of colloidal gold suspension and 5 µg VlsE for each sinter body (n=3).*

Best conditions were found with a 10 -fold diluted AuNPs suspension and a VIsE concentration of 0.5 µg per sinter body. For the positive serum, an optical density of 0.47 ± 0.089 (n=3) was observed, where as the negative serum gave 0.041 ± 0.012.

This means that the optical density of the negative serum is 10-fold lower than that of the positive serum. 2 more positive and 2 more negative sera sample were then tested using the optimized conditions; results are summarized with the corresponding 3-DPESB in Figure 32.

3-DPESB loaded with positive samples display with reddish grey color, which produced as a result of silver ions reduction on AuNPs surface. Whereas, 3-DPESB loaded with negative samples did not show any change in color. This significant difference allows the differentiation between positive and negative sera. In general, the background was found to be very low and the cut off level is at about 0.05, which is also very low. Differences between positive and negative sera are significant with analysis time 12 min.
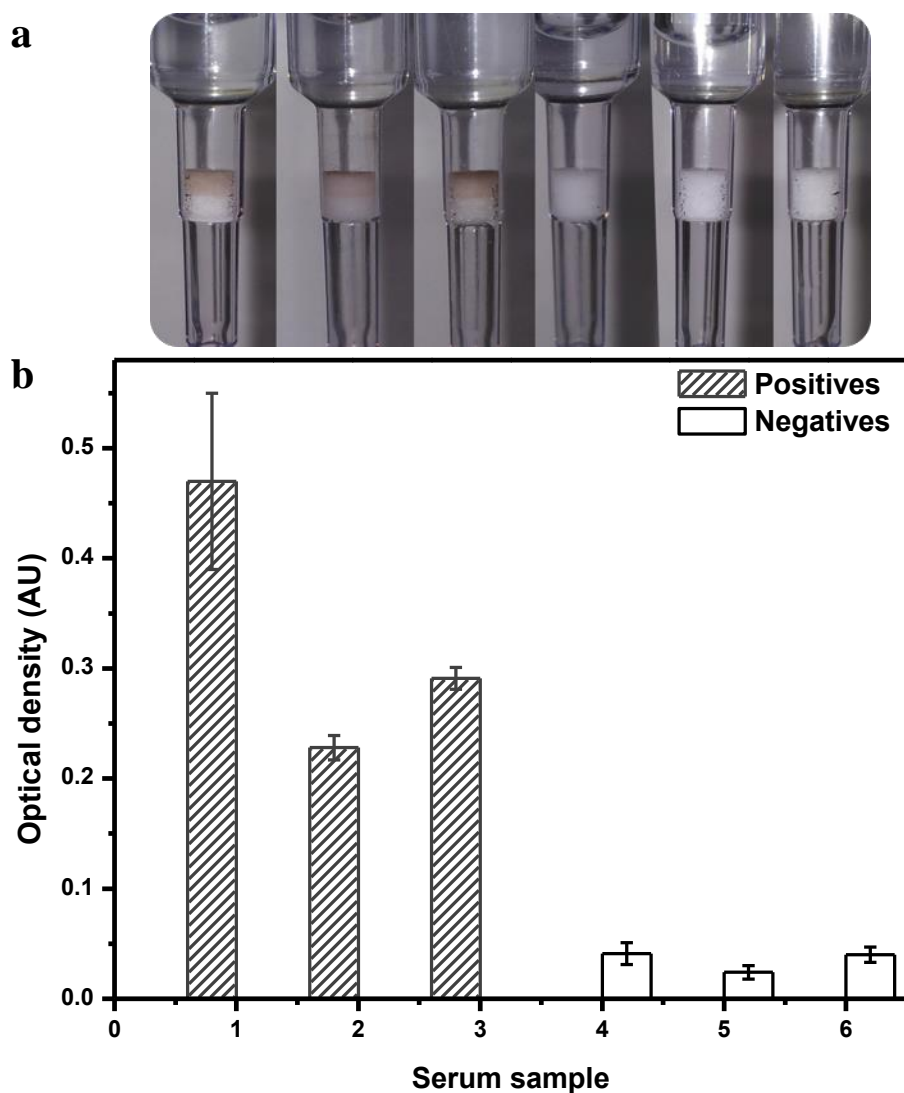
Figure 32 *(a) color development of 3 positive (left) and 3 negative sera (right) after detection with silver enhancer and (b) optical densities of the related sera samples after detection with silver enhancer at 650 nm (n=3).*

As alternative, absorbance intensities were measured directly after loading AuNP at 650 with exclusion of silver enhancer. The previously optimized conditions have been utilized; the direct detection of AuNPs resulted in lower signal intensity than the ones obtained from metallic silver. Optical density of 0.21 was acquired for a positive sample, in contrast to 0.47 when silver enhancer solution was added. However, as a huge advantage, direct detection of AuNPs results can be visibly observed exclusively after 5 min with convenient differentiation between positive and negative samples (Figure 33). More investigation could, however, enhance the signal in the same analysis time (5 min); this might be established with employing bigger nanoparticles or quantum dots for detection.
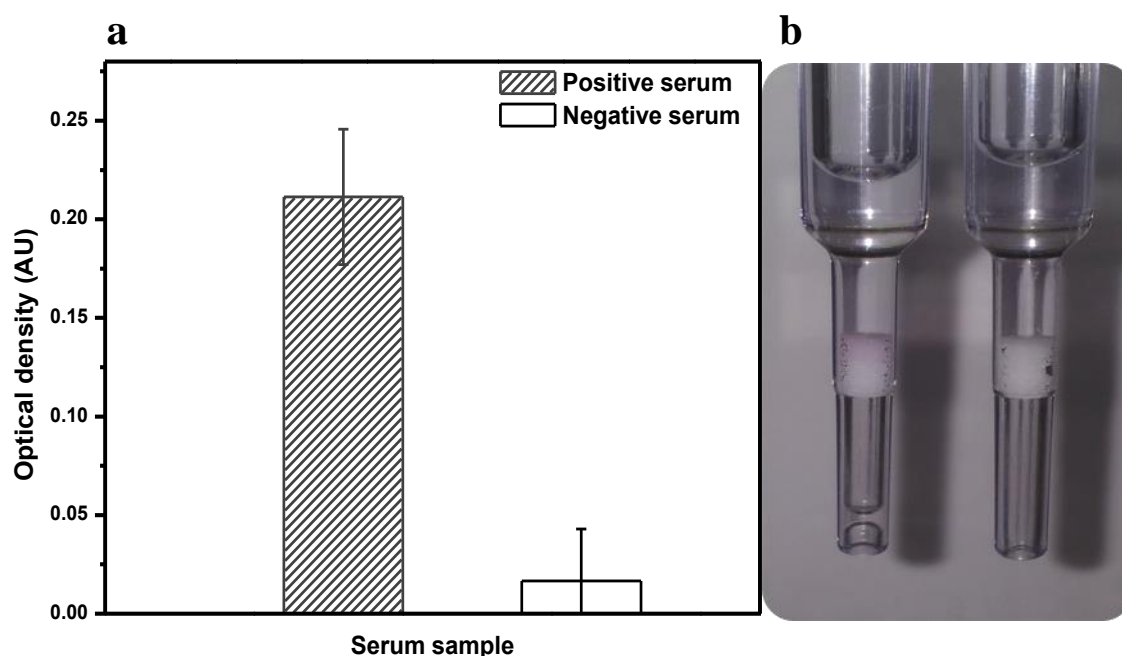
Figure 33 *(a) optical densities of the related sera samples after detection with gold nanoparticles at 650 nm (n=3), and (b) color development of one positive (left) and one negative sera (right) after detection with gold nanoparticles.*

5.6 Serological diagnosis using covalently modified 3-DPESB

Adsorptive immobilization of proteins on a hydrophobic surface is a convenient method. However, covalent immobilization provides more organized biomolecules layer; in effect, it would lower the steric hindrance effect, providing more sensitive and reproducible test.

Therefore, a covalent immobilization technique has been developed for the 3-DPESB modification. Polyethylene is rather resistant to most chemicals; therefore, its surface activation needs harsh and well-controlled conditions. In the here presented approach, hydroxyl groups were introduced to the 3-DPESB by UV photo grafting of 2-propenol at 254 nm over 6 h. Subsequently, N, N´-disuccinimidyl carbonate was used for hydroxyl-group activation. Finally, the VlsE antigen could be immobilized through free amino groups. In a final step, free binding sites have to be blocked by different reagents.

Different concentrations of the VlsE antigen, different concentrations of blocking reagents and different dilutions of serum sample have been tested to obtain the assay optimum performance. Best conditions were found at: 0.5 µg of immobilized VlsE antigen per sinter body, 40 mM ethanolamine for inactivation of active carbamate groups (for 35 min incubation), 0.5 % BSA + 5 % sucrose in PBS for blocking free binding sites (for 75 min incubation), and 500-fold serum dilution.

Again, HRP labeled secondary antibodies was used for detection. Employing the previously mentioned optimized conditions, positive and negative sera sample were examined; obtained optical densities with corresponding color development on the 3-DPESB are shown in Figure 34. Positive samples display with blue color, confirming the presence of the infecting agent. Negative samples display with colorless 3-DPESB. Difference between positive and negative sera can be considered significant. The cut off value for positive sera can be placed at optical densities between 0.15 and 0.2. Nevertheless, lower signal intensities were obtained in comparison to signal intensities obtained using the 3-DPESB modified with hydrophobic adsorption.

A second label, nanoparticles based on Sudan IV, was tested. Sudan IV is a synthetic dye; it has a maximum absorbance at 520 nm and displays with red color. Using the same assay optimized conditions, different dilutions of nanoparticle suspension were tested, 200, 133, 100, and 50-fold dilution. This step aimed to achieve the most sensitive and specific performance of the assay. 200-fold and 50-fold dilutions resulted in no significant difference between positive and negative samples. When 100 and 133 fold dilutions were tested, differentiation could be possible. Yet, the differences between positive and negative sera are rather low and could not be considered. More investigations are required to employ such nanoparticles on the proposed system. Depending on the solution, the cut off value has to be set between 0.2 and 0.3 (Figures 35 and 36).
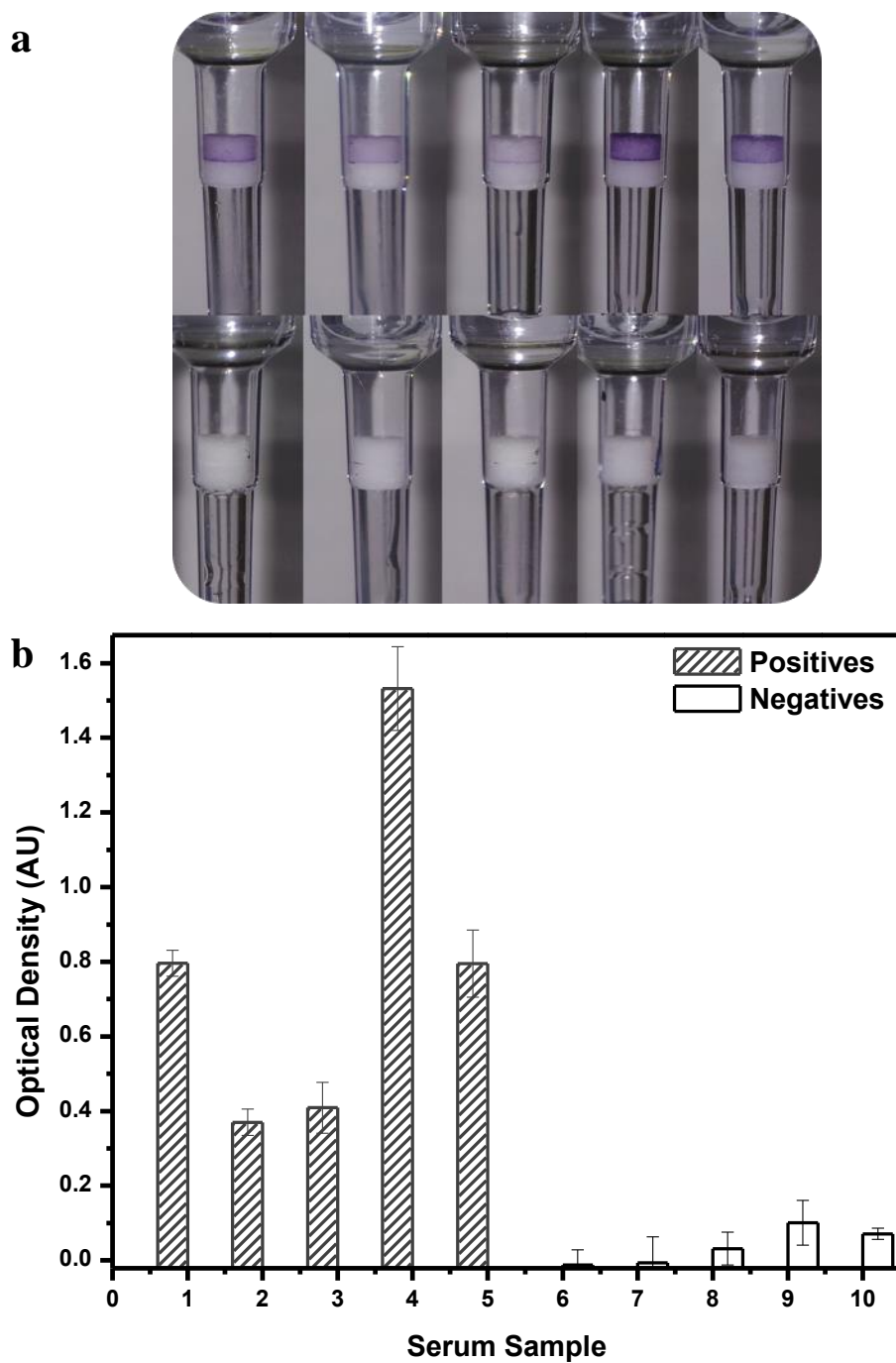
Figure 34 (a) *color development of 5 positive (upper row) and 5 negative (lower row) sera, and (b) related optical densities after performing the assay on covalently modified 3-DPESB. Detection was performed using HRP labeled secondary antibody and optical densities were measured at 650 nm (n=3).*
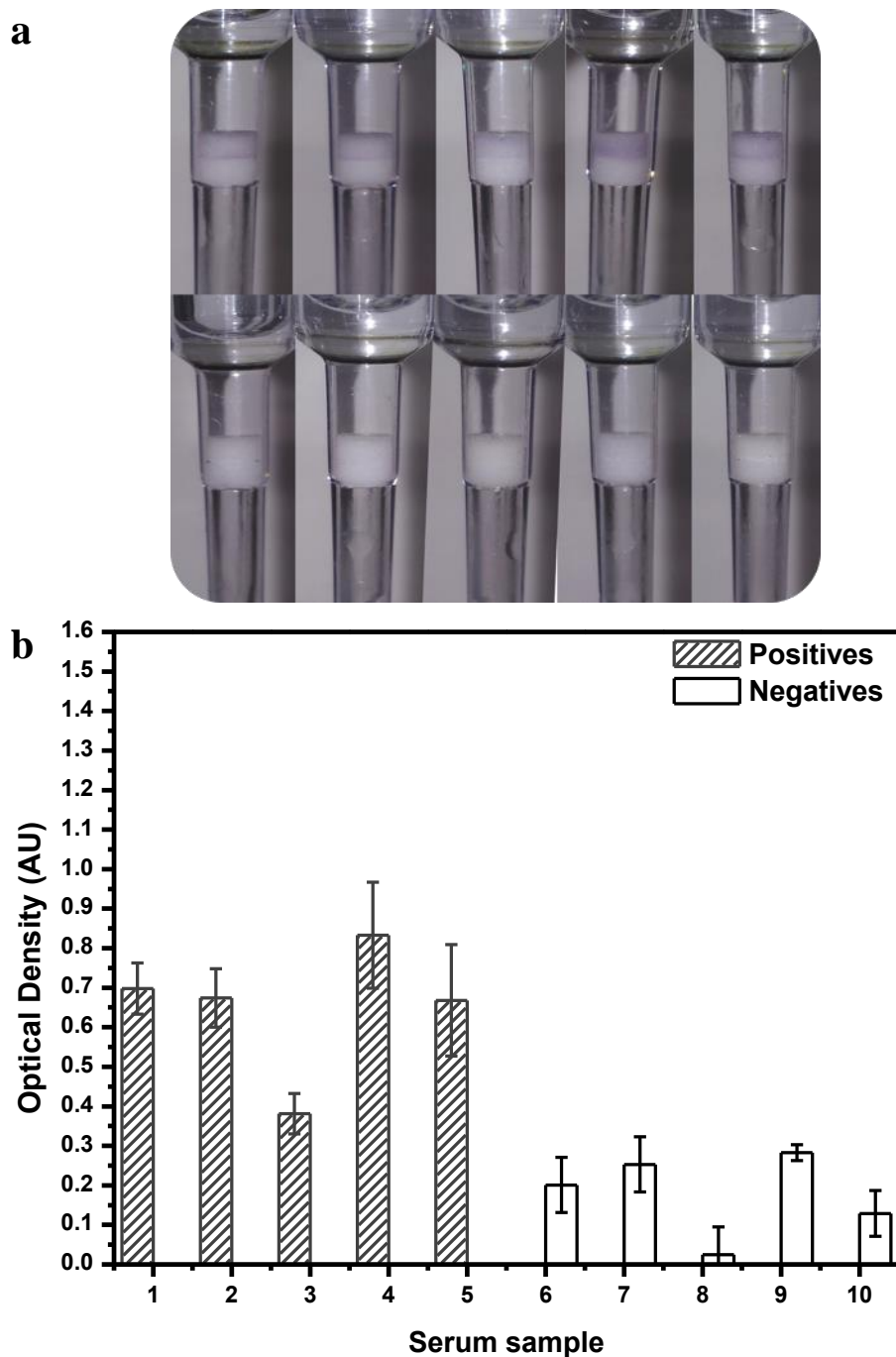
Figure 35 (a) *color development of 5 positive (upper row) and 5 negative (lower row) sera, and (b) related optical densities after performing the assay with streptavidin/Sudan IV/HRP nanoparticles in 100-fold dilution on covalently modified 3-DPESB. Detection of the blue TMB precipitate was conducted at 650 nm (n=3).*
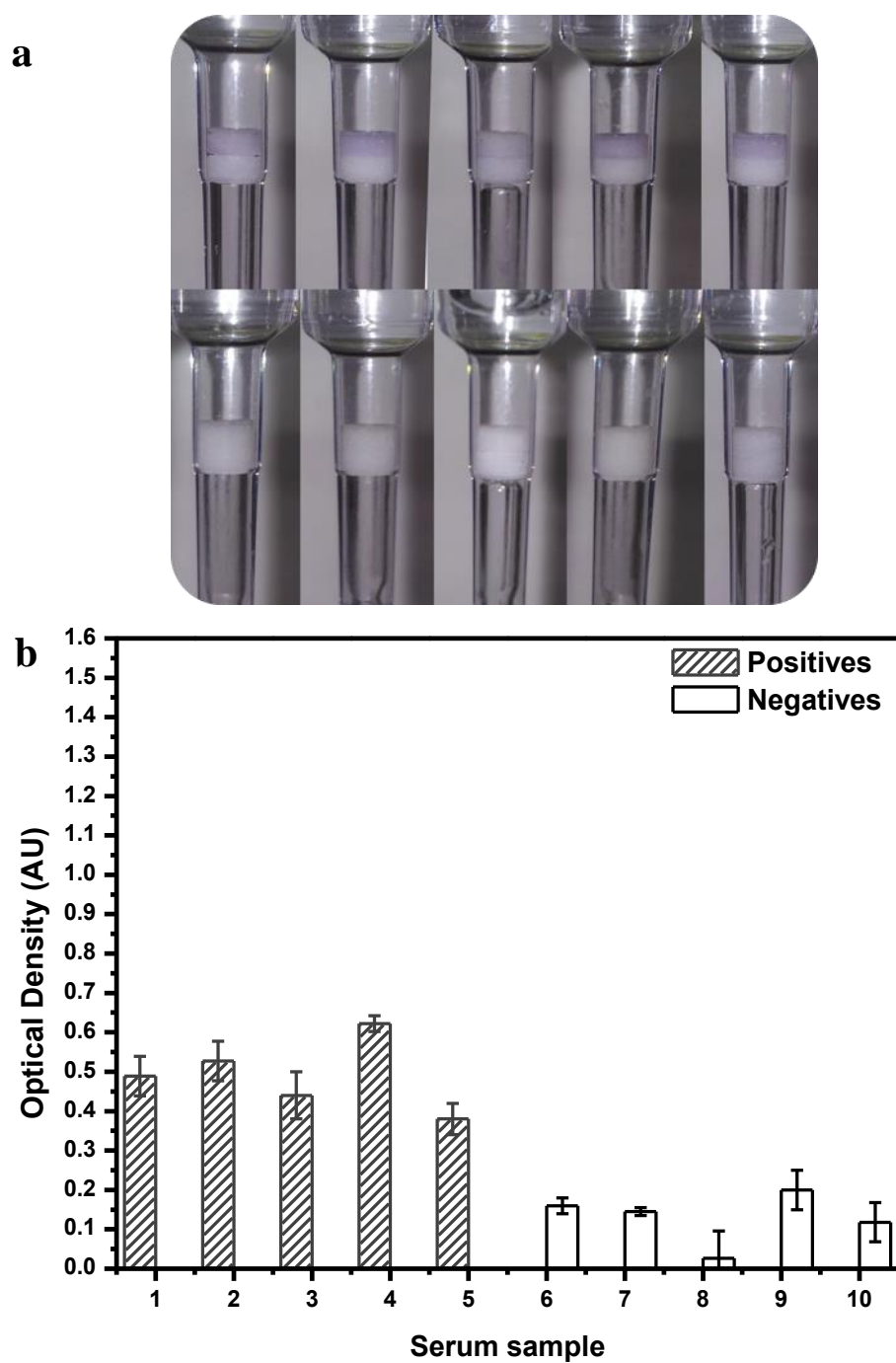
Figure 36 (a) *color development of 5 positive (upper row) and 5 negative (lower row) sera, and (b) related optical densities after performing the assay with streptavidin/Sudan IV/HRP nanoparticles in 133-fold dilution on covalently modified 3-DPESB. Detection of the blue TMB precipitate was conducted at 650 nm (n=3).*

5.7 Serological diagnosis using two-antigen modified gold nanoparticles

A second platform was proposed for rapid serological analysis; the developed method mainly employs AuNPs modified with two antigens, VlsE antigen and protein A, for diagnosis. To verify the test feasibility, three different sizes of AuNPs were synthesized and investigated. Synthesized nanoparticles showed maximum absorbance at 524, 527.5, and 531 nm, which are similar with previously reported absorbance measurements of AuNPs with average diameter around 20, 30, and 40 nm, respectively (Figure 37).
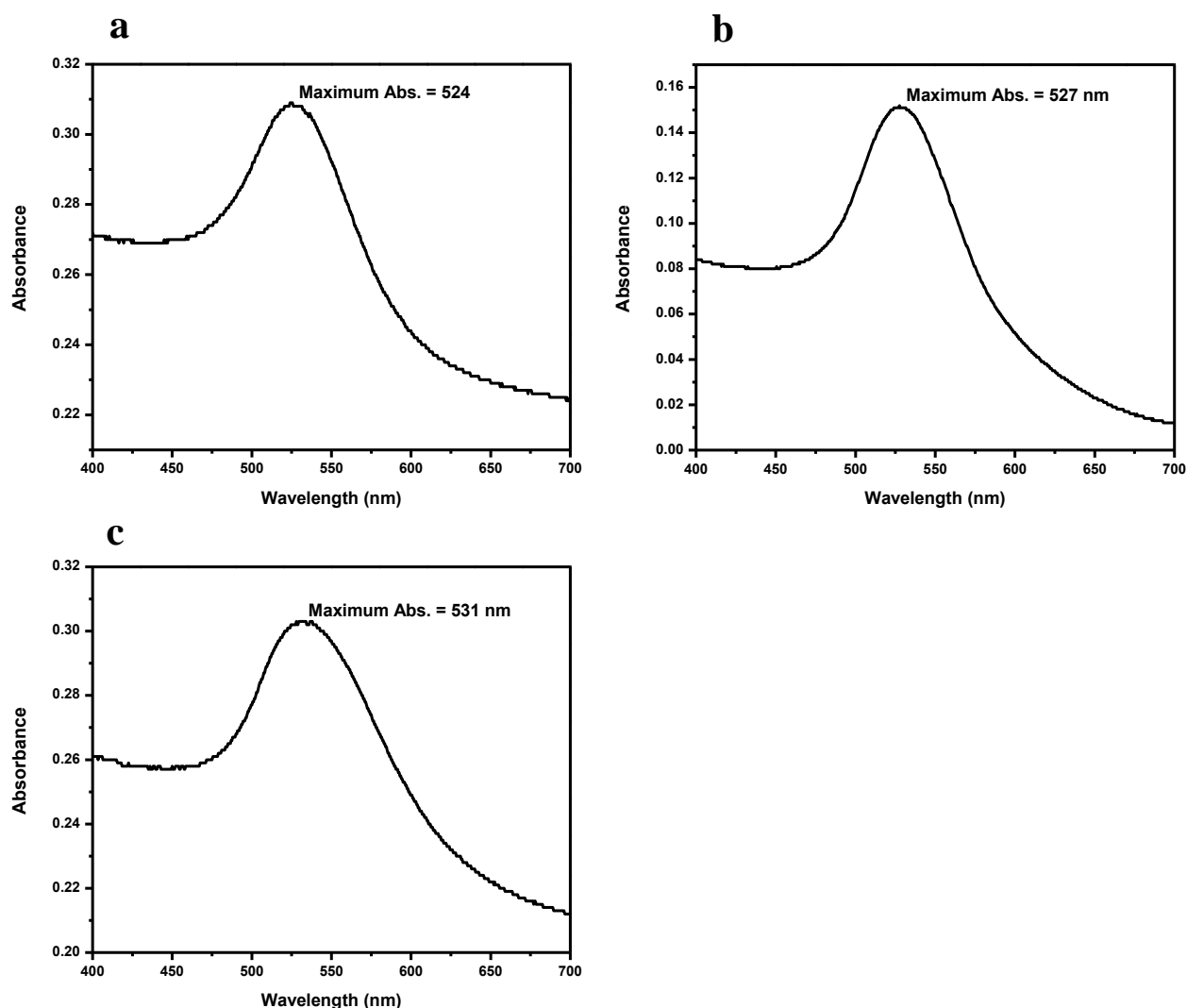
Figure 37 *UV-vis spectra of synthesized gold nanoparticles. 3 different sized have been synthesized, 20 nm AuNPs with maximum absorbance at 524 nm (a), 30 nm AuNPs with maximum absorbance at 527.5 nm (b), and 40 nm AuNPs with maximum absorbance at 531 nm (c).*

To modify the synthesized nanoparticles, covalent immobilization of the two antigens was utilized. Gold nanoparticles was capped with carboxyl groups using MUA at a first step (86). Then an EDC/NHS coupling reaction was pursued (109), which resulted in the attachment of antigens to the carboxyl groups on surface.

One positive serum and one negative serum were tested to confirm the feasibility of modified AuNPs as well as to optimize the assay conditions.

To select an optimal pH for the test, 50 mM phosphate buffer pH, 6.5, 7.4, and 8.7, were used to perform the assay. The different pH values, 6.5, 7.4, and 8.7, were examined based on the fact that the maximum equilibrium constant of antibody-antigen interaction in solution can be obtained between pH 6.4 and pH 8.7 (110, 111). AuNPs and serum sample were incubated in the buffer with the desired pH. UV-vis spectra were then recorded.

When phosphate buffer pH 7.4 was used, significant difference in absorbance between AuNPs incubated with positive sample and AuNPs incubated with negative sample was observed. The difference, as explained, is due to aggregation of AuNPs because of compatible antibodies found in positive serum.

UV-vis spectra were recorded after 3 h incubation. A red shift, 4 nm, in the maximum absorbance and broadening in the absorbance band in the region between 550-680 nm of AuNPs incubated with positive sample was seen as expected; on the other hand, no significant difference could be observed when pH 6.5 or pH 8.7 was used (Figure 38). The absorbance band in the region between 550-680 nm of AuNPs incubated with positive and negative were similar. This shows that there was no aggregation when positive serum was tested. PBS buffer pH 7.4 has been used further for all optimization steps.
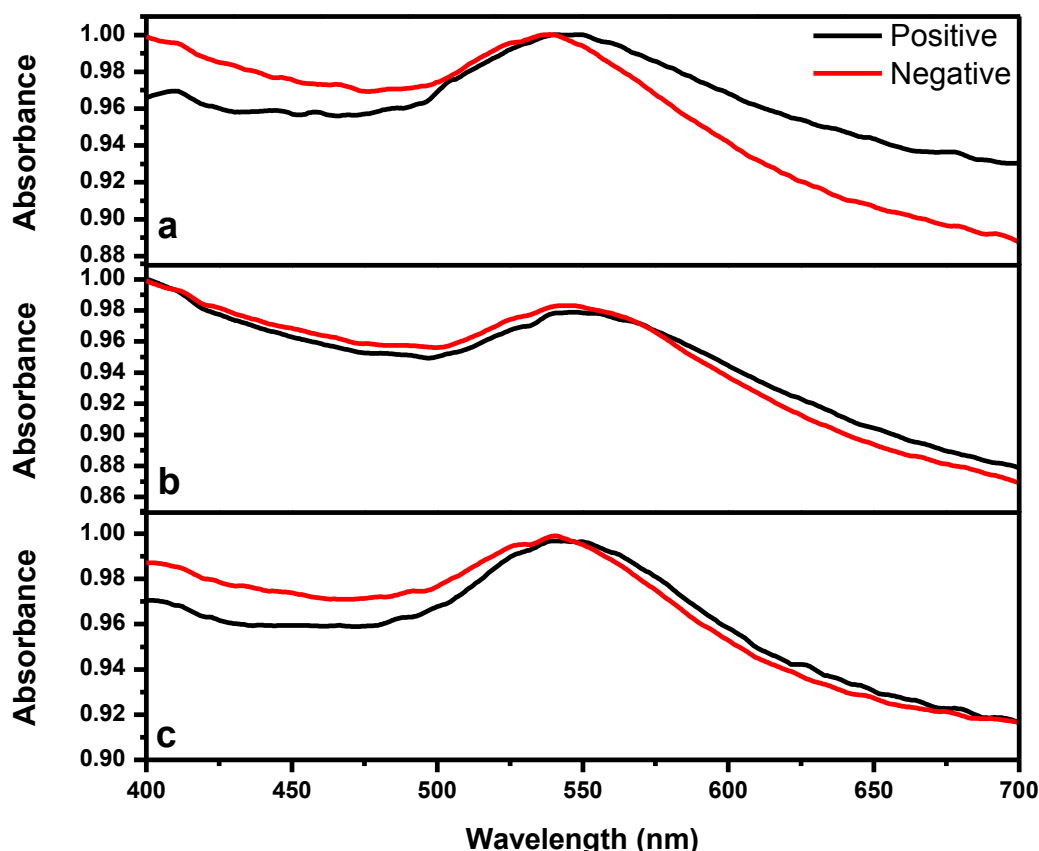
Figure 38 *Normalized UV-vis spectra of 20 nm AuNPs after 3 h incubation with positive serum (black) and negative serum (red). Spectra show the behavior of modified AuNPs at different pH values, 7.4 (a), 6.5 (b) and 8.7 (c). 50 mM phosphate buffer was used.*

Additives such as salt speed the protein interaction in solution. In the here case, effect of ionic strength was investigated on the assay incubation time. 50 mM and 100 mM NaCl were added to the phosphate buffer. Using the prepared buffers, 3 h incubation was necessary also to observe a difference in color. It seems that increasing salt concentration had no effect on the proteins interaction (Figure 39).

Moreover the aggregation of AuNPs caused by the positive sample was rather low when 50 mM NaCl was used; besides, 100 mM NaCl hindered and prevented the protein interaction (positive serum showed no effect on the AuNPs).

50 and 100 mM NaCl could be considered very high concentrations, which lower the affinity between proteins; or else the interaction between proteins seems to be less dependent on those high salt concentrations (112).

Figure 39 *Normalized UV-vis spectra of 20 nm AuNPs after 3 h incubation with positive serum (black) and negative serum (red). Spectra show the behavior of modified AuNPs at different NaCl concentrations, 0 mM (a), 50 mM (b) and 100 mM (c). 50 mM phosphate buffer was used.*

25-fold dilution of serum sample was used in the previous experiments. At this dilution, maximum absorbance intensity at 590 nm was measured when AuNPs were incubated with the positive sample. A calibration curve was needed in order to evaluate the test sensitivity; so absorbance intensities were recorded to different dilutions of a positive sample at 590 nm (Figure 40). At higher serum concentration, higher aggregation of nanoparticles was detected, which appeared as increasing in the absorbance intensities.

A good linear range could be obtained between 25 and 60-fold dilution with R-squared = 0.96144. Higher dilution (120-fold dilution) resulted in very low signal, which could not be considered for the calibration. 80-fold dilution as a limit of detection was calculated for the presented assay. The sensitivity seems to be low and developed ELISA assay showed better sensitivity (113). However, the sensitivity of such platform could be considered convenient. More investigations could, however, improve the sensitivity further.
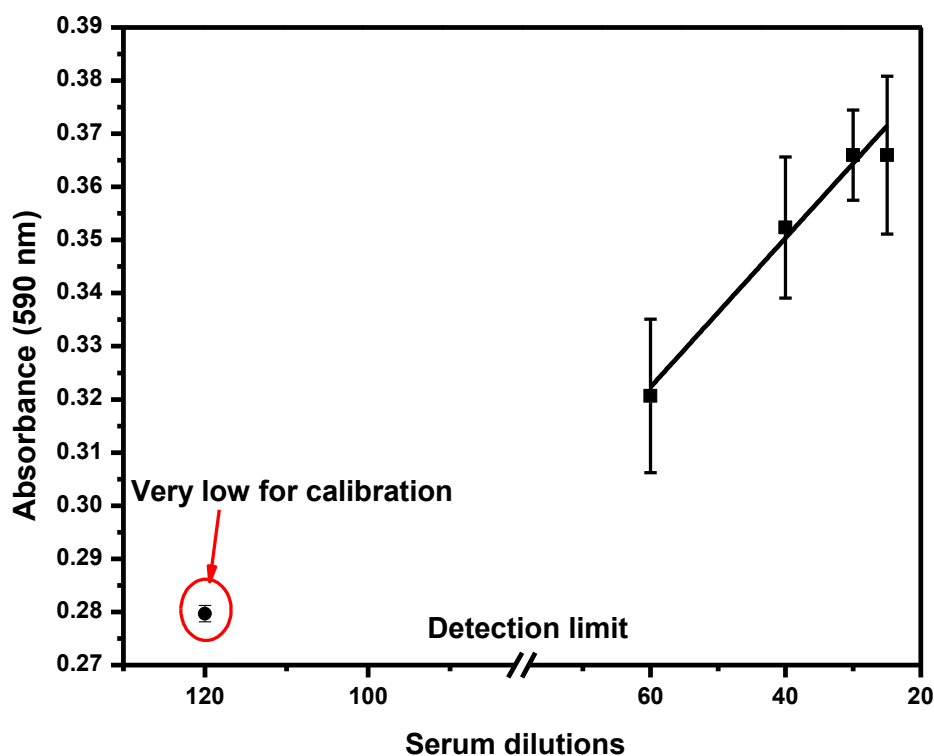
Figure 40 *Plot of absorbance intensities of modified 20 nm AuNPs at 590 nm after 3 h incubation with different dilutions of positive serum. Linear range obtained between 25-60 fold dilutions with R-squared = 0.96144. Higher dilution (120-fold) resulted in very low signal, which could not be considered.*

The main objective of the presented work was to develop a colorimetric test valid for point of care testing; that means a clear difference should be easily observed using naked eyes. The previous experiments showed a slight difference in color between positive and negative samples. Therefore bigger AuNPs sizes, 30 nm and 40 nm, were further tested as a trial to enhance the proteins interaction. Modified 30 nm AuNPs showed very promising results. Aggregation of AuNPs caused by positive samples could be easily observed using naked eyes. In addition, negative sample had no visible effect on AuNPs. 30 min incubation and phosphate buffer with 50 mM NaCl were necessary in the here case. Visual observation of AuNPs confirms the accumulation of particles to each other after incubation with positive samples; this could be due to the specific interactions to antibodies (Figure 41a).

UV-vis spectra showed also very low absorbance intensity and broadening of absorption band in the absorption region between 550 nm-680 nm of AuNPs that incubated with positive serum (Figure 41b). The shorter time could be due to the bigger size that enabled faster access to antibodies. This assumption was confirmed when 40 nm AuNPs was aggregated because of positive serum after 1 min.
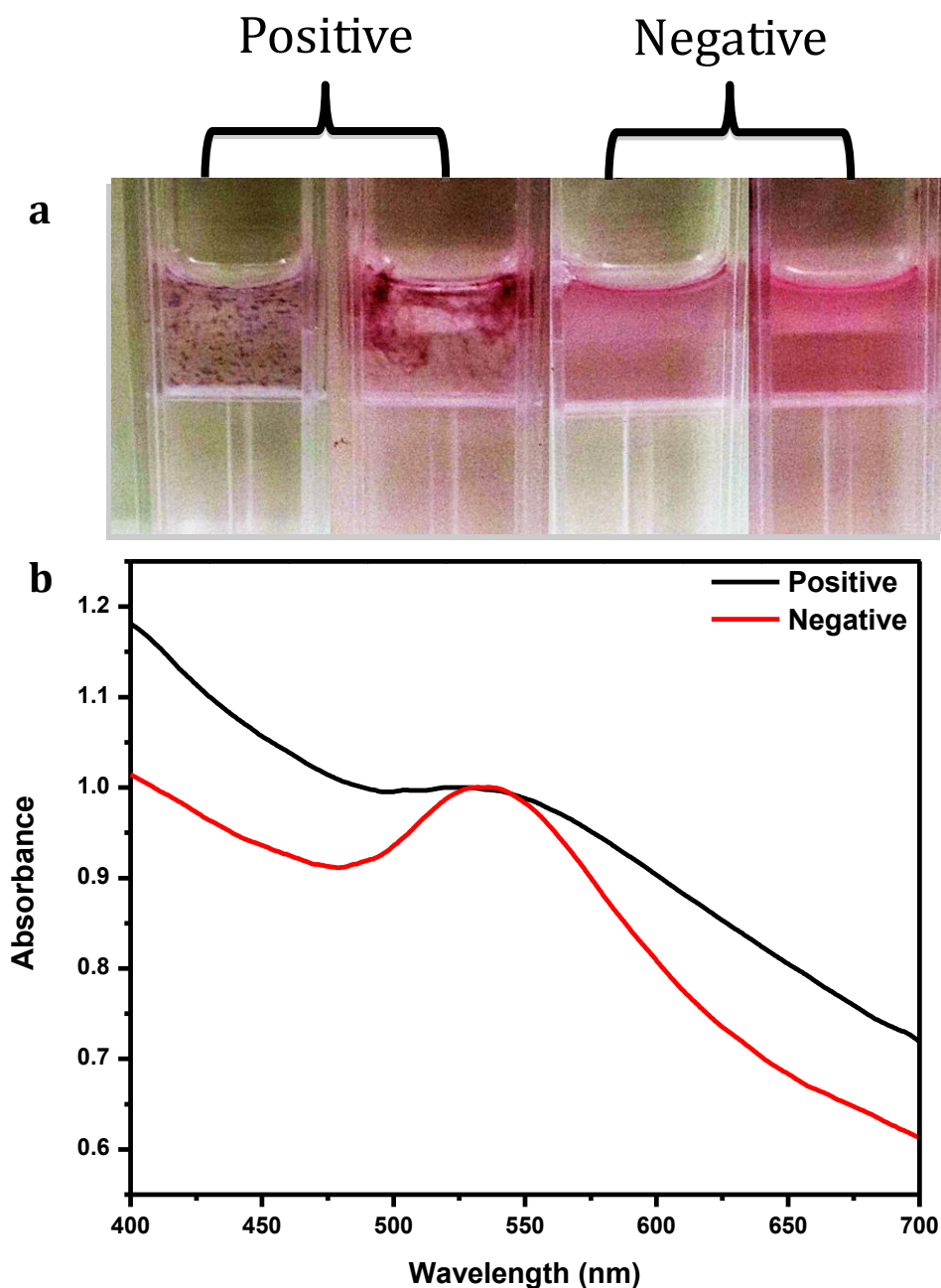
Figure 41 *(a) color development of 30 nm AuNPs after 30 min incubation with two positive sera (left) and two negative sera (right), and (b) normalized UV-spectra of 30 nm AuNPs incubated with one positive (black) and one negative (red) sera samples (b).*

Modified 40 nm AuNPs showed shifting in maximum absorption (25 nm) and broadening in the absorption band in the absorption region between 550 nm-680 nm when incubated with positive serum after only 1 min (Figure 42).

A significant difference between the positive and negative samples can be recorded using spectrometry measurements, however, a slight difference was visible using naked eyes.
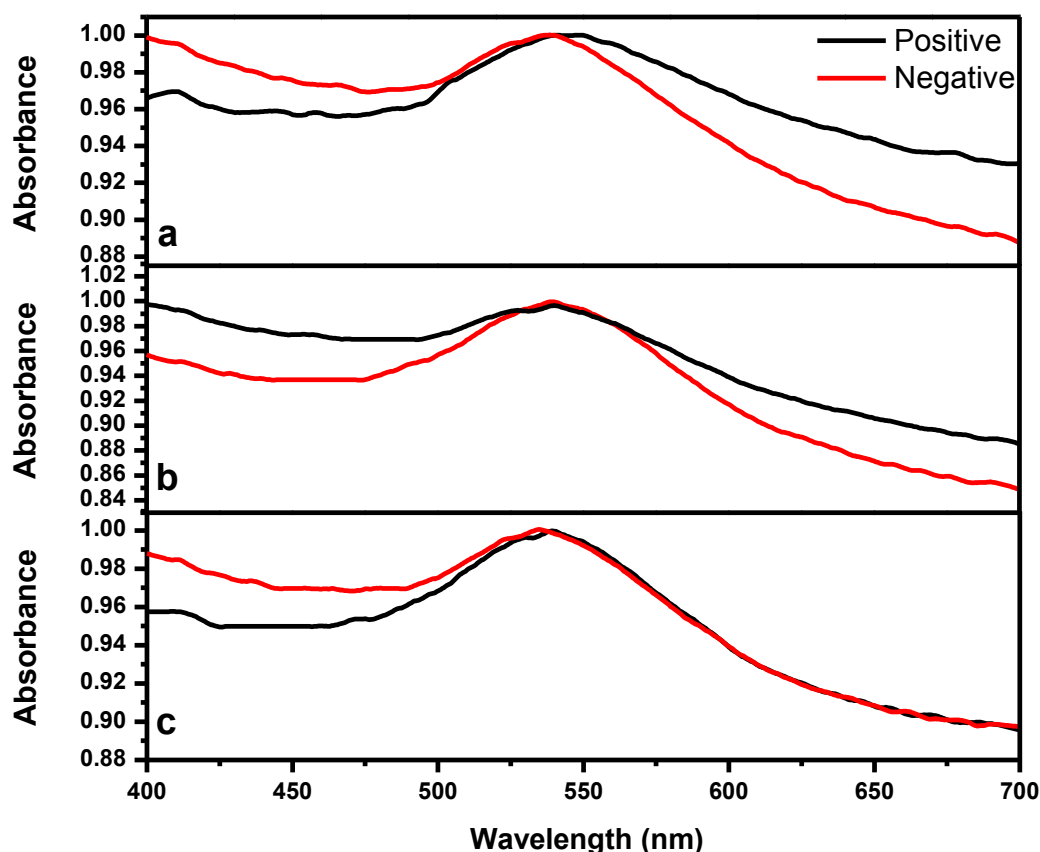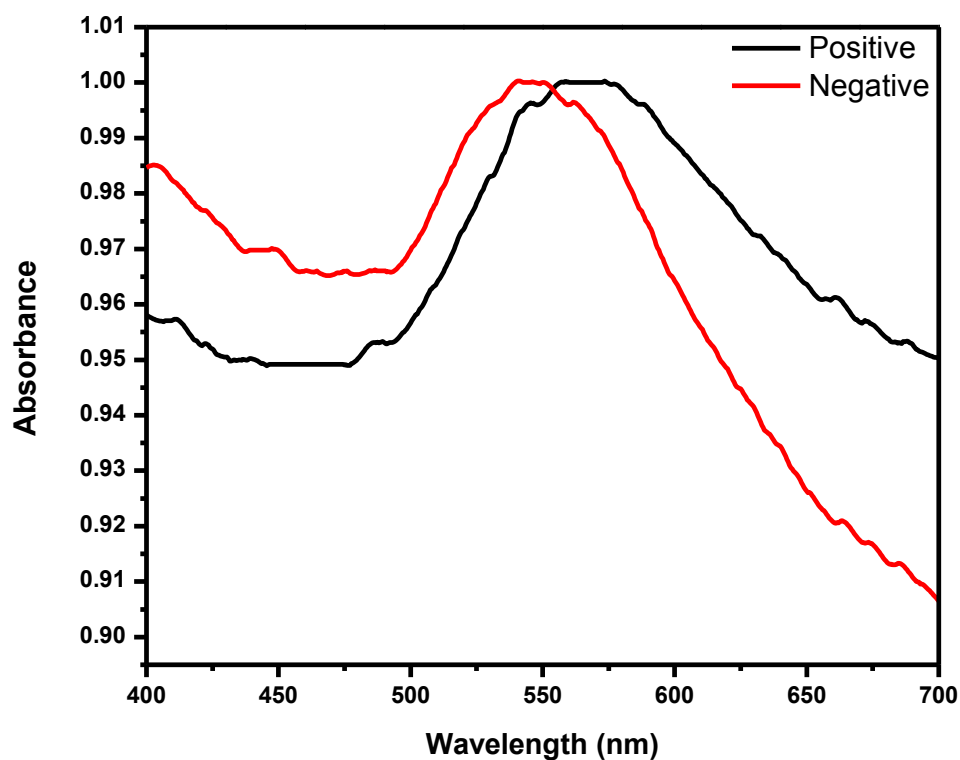

Figure 42 *Normalized UV-vis spectra of 40 nm AuNPs incubated with positive sample (black) and negative serum (red). Spectra recorded after 1 min incubation.*

6   Discussion

Serologic tests developed to detect antibodies directed to *borrelia burgdurferi* come mainly as a confirmation of the disease. Serologic diagnosis, as recommended, should be performed using a two-tiered testing in order to avoid the false positive results that caused by the cross-reaction with other spirochete infections (61). A first test should employ a sensitive enzyme immune assay for screening, followed by a western blot test for confirmation. Two-tiered testing is highly specific (95%-100%) and highly sensitive (>90%) in late stages of Lyme disease (114). As a drawback, it has low sensitivity in the early acute phase of the disease; besides, it is time consuming and labor intensive. Many studies have been focusing on developing alternatives to the two-tiered testing, which should be more rapid as well as they should be more specific in the early stage of the Lyme disease. Alternatives could be established in one-tier manner that are principally based on using highly specific recombinant antigens or synthetic peptides for antibodies detection. Such antigens offer the high specific detection of disease even in early stages; also they show low cross-reaction with other spirochete infections.

Bacon, et.al, developed a one-tier testing that is equal or exceed the performance of the two-tiered testing for detecting antibodies directed to *borrelia burgdorferi* (115). The assay is based on measuring IgG antibodies directed to, recombinant VlsE antigen (rVlsE1), a 10-mer conserved portion of OspC (pepC10), or a synthetic peptide C6 region of VlsE antigen. It was performed on ELISA microtiter plates and results revealed that the assay is simpler and more readily standardized than two-tiered analysis. The assay showed high specificity for detecting antibodies (99%) for the recombinant VlsE antigen and for the synthetic peptide C6.

Likewise, immunoblot assay could be performed based on using recombinant antigens of *Borrelia* burgdorferi, *Borrelia* afzelii and *Borrelia* garinii such as p100, VlsE, p39, OspA, OspC, p41. The test showed promising results and could be used as alternative to the two-tiered testing (116).

A second approach has been developed, which is based on using a multiplex assay technique; it showed also better results than two-tiered testing. Porwancher, et.al, developed a new multiplex immunoassay for detection of both VlsE1-IgG and pepC10-IgM antibodies simultaneously using the AtheNA Multi-Lyte test in a multiplex system (117). The test is a sandwich immunoassay based on flow cytometric separation of fluorescent micropaticles by use of Luminex xMAP technology (118); where the recombinant antigens are covalently bound to the microparticles before performing the test. The test showed specificity 95-100%

for the recombinant VlsE antigen. The multiplex technique can perform multiple antibody assays with the same serum sample. The technique, in addition, is able to distinguish up to 100 separate reactions in a single run.

A third approach can be considered also was developed based on a fully automated random-access Liaison analyzer, which employs two-step chemiluminescence immunoassay technology for Lyme borreliosis diagnosis (99). The operation of Liaison analyzer is straightforward, flexible and can be used as alternative to conventional immunoassays. The test showed overall specificity for the recombinant VlsE antigen (98%) and for the peptide C6 (97.8%).

Yet the abovementioned assays, which are considered most recent and most common approaches for diagnosis of Lyme disease, are time-consuming need lot of incubation steps and are not suitable for rapid point of care testing (100). For example, the multiplex based test needs several steps including mixing using shaker, vortexing and sonication as well as the several long incubation times of reagents (30 min each). In addition, the covalent immobilization of antigen on microparticles is needed before conducting the assay. The microtiter ELISA based assays and immunoblot assays need long incubation time to provide the results, 12- 24 hours. The Liasion *Borrelia* test is advantageous over others in terms of assay time; the test can be performed in 60 min; yet the analyzer needs well-trained personnel to perform the test and interpret the results.

All the abovementioned alternatives are performed in a stationary manner, which in turn require large volume of the sample as well as high concentration of the analyte. This is considered unfavorable in case of studies with limited sample volume or when the sample needs to be further tested. For example, ELISA on microtiter plates applies serum with dilution 1:100, multiplex assays require serum with dilution 1:21, immunoblot assays load serum with dilution 1:200, and the Liasion test requires serum with dilution 1:100.

In our investigations, new assays based on one-tier testing could be developed with high selectivity behavior for diagnosis of Lyme disease. This returns to the used recombinant VlsE antigen and the synthetic peptide C6 region of VlsE antigen, which induce a strong and specific antibody response that can be detected from early to late phase during the disease in humans infected with *Borrelia burgdorferi* or with European genospecies including *Borrelia afzelli* and *Borrelia garlnii*. Simultaneous, they show low cross-reaction with the other non-pathogenic *Borrelia* strains.

Discussion

In our work, VlsE and C6 antigens could be utilized, enabling the specific recognition of anti-*Borrelia*-antibodies in shorter analysis time and more sensitive manner than ELISA, immunoblot, multiplex-based assays, and chemiluminescence Liaison analyzer based assays. Our developed assays take around 5 to 30 min to obtain the results. They are easy to handle and cost effective. Besides, they are very rapid and suitable for point of care testing. Developed immunoassays are considered superior over the conventional methods in terms of analysis time, sensitivity, and the very small volume of the sample.

The main element in our development was to employ new platforms, on which the interaction should be conducted. 3-DPESB with dimension of 2×2.5 mm could be used as the first platform in an immune affinity flow system based on a little disposable plastic column (ABICAP^{TM}) (119). ABICAP^{TM} based assays are advantageous in terms of rapidity, easiness and specificity. The flow of reagents through the column, which depends mainly on gravity, is advantageous because incubation steps can be eliminated, reducing the nonspecific interaction and shortening the test time. In addition, large sample volumes can be applied when needed, providing an increased sensitivity by means of enrichment of the analyte through immune separation. A visible detection of analyte is also likely, allowing colorimetric point of care testing.

VlsE and C6 antigens could be easily immobilized on 3-DPESB surface. The used immobilization techniques provide the long storage time of the antigen-modified platform at 4 °C. Hereby, the assay starts by applying the serum sample and any prior steps are unnecessary; this is superior over the conventional methods in terms of the quick and easy performance. The 3-DPESB can be either placed in a miniaturized cartridge as used in the here presented investigation or alternatively placed in a pipette tip ('Dia Tip'). In the latter case, a programmable electronic pipette or a pipette robot is required. Further on, required instrumentation (pipette, simple hand-held photometer with one or two wave length) is simple and inexpensive so that this assay format is suitable for POC diagnostics even under difficult conditions in developing countries.

Our results showed that, VlsE-modified 3-DPESB coupled with HRP labeled antibody as a label offered very high sensitivity for detecting antibodies directed to *Borrelia* in human sera samples, particularly when hydrophobic adsorption of VlsE was used. This approach offered the highest sensitivity among our developed approaches. The hydrophobic immobilization seems to be very promising with such 3-D structural; it seems to preserve the antigen structure and activity, providing a maximum performance. The overall performance of the assay seems to be superior. Antibodies could be detected in 1000-fold dilution of sera

samples with very short time for the entire analysis (20 min). Also the limit of detection can reach 2000-3000 -fold serum dilutions.

For 16 of the 17 positive sera there is a clear differentiation from the negative sera in addition there was no false positive out of 20 negative samples (Section 5.5.1). There is only a problem with sample 11, which is false negative. The reason for this needs further investigation. It might be possible that the *Borrelia* infection represented by this serum is atypical or the VIsE antigen on the *Borrelia* cell wall shows some modifications leading to antibody production which cannot be detected by the used recombinant VIsE antigen. Therefore it can be recommended to use at least one further antigen structure like the Decorin binding protein A (DbpA), outer surface protein C (OspC) or the *Borrelia* membrane Protein A (BMPA) for safe detection.

Results showed also when VlsE covalently immobilized on 3-DPESB surface, detection of antibodies using HRP labeled antibody was possible in 500-fold serum dilution with analysis time 20 min. Taking into account that higher amounts of VIsE antigen were necessary for covalent immobilization and the dilution of the serum sample was lower, there seems to be no overall advantage of covalent immobilization in the assay performance. Nevertheless, the assay seems to be promising and showed better results than the conventional serologic tests; the difference between negative and positive sera is significant. It can be suggested that the storage properties of the covalently modified 3-DPESB are better.

From results it is clear that lower signal intensities were obtained comparing to the 3-DPESB hydrophobically modified with VlsE (Section 5.6). The reason could be due to a loss in the antigen activity, which could be caused by the used coupling method. The antigen could be immobilized through more than one functional group; this could cause a conformation in the antigen's active region and loss of its activity.

A highly sensitive and selective detection of anti-*borellia* antibodies could be accomplished using HRP labeled secondary antibody. A blue TMB-precipitate was produced when Borreliosis-positive sera were applied. The antigens could recognize anti-*Borrelia* antibodies in serum sample; in effect HRP labeled antibody could be attached to the surface when loaded, enabling afterwards the oxidation of the TMB solution. This resulted in producing a blue precipitate, which can be detected at 650 nm. On the other hand, only little coloration was visible when negative sera were tested, suggesting the absence of the anti-*Borrelia* antibodies from samples. Using alternative labels like fluorescence should increase sensitivity even further.

Discussion

In our work we were able to perform the serologic test only in 5 min with good specificity, which is considered as a huge advantage. VlsE-modified 3-DPESB coupled with AuNPs as a label provides a specific detection of antibodies in 250-fold dilution of serum sample in 5 min. The obtained signals are not considered high but the specific detection could be considered significant, particularly after the visible observation of both positive and negative samples. A clear difference can be seen using only naked eyes (Section 5.5.3). AuNPs display a reddish color so that direct detection of AuNPs absorbance at 520 nm should be possible. However, with the used photometer optical density was too low. In contrast detection at 650 nm gave better results. This might be caused by the structure of the used polyethylene, which is not transparent but opaque. It could be also due to aggregation of AuNPs on the 3-DPESB surface; the aggregation in turn caused a shift in the AuNPs absorbance to higher wavelength, at the region between 600 and 680 nm. Thus, results could be recorded with higher intensities at 650 nm. Adhesive AuNPs on 3-DPESB could be seen as a light red color when positive sample was tested. This could be attributed to the specific interaction of AuNPs with the recognized antibodies. In contrast, the final washing step could remove all AuNPs from the column, leaving a colorless 3-DPESB when negative sample was tested; this in turn confirmed the lacking of the antibody-antigen interaction. Signal might be further enhanced with the same analysis time if bigger nanoparticles or quantum dots would be used; this should be further investigated.

Additional advantage when using AuNPs as a label is the ability of AuNPs to catalyze the reduction of silver ions to elementary silver, giving a strong absorption of visible light. Results showed that detection of metallic silver produced after applying a silver enhancer solution improved the test sensitivity with analysis time only 12 min. As advantage of detecting gold nanoparticles or elementary silver, background was found to be very low; somehow, AuNPs enhance the specific interaction of the immobilized protein A with the detected antibodies. The reason could be due to the big size of AuNPs compared to conventional labeled proteins. The big size of AuNPs seems to overcome the weak unspecific interaction, moving all unbound AuNPs with the washing buffer out of the system.

As an interesting alternative, nanoparticles consisting out of Sudan IV, streptavidin, and HRP were used for detection. Sudan IV is a synthetic dye that displays with red color. It has an absorbance at 520 nm. TMB substrate can be oxidized by HRP on the nanoparticle surface giving a blue precipitate with absorption at 650 nm. In effect, these nanoparticles allows a simultaneous detection at two different wavelengths. This can be achieved using ABICAP[TM]

photometer, which facilitates the measurements at two wavelengths, 520 and 650 nm. Yet, Sudan IV particles absorption at 520 nm was too low for detection; only the blue TMB precipitate could be evaluated at 650 nm. Results showed that detection using such nanoparticles was not beneficial in our system. Very high background was observed, which limited further testing of the nanoparticles (Section 5.6). The reason for the high background could be related to the functionalization method of the nanoparticles. Hydrophobic adsorption of biomolecules was conducted; a protective layer of bovine serum albumin was adsorbed at a first place on Sudan IV particles, then HRP enzyme and anti-human biotin antibody were immobilized by hydrophobic manner. The affinity of BSA to the fat-soluble dye, Sudan IV, might not be strong enough to preserve BSA on the surface. BSA could be washed away by buffer solutions, exposing the particles surface. Thus non-specific interaction of nanoparticles to the surface might be occurred. In summary, the use of the multi-functional streptavidin/Sudan IV/HRP did not give any advantage. In theory, simultaneous detection of the Sudan IV at 520 nm and the polymerized TMB at 650 nm should be possible, but failed with the used real human samples.

In our work we showed also a development of a second approach, which is based also on ABICAP$^{\mathrm{TM}}$ technology; the proposed approach utilize the high specific interaction between the ConA lectin and the mannan polysaccharides. A fusion protein containing the antigen C6 part and the ConA part could be immobilized by self-organization on 3-DPESB surface modified with mannan; this resulted in a good accessibility of the *Borrelia* C6 antigen. In consequence testing human sera samples was performed in a simple and convenient ABICAP$^{\mathrm{TM}}$ format, allowing POC diagnosis. Results revealed that the fusion protein with C6 antigen part produced in our group showed similar specificity like the commercially available recombinant VlsE antigen. The test takes 20 min only and detection using HRP labeled antibody offered also excellent sensitivity; 1000-fold dilution of sera could be tested with high specific interaction (Section 5.4). Employing mannan modified 3-DPESB and a fusion protein is considered generic because a huge variety of protein structures can be linked to the ConA moiety in a similar manner as here presented. Outer protein sequences of pathogenic bacteria and viruses (like Zika virus) can be easily fused to the ConA moiety and a serological assay on the here presented platform can be established within a couple of weeks. This is of huge importance in case of an unexpected outbreak like Ebola in 2014 and Zika in 2015. As a further advantage of the method, the protein component is added shortly before the assay is started. Storage conditions can be specifically adapted to the need of the 3-DPESB and the fusion protein separately.

Discussion

The ABICAP[TM] technology has been used in the development of some immunoassays, e.g. the rapid diagnosis of Ebola virus infection (120) and the detection of *Yersinia pestis* (121). Yet, the used platform (3-DPESB) in the here investigations is smaller in size, which has not been previously studied. The small size would provide a cost effective and more rapid assay due to the lower amounts of proteins that are required to establish the assay. Polyethylene has been proposed as a convenient and inexpensive carrier in integration with the ABICAP[TM] technology. Granular material can be easily brought in different shapes, even with complex geometry. For our investigations, small porous cylinders with a diameter of 2.5 mm were chosen for the immunoassay. A porous polyethylene surface enables a smooth flow of the sample even with whole blood. Moreover, the large surface area allows high stable immobilization of proteins even by hydrophobic interactions.

As a disadvantage, covalent immobilization of biomolecules on polyethylene surface is only possible after surface activation. However, electromagnetic waves, plasma and highly reactive gases like ozone can be used to accomplish the surface activation. The activation of polyethylene has been easily achieved in our work using UV irradiation. The UV irradiation enabled, in addition, the activation of the inner surface of the small 3-DPESB over several hours, which has been proved by staining experiments. In effect, sufficient amounts of biomolecules can be immobilized, which enhance the test sensitivity further.

Our results showed the potential to develop a third approach that showed promising results and can be used as alternative to the conventional serologic tests. This approach employed AuNPs successfully to carry antigens; simultaneously it acted as a label for detection. As reported in literature (122), color of two gold nanoparticles shift to blue when the distance between them is less or equal to the diameter of the gold nanoparticle itself. The reason for that is the coupling of plasmon fields of the adjacent particles. This results in changing the frequency of the oscillated conduction electrons. Consequently, gold nanoparticles would maximally absorb light at higher wavelength, which appear as a blue color (123). This phenomenon (aggregation of gold) was successfully utilized in our experiments to detect anti-*Borrelia* antibodies in human sera samples.

Results indicate that AuNPs modified with VlsE and protein A showed very specific style to detect antibodies directed to *Borrelia*. The assay can be performed in 30 min in a homogeneous one-step assay (Section 5.7). A clear distinguish between positive and negative samples can be observed using only naked eyes. Also, measurement of absorbance intensity at 590 nm of AuNPs after a test is able to provide the necessary data for quantitative analysis.

Discussion

20-fold serum dilution was used in the proposed assay. The test is not highly sensitive; however, the simple performance of the test in one-step manner is considered very advantageous. The reason for the low sensitivity might be due to the immobilization step, which lack the full coverage and proper organization of proteins on the AuNPs surface. Employing another immobilization technique could result in better sensitivity. This study was to verify the hypothesis of employing the aggregation of AuNPs phenomenon caused by specific interaction to detect antibodies in sera sample. Thus, more investigations are believed would improve the test sensitivity and performance further.

Results showed that UV-vis spectra of 20, 30 and 40 nm AuNPs confirmed the aggregation of particles, which incubated with the positive sample. Also from results we can confirm that the size of AuNPs has a crucial consequence on both assay time as well as assay sensitivity. Big AuNPs sizes (such as 30 and 40 nm) enabled faster access of immobilized antigens to antibodies, shortening the test time. 30 min was needed with 30 nm AuNPs to obtain convenient results and only 1 min with the 40 nm AuNPs; on contrary, 3 hours incubation of sample was needed when 20 nm AuNPs was used. The enhancement in the colorimetric detection caused by the bigger particle sizes could be due to the fact that color of two gold nanoparticles shifts maximally to blue when the distance between them is less or equal to the diameter of the gold nanoparticle itself (122). Based on that, the length of the immune complex (VlsE-Antibody-Protein A) produced between two particles might be above 20 nm. Therefore, the aggregation could be easily seen when bigger particle sizes were tested.

Spectroscopy measurements are beneficial, however one main concern of the present work was to offer a rapid colorimetric point of care test. Thus prompt detection; particularly using naked eyes should be approached. A change in color from red to blue (caused by positive sample) was observed when 20 and 40 nm particles were tested; however, it could not be considered for a colorimetric detection. Only 30 nm AuNPs could undergo physical changes that can be clearly observed using naked eyes after aggregation. 30 nm AuNPs accumulated together forming a cloud like structure; the structure could appear with a blue shift in color (Section 5.7). This can explain the very low optical density obtained when 30 nm AuNPs incubated with positive sample; AuNPs was not distributed in solution rather than precipitated, so the incident light could interact only with few amount of particles.

Although results could be obtained after only one minute using the 40 nm AuNPs, which consider a huge and pioneer advantage, main disadvantage limited working with 40 nm size was the aggregation of AuNPs caused by negative serum. It is believed that aggregation caused by negative sample, which took place after 5-10 minutes, was raised form unspecific

interactions. It seems like that the amount of immobilized antigens were not enough to cover the surface of AuNPs. As a result unspecific interaction was observed as aggregation with the negative sample. More investigations are required to improve the performance of this size. In general, the assay is very simple and easy to handle; applying the serum sample to the AuNPs mainly performs the assay with no additional steps. Aggregation of gold nanoparticles was mainly and successfully utilized for antibodies recognition in real sera samples. The high affinity of both protein A and antigen to a target antibody could be generally suggested in developing other line assays.

6.1 Mannan-modified 3-DPESB platform

As a first approach, 3-DPESB surface was modified with mannan polysaccharide, which served as the platform to capture a fusion protein with the C6 region of VlsE antigen. Mannan is a very hydrophilic molecule; its hydrophobic immobilization on polyethylene surface is not favorable. Therefore, primary functionalization of the 3-DPESB was necessary for a covalent immobilization procedure.

Results showed that one-step UV photografting method seems to be easy and suitable for activation of such 3-dimensional structures. UV irradiation has a unique ability to manipulate the polymer surface without any influence on the bulk properties. UV photografting of small allyl monomers was selected for surface activation. Ally monomers generally able to provide the polymer surface with functional groups. They form active radicals after interaction with light; the grafting of radicals can then be achieved on the polymer surface in presence of initiator. 2-propenol was successfully used here as a building block to establish the active surface. The allyl alcohol, 2-propenol, tends to form an active polymer layer on the polyethylene surface rather than forming a homopolymer, this is due to its low reaction rate of polymerization. The grafting of 2-propenol monomers, which lasted 6 h, was conducted in one-step grafting process; the benzophenone as initiator and 2-propenol were incubated and irradiated in the same solution. It is believed that benzophenone abstracted hydrogen from the polyethylene surface, providing a macro radical that can react easily with the 2-propenol radicals.

The intensity of the absorption bands increases over time so that best results were achieved after 6h. The improved yield of grafting when irradiation time increased could be due to the low reaction rate of the 2-propenol; as a consequence, more monomers can be grafted with

time. The low reaction rate, in addition, is supposed to provide the surface with a rather organized active layer (124, 125). Longer exposure times seem to be possible but will give some problems because of evaporation of solvent accompanied by bubble formation at 3-DPESB surfaces. Therefore, longer reaction times than 6h are not recommended. Methanol as an organic solvent was used in the grafting process. Methanol showed inactivity toward UV light; unlike acetone, which was also tested and showed some activity and radical participating, leading to many difficulties in the grafting process.

Amounts of both the photoinitiator and the monomer should be sufficient; with those amounts a new grafted layer can be obtained. Best results, which yield in covering the full sinter bodies, were found to be when the reaction mixture contained 3 % (w/v) of benzophenone and 25 % volume of 2-propenol. Volume ratios of 2-propenol like 1:1 or strongly diluted solutions like 5 % did not give any advantage in the obtained FTIR spectra. It is assumed that the ratio between the used benzophenone and the 2-propenol is of importance.

Active hydroxyl groups, which enabled further immobilization steps, were introduced to the surface after a grafting step. Results showed that mannan could be attached to the activated surface through a monolayer with defined orientation (APTES). A densely packed monolayer of APTES was introduced, simply by dipping the polyethylene in an organic solvent containing the APTES. A condensation reaction takes place between the hydroxyl groups and the APTES molecules with the loss of ethanol and hydrolysis of alkoxy groups (126). This resulted in the covalent grafting of hydroxyl silane product on the surface and formation of aminopropyl silane film. Drying the 3-DPESB under high temperature is assumed to strengthen and densify the aminopropyl silane layers; horizontal polymerization (i.e., the formation of Si-O-Si bonds between adjacent surface aminopropyl silane molecules) is enhanced upon heating after the SAM is attached (127). The monolayer would aid to adopt the proteins in a more uniform orientation on the surface; this in turn enhanced the reproducibility and specificity of the assay, as can be seen when sera samples were tested (Section 5.4). It seems that the silane monolayer plays a key role in decreasing the non-specific interaction in the presented assay. Using silane layer in the immobilization procedure, as has been previously reported, assures a highly specific interaction of proteins (128, 129).

The APTES introduced amino groups all over the surface, which has been confirmed after a Bradford protein quantitation assay. The Bradford method has the advantages of being fast, simple, and highly sensitive. The method has been developed for protein quantitation based

on a reaction between basic amino acid residues and Coomassie brilliant blue G-250 in acidic solution. The reaction can be observed as a blue shift in the dye form. The absorbance intensity can be measured at 520-590 nm. The Bradford method could be utilized to confirm the presence of amino groups on the sinter body's surface after APTES grafting; sinter bodies modified with APTES could react with the Coomassie dye, causing a shift in the dye color, which can be seen as a dark blue. The APTES grafting provided a homogenous distribution of amine groups on the surface, which could be observed as a fully coloration of the 3-DPESB (Section 5.2). On the other hand, the unmodified 3-DPESB without any treatment (reference) display with a pale blue color. Based on the control experiments, it seems that the silanization grafting was successfully performed (Section 5.2).

Mannan could react with the amine groups on surface and be immobilized via imide bond. However activation of mannan to carbamate intermediate was required prior to its immobilization. N, N`-disuccinimdyl carbonate, a highly reactive toward nucleophiles, could attack hydroxyl groups of the mannan in a nonaqueous solution, producing active intermediate that is able to react with amine groups on 3-DPESB surface and form cross-linked product. The activated mannan (succinimidyl carbonate-mannan) was incubated in a final step with the silanized polyethylene, resulting in covalent binding of mannan to the surface. All activation process has been performed in organic solvent since the DSC and the intermediate groups are susceptible to hydrolysis in aqueous solutions to form two molecules of NHS.

In conclusion, it could be demonstrated that 3-dimensional polyethylene is a suitable carrier for immunoassays. As a disadvantage, UV radiation in combination with photografting takes a rather long time. The time can be probably reduced if direct oxidation of the polyethylene would be performed either with ozone or by plasma technologies. The here presented method seems to produce at least partially multilayers. This might influence the stability of immobilized mannan, but in practice there was no problem with this. The addition of the silane layer seems to stabilize the primary formed polyalcohol-layer. Obtained results demonstrate that i) the functionalization procedure summarized in Scheme 1 could be performed successfully. The successful immobilization of mannan could be observed after testing the sera sample with the help of the fusion protein. Mannan-modified polyethylene enabled a specific interaction with the recombinant fusion protein. Highest affinity between Con A and mannan could be achieved in presence of metal ions such as the transition metals and/or Ca^{2+} or Mg^{2+}; thus the fusion protein was diluted in HEPES buffer containing calcium, manganese, and magnesium ions before it was applied to the surface.

6.2 Antigen-modified 3-DPESB platform

A second approach based on employing 3-DPESB modified with VlsE antigen could be successfully developed for rapid analysis. Two different immobilization techniques (hyordophobic and covalent) have been well established for the 3-DPESB modification. Regardless the used immobilization method, it should be simple and reproducible; in addition, the immobilized proteins should be easily accessible and correctly oriented. In general, protein immobilization on surface of polymers such as polyethylene is controlled by many factors, e.g. the nature of the polymer, whether aliphatic or aromatic, the number of carbons of immobilized molecule, and the introduction of functional groups on the surface.

Results revealed that with a special washing routine, VlsE could be easily adsorbed to the polyethylene surface. Hydrophobic adsorption is considered the easiest method for protein immobilization on polymer surface. The strong hydrophobic characteristic of polyethylene makes the physical adsorption of antigen rather easy. To achieve higher adsorption affinity of antigen, all immobilization steps have been conducted under vacuum; this in turn would remove any bubbles distributed inside the 3-DPESB, which may hinder the adsorption of antigen. Washing in 96 % ethanol, then washing with ethanol-water (50:50), and finally washing with the carbonate buffer enabled 3-DPESB to be easily functionalized with the VlsE *Borrelia* antigen. The washing steps were performed to eliminate any impurities, which could disturb the immobilization process. Besides, it aimed to adapt the 3-DPESB in carbonate buffer pH 9.6, in which the immobilization would take place. Carbonate buffer pH 9.6 has been chosen based on a previously published study, which reported that carbonate buffer pH 9.6 yield the best conditions for hydrophobic immobilization (103). It is supposed that the hydrophobic parts of the antigen tend to exclude water molecules from solution and interact with the hydrocarbon chain of the polymer surface, causing the strong adsorption of antigen. This in addition to the Wan Dar Waals forces and electrostatic interactions, which contribute and improve the protein immobilization process. Adsorptive immobilization of proteins on a hydrophobic surface is a convenient method and yielded in highly sensitive detection of antibodies in sera samples as shown in results.

In our work we showed the potential to immobilize VlsE antigen on the 3-DPESB by covalent bonding as an alternative. This aimed to provide the surface with a rather organized biomolecules layer, which would lower the steric hindrance effect, providing more sensitive and reproducible test. Using the UV-photografting of 2-propenol, hydroxyl groups could be introduced and used to catch the VlsE antigen. Hydroxyl groups are not reactive toward the

protein functional groups such as free amine groups. Thus, hydroxyl groups have been firstly activated to DSC-activated hydroxylic compound after a reaction with N, N-disuccinimidyl carbonate (DSC) (102). The activation process has been performed in organic solvent since the DSC and the intermediate groups are susceptible to hydrolysis in aqueous solutions. The activated hydroxylic compound could then react with the free amine groups to form a carbamate bond, which display excellent stability. This resulted in fixing the antigen on the surface after a simple incubation step.

Results showed also that, covalent immobilization required higher amounts of antigen on the surface than hydrophobic adsorption to establish a working assay. The reason might be due to the few free amine groups on antigen surface, which were used to couple the protein. Unlikely, hydrophobic adsorption utilized the long hydrophobic chain of the protein to interact with the polyethylene surface. As a result less amount of antigen was required to cover the surface. Using a ELISA like assay, the antibodies could be successfully recognized by the immobilized VlsE antigen. Both hydrophobic and covalent immobilization resulted in a surface, which is selective and sensitive toward detection of anti-*Borrelia* antibodies in human sera samples.

In our work we showed also the successful modification of AuNPs with protein A by hydrophobic adsorption. The modification process provided AuNPs that enables a rapid and specific detection of antibody-antigen interaction in ABICAP[TM] system. Hydrophobic modification of AuNPs depends mainly on the nature, pH, and concentration of the used buffer. It has a crucial impact on the stability and performance of AuNPs; irrelevant buffer would cause aggregation of AuNPs during immobilization, preventing protein adsorption.

100 mM borate buffer pH 7.4 was found to be suitable for full coverage of AuNPs with protein A, which could be predicted when no aggregation was observed during immobilization (104); in contrast AuNPs aggregation was observed when phosphate buffer pH 7.4 as well as PBS buffer pH 7.4 were used for immobilization.

SPR device could be employed to confirm the feasibility of the prepared AuNPs. The SPR C18 chip surface was efficient that enabled retaining the OspC antigen structure on the surface with maintained activity. OspC in turn caught antibodies from a positive serum sample. Subsequently, AuNPs modified with protein A could be tested. Results confirmed the successful modification of AuNPs with Protein A. More, AuNPs could be used successfully as a label for further experiment in the ABICAP[TM] system as shown in results.

6.3 Two-protein modified AuNPs platform

A third approach was developed based on employing two-antigen modified AuNPs for rapid analysis. AuNPs colloid that aggregates as a consequence of a positive sample addition could be successfully established. Simultaneously, the colloid remained stable with no alteration when a negative sample is being added. The two antigens (*Borrelia* VlsE antigen and protein A) have been immobilized on AuNPs surface; the antigens showed a specific interaction behavior to the target antibody found in sample, indicating the presence of an infection through the aggregation of gold nanoparticles. Turkevich method for AuNPs synthesis enabled the easy synthesis of three different sizes (20, 30, and 40 nm) of particles. The advantage of the method is the capability of controlling the AuNPs size easily by controlling the concentration of both gold (III) chloride hydrate and the trisodium citrate salt in the reaction solution.

Most important step after AuNPs synthesis was to modify them with the chosen antigens; modification of AuNPs can be achieved using hydrophobic or covalent techniques. Covalent technique was chosen because, as previously mentioned, it enables a highly stable biomolecules bonding and allows a rather organized biomolecules layer, which would lower the steric hindrance effect, providing more sensitive and reproducible test. One common method, which we used, was to immobilize antigen through the free amino groups of lysine (or hydroxy) residues when considering the presence of carboxylate groups on gold surface. Hence, AuNPs was capped first with a self-assembled monolayer of 11-mercaptoundecanoic acid (MUA), which provided the surface with the carboxylate groups. MUA is a thiol acid mostly used to functionalize nanoparticles surface. The thiol end, which has strong affinity to gold, reacts with the gold surface, leaving a carboxyl group free and exposed for further immobilization. Then with a controlled pH solution, antigens could be immobilized using EDC/NHS coupling procedure. Concentration of MUA should be carefully optimized because high concentration of MUA would result in aggregation of gold nanoparticles.

The aggregation takes place due to increasing hydrogen ions' concentration, decreasing the pH. For that, two factors were adjusted prior to AuNPs functionalization: i) increasing the pH of gold colloid using NaOH and ii) testing different concentrations of MUA. 4 µL of NaOH in 2 mL gold suspension had to be used before addition of MUA to prevent aggregation. 5 µL of 1mg mL^{-1} MUA (dissolved in ethanol) found to be a proper concentration; functionalization of gold nanoparticles was achieved with no observed aggregation.

Discussion

From results it is believed that gold surface with carboxylate groups was activated after using a zero-length cross-linker EDC in presence of NHS. NHS prevents the hydrolysis of the EDC that tend to take place in the aqueous solution. Accordingly, an *o*-isoacyl urea intermediates was produced that can react with the free amine groups of antigens, resulting in a strong amide covalent bond dragging antigens to the surface (130). The performance of modified AuNPs can be verified as a red shift in the maximum absorbance as well as broadening of the absorbance band when incubated with positive serum. The AuNPs aggregation results in a visible change appear in the absorption region between 550 nm-680 nm. The change can be observed as a new peak (131); or else it can be observed as an increasing in absorption intensity, broadening of absorption band (132).

Our results showed that broadening of absorption band rather than appearance of a new peak can be seen. One factor might play a key role in appearance of a new peak is the concentration of the analyte or the concentration of AuNPs. It could be that in our experiments the concentrations of either AuNPs or antigens were not sufficient to cause the appearance of a new peak around 550-680. So, broadening of absorption band in UV-vis measurements was taken as a confirmation of accumulation in the present work. Yet, visible observation was sufficient to distinguish between positive and negative samples.

At first 20 nm AuNPs was used for assay conditions optimization because of their higher stability and lower sedimentation over the others. Optimum performance of AuNPs could be obtained when 10 μL 1 mg mL^{-1} VlsE and 12 μL 1 mg mL^{-1} protein A were used. The optimum antigen concentrations should cause higher difference in absorbance intensities between AuNPs incubated with positive serum and AuNPs incubated with negative serum. Higher difference, in other words, means a maximum interaction should take place between immobilized antigens and antibodies found in the positive serum; simultaneously, the negative sample should not cause any non-specific interaction with the AuNPs.

Results showed also that higher affinity between immobilized antigens and anti-*Borrelia* antibody, which was observed as maximum aggregation of AuNPs incubated with positive serum, could be seen when phosphate buffer pH 7.4 was used. This is compatible with previously reported studies, which reported that maximum interaction of antibody-antigen interaction as well as protein A-antibody interaction could take place at pH 7.4.

Results showed that increasing salt concentration hindered the interaction between immobilized proteins and anti-*Borrelia* antibodies when 20 nm AuNPs was used. 50 mM NaCl weakened the proteins interaction; this can be observed by the weak aggregation of AuNPs incubated with positive serum. Moreover, 100 mM NaCl totally prevented the

proteins interaction. Nevertheless, 30 nm AuNPs gave higher sensitive and more rapid test when 50 mM NaCl was added to the assay buffer.

A convenient recognition of anti-*Borrelia* antibodies in sera samples was achievable using the three different sizes of AuNPs. UV-vis spectra showed the aggregation of nanoparticles incubated with positive sample. The aggregation is observed as a red shift in maximum absorbance and broadening in the absorption band. The reason for the aggregation as supposed should be due to the specific interaction of both antigens on the gold surface with the antibodies. This can be confirmed also when negative sample is tested and no visible change could be observed.

Summary

The presented work describes the development of new ligand-binding assay platforms for rapid serological diagnosis. 3-D polyethylene sinter bodies and monodisperse gold nanoparticles have been successfully employed as protein carriers, providing sensitive, selective and rapid serological diagnosis. Detection of anti-*Borrelia* antibodies in human sera samples was taken as a model in our work. Antibodies recognition either by visible observation or by spectroscopic measurements was easily practicable. All developed assays could be performed in a short time, 5-30 min, providing a suitable colorimetric point of care test. The established assays offer simple, rapid and reliable tools of analysis with minimal cost, which can be easily transferred to other infectious diseases. In brief, thesis can be divided into three different parts; each part based on one new approach.

In the first part, diagnosis of Lyme borreliosis has been carried out on chemically modified porous polyethylene sinter bodies. Photografting of 2-propenol on the polyethylene surface was performed as a first step. Active hydroxyl groups were introduced as a result of polyalcohol formation, which has been confirmed using different analysis techniques such as FTIR, SEM, and AFM. The hydroxyl groups were used for further immobilization and could be linked via 3-aminopropyltriethoxysilane to polysaccharides like mannan. Prone to mannan coupling, mannan was activated using N, N´-disuccinimidyl carbonate to allow smooth reaction with the primary amine groups of the silane layer. The high specific interaction between mannan polysaccharides and lectins was employed in a final preparation step; a recombinant fusion protein consisting of the mannan-binding domain of the lectin Concanavalin A (ConA) and a specific *Borrelia* surface antigen was immobilized by self-organization on the mannan surface. This strategy is highly efficient and resulted in a defined orientation of the antigen part of the fusion protein. The binding of anti-*Borrelia* antibodies in human sera samples was detected by a color reaction in an ELISA-like manner in only 20 min. Horseradish peroxidase (HRP) secondary labeled antibody was used as a label. The assay enabled a rapid and convenient differentiation between *Borrelia*-negative and -positive sera even in 1000-fold diluted samples and allows detection of Lyme borellioses in a rather early stage. This generic strategy can be easily transferred to other bacterial or viral antigen structures.

In the second part, diagnosis of Lyme borreliosis has been carried out on porous polyethylene sinter bodies, which have been coated with VlsE antigen rather than mannan.

Summary

Sufficient amounts of VlsE antigen could be successfully immobilized on the surface using both hydrophobic adsorption and covalent immobilization. A special washing routine could be developed for the easy physical adsorption of the antigen. Covalent immobilization has been proposed as alternative to immobilize the antigen. Photografting of 2-propenol was conducted primarily to launch the covalent immobilization procedure. Activation of the produced hydroxyl groups enabled eventually an amine-coupling reaction to be pursued, resulting in binding of the antigen's N-terminus lysine amino groups to the activated intermediate on the surface. Detection of anti-*Borrelia* antibodies has been easily achieved using a ELISA like assay. Three labels were tested: i) a horseradish peroxidase (HRP) labeled secondary antibody, ii) nanoparticles based on Sudan IV, and iii) gold nanoparticles modified with protein A. HRP secondary labeled antibody provides the most sensitive test when integrated with 3-DPESB modified with hydrophobic adsorption; 1000 fold dilution of serum sample can be clearly detected in only 20 min. Gold nanoparticles modified with protein A could be employed in the ABICAP^{TM} technology as a very promising label. Detection of antibodies could be conducted in only 5 min; this advantageous approach could be established based on direct detection of AuNPs. Detection of metallic silver produced by catalytic activity of AuNPs was possible. Detection of metallic silver required longer time (12 min), but with improved sensitivity. Nanoparticles based on Sudan IV showed high background and were less favorable when real samples were tested.

In the third part, the physical properties of AuNPs could be successfully employed to develop AuNPs able to detect target antibodies in human sera sample. AuNPs has been modified with two antigens, surface VlsE *Borrelia* antigen and protein A. The specific interaction of the two antigens with anti-*Borrelia* antibodies enabled the detection of the antibodies in human sera samples. Three different sizes (20, 30, and 40 nm) were tested; a convenient recognition of antibodies was achieved with all sizes using spectroscopy measurements. Moreover, 30 nm particles showed a very promising colorimetric detection; accumulation of nanoparticles could be visibly observed using naked eyes. The size of nanoparticles showed a crucial impact on the assay time; 3 h incubation was needed to obtain considerable results when 20 nm particles was used, while 30 min was needed with the 30 nm particles and only 1 min with the 40 nm particles. The proposed test can be performed only in one step with no additional washing steps. The test is promising, simple and suitable for point-of-care testing. Applying the proposed platform to other assays is suggested for rapid analysis.

Zusammenfassung

In der vorliegenden Arbeit wird die Verwendung von neuartigen Analytik-Plattformen beschrieben, mit denen Immunoassays für die schnelle serologische Diagnostik durchgeführt werden konnten. „3-D-Polyethylen-Sinterkörper" und monodisperse Goldnanopartikel wurden hierbei als Träger für proteinerge Erkennungsstrukturen erfolgreich eingesetzt. Es konnte dadurch eine sensitive, selektive und schnelle Diagnostik einer Borrelien-Infektion erreicht werden. Da der gewählte experimentell Ansatz generisch ist, kann er auch auf andere Krankheitserreger übertragen werden. Die Detektion der Antikörper erfolgte sowohl durch visuelle Auswertung als auch durch spektroskopische Messungen. Die entwickelten Assays können in einem Zeitraum von 5 – 30 Minuten durchgeführt werden; somit sind sie für Point of Care Tests geeignet. Die experimentellen Arbeiten sind in drei Bereiche Aufgeteilt:

In dem ersten Teil wurde die Diagnostik der Lyme-Borreliose auf chemisch modifizierten porösen Polyethylensinterkörpern als Trägerstruktur durchgeführt. Es wurde 2-Propenol auf die Polyethylenoberfläche mit der Hilfe von UV-Strahlung immobilisiert. Aktive Hydroxylgruppen wurden durch Polymerisation eingeführt und durch verschiedene Analysetechniken wie FTIR, REM, AFM bestätigt. An diese konnten über 3-Aminopropyltriethoxysilan Polysaccharide wie Mannan an die Oberfläche gebunden werden. Mannan wurde zuvor durch N,N´-Disuccinimidylcarbonat aktiviert, um die Bildung von Säureamidgruppen zu ermöglichen.

Die hohe spezifische Wechselwirkung zwischen Mannan und Lektinen wie Concanavalin A (ConA) wurde in einer abschließenden Präparationphase ausgenutzt. Zur Verwendung kam hierbei ein rekombinantes Fusionsprotein, das sich aus dem Mannan-bindenden Domäne des ConA und einem spezifischen Borrelia-Oberflächenantigens, VlsE, zusammensetzt. Es wurde durch Selbstorganisation auf der Mannanoberfläche immobilisiert. Diese effiziente Strategie resultierte in einer definierten Orientierung des Antigen-Teils des Fusionsproteins. Die Bindung von anti-*Borrelia* Antikörpern aus humanen Seren wurde durch eine Farbreaktion in einem ELISA-ähnlichen Test binnen 20 Minuten bestimmt. Dabei wurden mit Meerrettichperoxidase (HRP) markierte, sekundäre Antikörper verwendet. Der Test ermöglicht sowohl eine schnelle und effiziente Unterscheidung zwischen Borrelien-negativen und –positiven Seren in bis zu 1000-fach verdünnten Proben und erlaubt somit den Nachweis von Lyme-Borreliose in einem relativ frühen Stadium. Diese Methodik kann leicht auf andere bakterielle oder virale Antigenstrukturen übertragen werden.

Zusammenfassung

In dem zweiten Teil dieser Studie wurde der erhaltene Assay optimiert und unterschiedle Immobilisierungsstrategie und Detektionsmethoden vergleichend untersucht. Die Immobilisierung des Antigens auf der Polyethylenoberfläche konnte sowohl durch hydrophobe Adsorption sowie kovalente Bindung des Antigens auf der Oberfläche erfolgreich durchgeführt werden. Zur einfachen physikalischen Adsorption des Antigens konnte eine spezielle Wasch-Routine entwickelt werden. Die Oberflächenmodifikation des Polyethylens erfolgte durch UV-induzierte Polymerisation von 2-Propenol. Die erzeugten Hydroxylgruppen wurden zuerst zu Carbamaten umgesetzt. Hierzu wurden Amin-Kupplungsreaktion durchgeführt; die Proteine wurden über die freie Aminogruppe des N-Terminus oder des Lysins an diese gebunden. Der Nachweis von anti-*Borrelia* Antikörpern in den Serumproben wurde durch einen kolorimetrischen Assay ermöglicht. Drei Label wurden getestet: i) ein Meerrettichperoxidase (HRP) markierte sekundärer Antikörper ii) Nanopartikel auf Basis von Sudan IV, und iii) Gold-Nanopartikel, die mit Protein A modifiziert wurden. HRP markierte sekundärer Antikörper lieferten den empfindlichsten Test; ein 1000-fache Verdünnung der Serumproben konnte deutlich in nur 20 min detektiert werden. Die Protein A modifizierten Gold-Nanopartikel stellen eine vielversprechende Alternative dar. Der Nachweis von Antikörpern konnte in sehr kurzer Zeit erreicht werden (5 min). Diese Steigerung der Nachweisgeschwindigkeit konnte durch die direkte Detektion von Goldnanopartikeln erreicht werden. Als weiteres Label konnte Silber verwendet werden, um die Sensitivität des Tests zu erhöhen. Silber-Ionen wurden reduziert, um elementares Silber zu erhalten. Die Detektion benötigt eine längere Zeit (12 min), jedoch mit verbesserter Sensitivität. Nanopartikeln auf Basis von Sudan IV zeigten einen hohen Hintergrund und waren nur mäßig für Seren-Proben geeignet. Das entwickelte Verfahren bietet eine einfache, schnelle und zuverlässige Analysemethode mit minimalen Kosten und kann leicht an andere Infektionen angepasst werden.

In dem dritten Teil der Arbeit wurden die besonderen spektroskopischen Eigenschaften von Gold-Nanopartikeln ausgenutzt, um anti-*Borrelia* Antikörper in menschlichen Seren nachzuweisen. Gold-Nanopartikeln wurden mit zwei Proteinen modifiziert; VlsE *Borrelia*-Antigen und Protein A. Die spezifische Wechselwirkung der beiden Proteine mit anti-*Borrelia* Antikörpern in menschlichen Serumproben führte zu einer Aggregation der Goldnanopartikel. Goldnanopartikel wurden in drei verschieden Größen (20, 30 und 40 nm) getestet; eine geeignete Identifikation von Antikörpern wurde bei allen Größen mittels spektroskopischer Messungen erreicht. Zusätzlich zeigten die 30 nm Partikel eine

vielversprechende kolorimetrische auswertbare Reaktion; Die Akkumulation von Nanopartikel konnte mit dem bloßen Auge beobachtet werden. Die Größe der verwendeten Nanopartikel hatte einen entscheidenden Einfluss auf die Dauer der Testverfahren. Es wurden 3 h Inkubationszeit benötigt um auswertbare Ergebnisse bei den 20 nm Partikeln zu erhalten, 30 min bei den 30 nm Partikeln und lediglich 1 min bei den 40 nm Partikeln. Der vorgeschlagen Test kann auch in nur einem Schritt ohne weitere Waschschritte durchgeführt werden. Dieser Ansatz erscheint vielversprechend, einfach und somit gut geeignet für Point of Care Tests. Die Verwendung dieser Plattform für andere Tests auf verschiedenste Viren und Bakterien (bzw. dagegen gerichtete Antikörper) kann in Zukunft zu schnellen Ergebnissen führen, ohne dass eine Laborausrüstung erforderlich ist.

References

1.   Zhou L, Zhu A, Lou X, Song D, Yang R, Shi H, et al. Universal quantum dot-based sandwich-like immunoassay strategy for rapid and ultrasensitive detection of small molecules using portable and reusable optofluidic nano-biosensing platform. Analytica Chimica Acta. 2016;905:140-8.

2.   Imai S, Takahashi T, Naito S, Yamauchi A, Okada C, Notsu Y, et al. Development of a novel immunoassay specific for mouse intact proinsulin. Analytical Biochemistry. 2015;484:91-8.

3.   Yalow RS, Berson SA. Immunoassay of endogenous plasma in man. Journal of Clinical Investigation. 1960;39(7):1157-75.

4.   Burmistrova NA, Rusanova TY, Yurasov NA, Goryacheva IY, De Saeger S. Multi-detection of mycotoxins by membrane based flow-through immunoassay. Food Control. 2014;46:462-9.

5.   Tang L, Dong C, Ren J. Highly sensitive homogenous immunoassay of cancer biomarker using silver nanoparticles enhanced fluorescence correlation spectroscopy. Talanta. 2010;81(4–5):1560-7.

6.   Glass TR, Saiki H, Joh T, Taemi Y, Ohmura N, Lackie SJ. Evaluation of a compact bench top immunoassay analyzer for automatic and near continuous monitoring of a sample for environmental contaminants. Biosensors and Bioelectronics. 2004;20(2):397-403.

7.   Ma S, Tang Y, Liu J, Wu J. Visible paper chip immunoassay for rapid determination of bacteria in water distribution system. Talanta. 2014;120:135-40.

8.   Banga-Mboko H, Sulon J, Closset J, Remy B, Youssao I, De Sousa NM, et al. An Improved Radioimmunoassay for Measurement of Pepsinogen in Porcine Blood Samples. The Veterinary Journal. 2003;165(3):288-95.

9.   Larose P, Ong H, Du Souich P. Simple and rapid radioimmunoassay for the routine determination of vasopressin in plasma. Clinical Biochemistry. 1985;18(6):357-61.

10.   Yalow RS. The limitations of radioimmunoassay (RIA). TrAC Trends in Analytical Chemistry. 1982;1(6):128-31.

11.   Draisci R, Volpe G, Compagnone D, Purificato I, delli Quadri F, Palleschi G. Development of an electrochemical ELISA for the screening of 17[small beta]-estradiol and application to bovine serum. Analyst. 2000;125(8):1419-23.

12.   Engvall E, Perlmann P. Enzyme-linked immunosorbent assay (ELISA) quantitative assay of immunoglobulin G. Immunochemistry. 1971;8(9):871-4.

References

13.   Van Weemen BK, Schuurs AHWM. Immunoassay using antigen—enzyme conjugates. FEBS Letters. 1971;15(3):232-6.

14.   Josephy PD, Eling T, Mason RP. The horseradish peroxidase-catalyzed oxidation of 3,5,3',5'-tetramethylbenzidine. Free radical and charge-transfer complex intermediates. Journal of Biological Chemistry. 1982;257(7):3669-75.

15.   Woodhead JS, Weeks I. Chemiluminescence immunoassay. Pure and Applied Chemistry1985. p. 523.

16.   Whitesides GM. The origins and the future of microfluidics. Nature. 2006;442(7101):368-73.

17.   Giri B, Pandey B, Neupane B, Ligler FS. Signal amplification strategies for microfluidic immunoassays. TrAC Trends in Analytical Chemistry.

18.   Lim CT, Zhang Y. Bead-based microfluidic immunoassays: the next generation. Biosensors and Bioelectronics. 2007;22(7):1197-204.

19.   Dzantiev BB, Byzova NA, Urusov AE, Zherdev AV. Immunochromatographic methods in food analysis. TrAC Trends in Analytical Chemistry. 2014;55:81-93.

20.   Young S-H, Antonini JM, Roberts JR, Erdely AD, Zeidler-Erdely PC. Performance evaluation of cytometric bead assays for the measurement of lung cytokines in two rodent models. Journal of Immunological Methods. 2008;331(1–2):59-68.

21.   Zhang Y, Li L, Lu J, Ge L, Ge S, Yan M, et al. Triple catalysis amplification strategy for simultaneous multiplexed electrochemical immunoassays based on cactus-like MnO2 functionalized nanoporous gold. Sensors and Actuators B: Chemical. 2013;186:545-9.

22.   Wang X, Niessner R, Tang D, Knopp D. Nanoparticle-based immunosensors and immunoassays for aflatoxins. Analytica Chimica Acta.

23.   Lin P, Wang S-H, Wang Y-L. Development of phase separation immunoassay. Chinese Journal of Analytical Chemistry. 2009;37(12):1839-46.

24.   Pei X, Zhang B, Tang J, Liu B, Lai W, Tang D. Sandwich-type immunosensors and immunoassays exploiting nanostructure labels: a review. Analytica Chimica Acta. 2013;758:1-18.

25.   Qi Y, Xiu F-R, Li B. One-step homogeneous non-stripping chemiluminescence metal immunoassay based on catalytic activity of gold nanoparticles. Analytical Biochemistry. 2014;449:1-8.

26.   Venn RF. Principles and practice of bioanalysis. London; New York: Taylor & Francis; 2000.

27.   Kato K, Hamaguchi Y, Okawa S, Ishikawa E, Kobayashi K, Katunuma N. Enzyme immunoassay in rapid progress. The Lancet. 1977;309(8001):40.

28.   Harlow E, Lane D. Antibodies : a laboratory manual. New York: Cold Spring Harbor Laboratory.; 1988.

29.   Lipman NS, Jackson LR, Trudel LJ, Weis-Garcia F. Monoclonal versus polyclonal antibodies: distinguishing characteristics, applications, and information resources. ILAR Journal. 2005;46(3):258-68.

30.   Bradley J. Immunoglobulins. Journal of Medical Genetics. 1974;11(1):80-90.

31.   Bird RE, Hardman KD, Jacobson JW, Johnson S, Kaufman BM, Lee SM, et al. Single-chain antigen-binding proteins. Science. 1988;242(4877):423-6.

32.   Schroeder Jr HW, Cavacini L. Structure and function of immunoglobulins. Journal of Allergy and Clinical Immunology. 2010;125(2, Supplement 2):S41-S52.

33.   Higel F, Seidl A, Sörgel F, Friess W. N-glycosylation heterogeneity and the influence on structure, function and pharmacokinetics of monoclonal antibodies and Fc fusion proteins. European Journal of Pharmaceutics and Biopharmaceutics. 2016;100:94-100.

34.   Ramaraj T, Angel T, Dratz EA, Jesaitis AJ, Mumey B. Antigen–antibody interface properties: composition, residue interactions, and features of 53 non-redundant structures. Biochimica et Biophysica Acta (BBA) - Proteins and Proteomics. 2012;1824(3):520-32.

35.   Reverberi R, Reverberi L. Factors affecting the antigen-antibody reaction. Blood Transfusion. 2007;5(4):227-40.

36.   Hnaien M, Diouani MF, Helali S, Hafaid I, Hassen WM, Renault NJ, et al. Immobilization of specific antibody on SAM functionalized gold electrode for rabies virus detection by electrochemical impedance spectroscopy. Biochemical Engineering Journal. 2008;39(3):443-9.

37.   Shimabukuro FH, Da Costa VM, Da Silva RC, Langoni H, Da Silva AV, De Carvalho LR, et al. Prozone effects in microscopic agglutination tests for leptospirosis in the sera of mice infected with the pathogenic Leptospira interrogans serovar Canicola. Memórias do Instituto Oswaldo Cruz. 2013;108(5):668-70.

38.   De Azevedo PZ, Sylvestre TF, Cavalcante RdS, De Carvalho LR, Moris DV, De Oliveira MLCS, et al. Evaluation of the double agar gel immunodiffusion test and of the enzyme-linked immunosorbent assay in the diagnosis and follow-up of patients with chronic pulmonary aspergillosis. PLoS ONE. 2015;10(8):e0134841.

References

39.   Lai W, Wei Q, Zhuang J, Lu M, Tang D. Fenton reaction-based colorimetric immunoassay for sensitive detection of brevetoxin B. Biosensors and Bioelectronics. 2016;80:249-56.

40.   Zhang B, Zhang Y, Liang W, Cui B, Li J, Yu X, et al. Nanogold-penetrated poly(amidoamine) dendrimer for enzyme-free electrochemical immunoassay of cardiac biomarker using cathodic stripping voltammetric method. Analytica Chimica Acta. 2016;904:51-7.

41.   Mazumdar SD, Barlen B, Kämpfer P, Keusgen M. Surface plasmon resonance (SPR) as a rapid tool for serotyping of Salmonella. Biosensors and Bioelectronics. 2010;25(5):967-71.

42.   Day MJ. Introduction to Antigen and Antibody Assays. Topics in Companion Animal Medicine.

43.   Schnarr S, Franz JK, Krause A, Zeidler H. Lyme borreliosis. Best Practice & Research Clinical Rheumatology. 2006;20(6):1099-118.

44.   Burgdorfer W, Barbour AG, Hayes SF, Benach JL, Grunwaldt E, Davis JP. Lyme disease-a tick-borne spirochetosis? Science. 1982;216(4552):1317-9.

45.   Steere AC. Lyme borreliosis in 2005, 30 years after initial observations in Lyme Connecticut. Wien Klin Wochenschr. 2006;118(21-22):625-33.

46.   Rosa PA, Tilly K, Stewart PE. The burgeoning molecular genetics of the Lyme disease spirochaete. Nat Rev Micro. 2005;3(2):129-43.

47.   Charon NW, Goldstein SF. Genetics of motility and chemotaxis of a fascinating group of bacteria: the spirochetes. Annual Review of Genetics. 2002;36(1):47-73.

48.   Pfister HW, Wilske B, Weber K. Lyme borreliosis: basic science and clinical aspects. The Lancet. 1994;343(8904):1013-6.

49.   Humair P-F, Gern L. The wild hidden face of Lyme borreliosis in Europe. Microbes and Infection. 2000;2(8):915-22.

50.   Barbour AG, Zuckert WR. Genome sequencing: new tricks of tick-borne pathogen. Nature. 1997;390(6660):553-4.

51.   Singh SK, Girschick HJ. Lyme borreliosis: from infection to autoimmunity. Clinical Microbiology and Infection. 2004;10(7):598-614.

52.   Wagemakers A, Staarink PJ, Sprong H, Hovius JWR. Borrelia miyamotoi: a widespread tick-borne relapsing fever spirochete. Trends in Parasitology. 2015;31(6):260-9.

53.   Singh SK, Girschick HJ. Toll-like receptors in Borrelia burgdorferi-induced inflammation. Clinical Microbiology and Infection. 2006;12(8):705-17.

References

54.   Liveris D, Schwartz I, McKenna D, Nowakowski J, Nadelman R, DeMarco J, et al. Comparison of five diagnostic modalities for direct detection of Borrelia burgdorferi in patients with early Lyme disease. Diagnostic Microbiology and Infectious Disease. 2012;73(3):243-5.

55.   Barbour AG, Burgdorfer W, Hayes SF, Péter O, Aeschlimann A. Isolation of a cultivable spirochete fromIxodes ricinus ticks of Switzerland. Current Microbiology. 1983;8(2):123-6.

56.   Schmidt BL. PCR in laboratory diagnosis of human Borrelia burgdorferi infections. Clinical Microbiology Reviews. 1997;10(1):185-201.

57.   Brunner M. New method for detection of Borrelia burgdorferi antigen complexed to antibody in seronegative Lyme disease. Journal of Immunological Methods. 2001;249(1–2):185-90.

58.   Kelly R. Cultivation of Borrelia hermsi. Science. 1971;173(3995):443-4.

59.   Molloy PJ, Persing DH, Berardi VP. False-positive results of PCR testing for Lyme disease. Clinical Infectious Diseases. 2001;33(3):412-3.

60.   Branda JA, Aguero-Rosenfeld ME, Ferraro MJ, Johnson BJB, Wormser GP, Steere AC. 2-tiered antibody testing for early and late Lyme disease using only an immunoglobulin G blot with the addition of a VlsE band as the second-tier test. Clinical Infectious Diseases. 2010;50(1):20-6.

61.   prevention Cfdca. Readers recommendations for test performance and interpretation from the second national conference on serologic diagnosis of Lyme disease. MMWR Morb Mortal Wkly Rep. 1995;44(31):590-1.

62.   Datta S, Christena LR, Rajaram YRS. Enzyme immobilization: an overview on techniques and support materials. 3 Biotech. 2012;3(1):1-9.

63.   Chen W-J, Ling X-M. Advances of methods of protein immobilization on capillary column. Chinese Journal of Analytical Chemistry. 2009;37(6):929-34.

64.   Sassolas A, Blum LJ, Leca-Bouvier BD. Immobilization strategies to develop enzymatic biosensors. Biotechnology Advances. 2012;30(3):489-511.

65.   Mohamad NR, Marzuki NHC, Buang NA, Huyop F, Wahab RA. An overview of technologies for immobilization of enzymes and surface analysis techniques for immobilized enzymes. Biotechnology, Biotechnological Equipment. 2015;29(2):205-20.

66.   Aggarwal SL, Sweeting OJ. Polyethylene: preparation, structure, and properties. Chemical Reviews. 1957;57(4):665-742.

67.   Domski GJ, Rose JM, Coates GW, Bolig AD, Brookhart M. Living alkene polymerization: new methods for the precision synthesis of polyolefins. Progress in Polymer Science. 2007;32(1):30-92.

68.   Nakabayashi K, Mori H. Recent progress in controlled radical polymerization of N-vinyl monomers. European Polymer Journal. 2013;49(10):2808-38.

69.   Pasanphan W, Chirachanchai S. Polyethylene film surface functionalized with chitosan via γ-ray irradiation in aqueous system: an approach to induce copper(II) ion adsorptivity on PE. Reactive and Functional Polymers. 2008;68(8):1231-8.

70.   Patel D, Wu J, Chan P, Upreti S, Turcotte G, Ye T. Surface modification of low density polyethylene films by homogeneous catalytic ozonation. Chemical Engineering Research and Design. 2012;90(11):1800-6.

71.   Daniloska V, Blazevska-Gilev J, Dimova V, Fajgar R, Tomovska R. UV light induced surface modification of HDPE films with bioactive compounds. Applied Surface Science. 2010;256(7):2276-83.

72.   Price GJ, Clifton AA, Keen F. Ultrasonically enhanced persulfate oxidation of polyethylene surfaces. Polymer. 1996;37(26):5825-9.

73.   Wickson BM, Brash JL. Surface hydroxylation of polyethylene by plasma polymerization of allyl alcohol and subsequent silylation. Colloids and Surfaces A: Physicochemical and Engineering Aspects. 1999;156(1–3):201-13.

74.   Austin ME, Busfield WK, Pomery PJ. Radiation-induced grafting of allyl alcohol onto oriented high density polyethylene. European Polymer Journal. 1995;31(7):683-7.

75.   Yang WT, Rånby B. The role of far UV radiation in the photografting process. Polymer Bulletin. 1996;37(1):89-96.

76.   Rahimpour A, Madaeni SS, Zereshki S, Mansourpanah Y. Preparation and characterization of modified nano-porous PVDF membrane with high antifouling property using UV photo-grafting. Applied Surface Science. 2009;255(16):7455-61.

77.   Vonk RJ, Wouters S, Barcaru A, Vivó-Truyols G, Eeltink S, Koning LJ, et al. Post-polymerization photografting on methacrylate-based monoliths for separation of intact proteins and protein digests with comprehensive two-dimensional liquid chromatography hyphenated with high-resolution mass spectrometry. Analytical and Bioanalytical Chemistry. 2015;407(13):3817-29.

78.   De Jong WH, Borm PJA. Drug delivery and nanoparticles: applications and hazards. International Journal of Nanomedicine. 2008;3(2):133-49.

References

79. Roller J, Laschke MW, Tschernig T, Schramm R, Veith NT, Thorlacius H, et al. How to detect a dwarf: in vivo imaging of nanoparticles in the lung. Nanomedicine: Nanotechnology, Biology and Medicine. 2011;7(6):753-62.

80. Doria G, Conde J, Veigas B, Giestas L, Almeida C, Assunção M, et al. Noble metal nanoparticles for biosensing applications. Sensors. 2012;12(2).

81. Terborg L, Masini JC, Lin M, Lipponen K, Riekolla M-L, Svec F. Porous polymer monolithic columns with gold nanoparticles as an intermediate ligand for the separation of proteins in reverse phase-ion exchange mixed mode. Journal of Advanced Research. 2015;6(3):441-8.

82. Zhang JZ, Noguez C. Plasmonic optical properties and applications of metal nanostructures. Plasmonics. 2008;3(4):127-50.

83. Mirkin CA, Letsinger RL, Mucic RC, Storhoff JJ. A DNA-based method for rationally assembling nanoparticles into macroscopic materials. Nature. 1996;382(6592):607-9.

84. Song J, Huang P-C, Wan Y-Q, Wu F-Y. Colorimetric detection of thiocyanate based on anti-aggregation of gold nanoparticles in the presence of cetyltrimethyl ammonium bromide. Sensors and Actuators B: Chemical. 2016;222:790-6.

85. Borghei Y-S, Hosseini M, Dadmehr M, Hosseinkhani S, Ganjali MR, Sheikhnejad R. Visual detection of cancer cells by colorimetric aptasensor based on aggregation of gold nanoparticles induced by DNA hybridization. Analytica Chimica Acta. 2016;904:92-7.

86. Chen H, Hu W, Li CM. Colorimetric detection of mercury(II) based on 2,2′-bipyridyl induced quasi-linear aggregation of gold nanoparticles. Sensors and Actuators B: Chemical. 2015;215:421-7.

87. Turkevich J, Stevenson PC, Hillier J. A study of the nucleation and growth processes in the synthesis of colloidal gold. Discussions of the Faraday Society. 1951;11(0):55-75.

88. Frens G. Particle size and sol stability in metal colloids. Kolloid-Zeitschrift und Zeitschrift für Polymere. 1972;250(7):736-41.

89. Brust M, Walker M, Bethell D, Schiffrin DJ, Whyman R. Synthesis of thiol-derivatised gold nanoparticles in a two-phase Liquid-Liquid system. Journal of the Chemical Society, Chemical Communications. 1994(7):801-2.

90. Khademi-Azandehi P, Moghaddam J. Green synthesis, characterization and physiological stability of gold nanoparticles from Stachys lavandulifolia Vahl extract. Particuology. 2015;19:22-6.

References

91.   Shang Y, Min C, Hu J, Wang T, Liu H, Hu Y. Synthesis of gold nanoparticles by reduction of HAuCl4 under UV irradiation. Solid State Sciences. 2013;15:17-23.

92.   Muddineti OS, Ghosh B, Biswas S. Current trends in using polymer coated gold nanoparticles for cancer therapy. International Journal of Pharmaceutics. 2015;484(1–2):252-67.

93.   Weiser HB. Inorganic colloid chemistry. 1933.

94.   Templeton AC, Wuelfing WP, Murray RW. Monolayer-protected cluster molecules. Accounts of Chemical Research. 2000;33(1):27-36.

95.   Lala N, Lalbegi SP, Adyanthaya SD, Sastry M. Phase transfer of aqueous gold colloidal particles capped with inclusion complexes of cyclodextrin and alkanethiol molecules into chloroform. Langmuir. 2001;17(12):3766-8.

96.   Cevenini R, Sambri V, Massaria F, Franchini R, D'Antuono A, Borda G, et al. Surface immunofluorescence assay for diagnosis of Lyme disease. Journal of Clinical Microbiology. 1992;30(9):2456-61.

97.   Magnarelli LA, Ijdo JW, Padula SJ, Flavell RA, Fikrig E. Serologic diagnosis of Lyme borreliosis by using enzyme-linked immunosorbent assays with recombinant antigens. Journal of Clinical Microbiology. 2000;38(5):1735-9.

98.   Porwancher R. A reanalysis of IgM western blot criteria for the diagnosis of early Lyme disease. Journal of Infectious Diseases. 1999;179(4):1021-4.

99.   Ledue TB, Collins MF, Young J, Schriefer ME. Evaluation of the recombinant VlsE-based Liaison chemiluminescence immunoassay for detection of Borrelia burgdorferi and diagnosis of Lyme disease. Clinical and Vaccine Immunology : CVI. 2008;15(12):1796-804.

100.   Boyd M, Woolley T. Point of care testing. Surgery (Oxford). 2016;34(2):91-3.

101.   Dassinger N, Vornicescu D, Merkl S, Kehrel M, Dayyoub E, Bakowsky U, et al. A fusion protein for regenerative surfaces. Physica Status Solidi (a). 2012;209(5):832-8.

102.   Miron T, Wilchek M. A simplified method for the preparation of succinimidyl carbonate polyethylene glycol for coupling to proteins. Bioconjugate Chemistry. 1993;4(6):568-9.

103.   Meyer MHF, Hartmann M, Krause H-J, Blankenstein G, Mueller-Chorus B, Oster J, et al. CRP determination based on a novel magnetic biosensor. Biosensors and Bioelectronics. 2007;22(6):973-9.

104.   Thobhani S, Attree S, Boyd R, Kumarswami N, Noble J, Szymanski M, et al. Bioconjugation and characterisation of gold colloid-labelled proteins. Journal of Immunological Methods. 2010;356(1–2):60-9.

References

105.   Van Regenmortel MHV. Analysing structure-function relationships with biosensors. Cellular and Molecular Life Sciences CMLS. 2001;58(5):794-800.

106.   Höbel S, Vornicescu D, Bauer M, Fischer D, Keusgen M, Aigner A. A novel method for the assessment of targeted PEI-based nanoparticle binding based on a static surface plasmon resonance system. Analytical Chemistry. 2014;86(14):6827-35.

107.   Brunt J, Webb MD, Peck MW. Rapid affinity immunochromatography column-based tests for sensitive detection of clostridium botulinum neurotoxins and Escherichia coli O157. Applied and Environmental Microbiology. 2010;76(13):4143-50.

108.   Kehrel M, Dassinger N, Merkl S, Vornicescu D, Keusgen M. A novel approach for increasing sensitivity in lateral flow assays: development of an enrichment module based on polyethylene sintered bodies. physica status solidi (a). 2012;209(5):917-24.

109.   Bartczak D, Kanaras AG. Preparation of peptide-functionalized gold nanoparticles using one pot EDC/sulfo-NHS coupling. Langmuir. 2011;27(16):10119-23.

110.   Hughes-Jones NC, Gardner B, Telford R. The effect of pH and ionic strength on the reaction between anti-D and erythrocytes. Immunology. 1964;7(1):72-81.

111.   Barnes AE. The specificity of pH and ionic strength effects on the kinetics of the Rh (D)-anti-Rh (D) system. The Journal of Immunology. 1966;96(5):854-64.

112.   Dumetz AC, Snellinger-O'Brien AM, Kaler EW, Lenhoff AM. Patterns of protein–protein interactions in salt solutions and implications for protein crystallization. Protein Science : A Publication of the Protein Society. 2007;16(9):1867-77.

113.   Peltomaa M, McHugh G, Steere AC. The VlsE (IR6) peptide ELISA in the serodiagnosis of Lyme facial paralysis. Otology & Neurotology. 2004;25(5).

114.   Johnson BJB, Robbins KE, Bailey RE, Cao B-L, Sviat SL, Craven RB, et al. Serodiagnosis of Lyme disease: accuracy of a two-step approach using a flagella-based ELISA and immunoblotting. Journal of Infectious Diseases. 1996;174(2):346-53.

115.   Bacon RM, Biggerstaff BJ, Schriefer ME, Gilmore RD, Philipp MT, Steere AC, et al. Serodiagnosis of Lyme disease by kinetic enzyme-linked immunosorbent assay using recombinant VlsE1 or peptide antigens of Borrelia burgdorferi compared with 2-tiered testing using whole-cell lysates. Journal of Infectious Diseases. 2003;187(8):1187-99.

116.   Park S-H, Hwang K-J, Chu H, Park M-Y. Serological detection of Lyme borreliosis agents in patients from Korea, 2005–2009. Osong Public Health and Research Perspectives. 2011;2(1):29-33.

117.   Porwancher RB, Hagerty CG, Fan J, Landsberg L, Johnson BJB, Kopnitsky M, et al. Multiplex immunoassay for Lyme disease using VlsE1-IgG and pepC10-IgM antibodies:

References

improving test performance through bioinformatics. Clinical and Vaccine Immunology : CVI. 2011;18(5):851-9.

118.   Gerritzen A, Brandt S. Serodiagnosis of Lyme borreliosis with bead based immunoassays using multiplex technology. Methods. 2012;56(4):477-83.

119.   ABICAP-fast quantification of antigens and antibodies. Biosensors and Bioelectronics. 1993;8(2):xv-xviii.

120.   Lucht A, Formenty P, Feldmann H, Götz M, Leroy E, Bataboukila P, et al. Development of an immunofiltration-based antigen-detection assay for rapid diagnosis of Ebola virus infection. Journal of Infectious Diseases. 2007;196(Supplement 2):S184-S92.

121.   Meyer MHF, Stehr M, Bhuju S, Krause H-J, Hartmann M, Miethe P, et al. Magnetic biosensor for the detection of Yersinia pestis. Journal of Microbiological Methods. 2007;68(2):218-24.

122.   Dusemund B, Hoffmann A, Salzmann T, Kreibig U, Schmid G. Cluster matter: the transition of optical elastic scattering to regular reflection. Zeitschrift für Physik D Atoms, Molecules and Clusters.20(1):305-8.

123.   Vilela D, González MC, Escarpa A. Sensing colorimetric approaches based on gold and silver nanoparticles aggregation: chemical creativity behind the assay. A review. Analytica Chimica Acta. 2012;751:24-43.

124.   Kritskaya DA, Pomogailo AD, Ponomarev AN, Dyaschkovskii FS. Functionalization of polymer supports for polymerization catalysts by graft polymerization method. Journal of Applied Polymer Science. 1980;25(3):349-57.

125.   Dowbenko R. Allyl monomers and polymers. Kirk-Othmer Encyclopedia of Chemical Technology: John Wiley & Sons, Inc.; 2000.

126.   Bluemel J. Reactions of ethoxysilanes with eilica: a solid-state NMR study. Journal of the American Chemical Society. 1995;117(7):2112-3.

127.   Pasternack RM, Rivillon Amy S, Chabal YJ. Attachment of 3-(aminopropyl)triethoxysilane on silicon oxide surfaces: dependence on solution temperature. Langmuir. 2008;24(22):12963-71.

128.   Carrara S, Cavallini A, Maruyama Y, Charbon E, De Micheli G. A new ethylene glycol-silane monolayer for highly-specific DNA detection on silicon chips. Surface Science. 2010;604(23–24):L71-L4.

129.   Schlingman DJ, Mack AH, Mochrie SGJ, Regan L. A new method for the covalent attachment of DNA to a surface for single-molecule studies. Colloids and surfaces B, Biointerfaces. 2011;83(1):91-5.

References

130.   Hermanson GT. Bioconjugate techniques. San Diego: Academic Press; 1996.

131.   Pu W, Zhao H, Huang C, Wu L, Xu D. Visual detection of arginine based on the unique guanidino group-induced aggregation of gold nanoparticles. Analytica Chimica Acta. 2013;764:78-83.

132.   Bui M-PN, Baek TJ, Seong GH. Gold nanoparticle aggregation-based highly sensitive DNA detection using atomic force microscopy. Analytical and Bioanalytical Chemistry. 2007;388(5):1185-90.

E R K L Ä R U N G

Ich versichere, dass ich meine Dissertation

" Development of new immunoassay platforms for rapid serological diagnosis of Lyme borreliosis''

selbständig ohne unerlaubte Hilfe angefertigt und mich dabei keiner anderen als der von mir ausdrücklich bezeichneten Quellen bedient habe. Alle vollständig oder sinngemäß übernommenen sind Zitate als solche gekennzeichnet.

Die Dissertation wurde in der jetzigen oder einer ähnlichen Form noch bei keiner anderen Hochschule eingereicht und hat noch keinen sonstigen Prüfungszwecken gedient.

Marburg, den..........................

....

(Unterschrift mit Vor- und Zuname)

Mohammed Alasel │ Curriculum vitae

Friedrich-Ebert-Str. 111 - 35039 Marburg, Germany
+49 (0) 17684468319
alaselm@staff.uni-marburg.de & maaalasel@yahoo.com

Personal Information

Date of birth:	10.05.1983
Nationality:	Egyptian

Education

April 2012 – present Doctoral studies at Philipps University, Institute of Pharmaceutical Chemistry, Germany.

Aug 2010 – January 2011 Molecules of life **course** (modern cell biology and biochemistry), at Umeå University, Department of Medical Biochemistry and Biophysics, Umeå, Sweden.

Aug 2008 – January 2009 Ion exchange separation and purification methods, **course,** (basics and applications of Ion Exchange separation in chemistry and chemical industry) at Royal Institute of Technology, Institute of Materials Science and Engineering, Stockholm, Sweden.

11/2005 – 02/2008   MSc of science with chemistry major at Lund University, Faculty of science, Lund, Sweden.

Master theses:

1. Development of an amperometric screen-printed array biosensor for glucose and ethanol determination.
2. Studying of glycoprotein-lectin interaction/affinity using Biacore analyser and immobilized lectins.
3. Studies of [lectin-glycan] interactions for the differentiation of pathogenic bacteria using Biacore analyser.

09/2000 – 05/2004 Bachelor of Science with chemistry major at Mansoura University, Faculty of Science, Egypt.

Work Experience

04/2012 – present   **Doctoral research**

Philipps University, Institute of Pharmaceutical chemistry, (Prof. Dr. M. Keusgen) Marburg, Germany.

- ❖ Working as a research scientist within the research project **Diagnostic pipette tip (DiaTip)** a collaboration between Philipps University, Seramun Diagnostica GmbH, Senova and Forschungszentrum für Medizintechnik und Biotechnologie, responsible for developing new and rapid platforms for bio analysis. Currently working on a PhD thesis that will summarize my research work of the last three and half years, completion expected in May 2016.

Detailed description:

- Developing new immunoassay platforms for serological diagnosis of infectious diseases.
- Gold nanoparticles synthesis and functionalization
- Surface functionalization of polymeric materials
- Protein-protein interaction using surface plasmon resonance
- Protein immobilization
- Bio-conjugation
- Working with FTIR, UV, UV-vis, SPR
- Documenting and publishing the results in international research journals
- Further contributions to university and institute affairs
    - ➢ Teaching assistant in instrumental analysis practical (Focus on HPLC)
    - ➢ Working with LC-MS (Electrospray ionization MS)
    - ➢ Giving scientific talks at international conferences   and group meetings
    - ➢ Supervising master and bachelor students during their thesis and practical work
    - ➢ Organizing project meetings and work-shops

05/2011 – 11/2011   **Internship Research**

Lund University, Faculty of Medicine, Stem Cell Center, (Prof.Dr. E. Pera) Lund, Sweden.

- ❖ Working as a research scientist within the research project **Retinoic acid biosynthesis in pancreas development and role of Rdh10 in adult diabetic mice.**

Detailed description:

- Genotyping by PCR
- Immunofluorescence
- Characterization of DNA sequences by Gel electrophoresis
- Extraction of genomic DNA from different tissues

Language Skills

English: Very good
German: Good
Arabic: Native

Publications

Published

- G. Safina, I.B. Duran, <u>M. Alasel</u>, B. Danielsson. Surface plasmon resonance for real-time study of Lectin-carbohydrate interactions for the differentiation and identification of glycoproteins. Talanta 84 (2011) 1284-1290.

Communicated to journals

- <u>M. Alasel</u>, M. Keusgen. A new 3-dimensional polyethylene based platform for a rapid serological diagnosis.
- <u>M. Alasel</u>, N. Dassinger, D. Vornicescu, K. Engelhardt, M. Keusgen. Mannan Modified sinter bodies for diagnosis of borreliosis in diagnostic pipette tip.
- <u>M. Alasel</u>, M. Keusgen. A one-step colorimetric test for serological diagnosis based on two-protein modified gold nanoparticles.

Conferences

- Nanax 7 conference on Nanoscience, Philipps University, Marburg, Germany, 2016. (**Poster presentation**)
- Workshop on Evaluation of Natural Resources in Afghanistan, Rauischholzhausen, Marburg, Germany, 2015. (**Attendee**)
- EnFI conference on Engineering of Functional Interfaces, Hannover Medical School, Hannover, Germany, 2015. (**Oral presentation**)
- The international society for optics and photonics (SPIE), San Francisco, USA, 2015. (**Oral presentation**)
- European Youssef Jameel PhD summer school, Cardiff University, UK, 2014. (**Oral presentation**)
- The Globalization of Pharmaceutics Education Network (GPEN), Helsinki, Finland, 2014. (**Poster presentation**)
- EnFI conference on Engineering of Functional Interfaces, Aachen University of Applied Sciences, Germany, 2014. (**Oral presentation**)
- Die Deutsche Pharmazeutische Gesellschaft (DPhG), Frankfurt, Germany, 2014. (**Poster presentation**)
- EnFI conference on Engineering of Functional Interfaces, Hasselt University, Campus Hasselt, Belgium, 2013. (**Oral presentation**)
- XVI Intl conference on Flow Injection Analysis, Pattaya, Thailand, 2010. My publication results were presented as a poster in the conference.